B6985
Encl to
9-17-84 ltr
to P. Brooks

PARAMETERS AND VARIABLES APPEARING IN COMPUTER CODES FOR WASTE PACKAGE STRUCTURAL AND THERMAL ANALYSIS

Prepared by:

CorSTAR Research, Inc.
7315 Wisconsin Avenue
Suite 702 North
Bethesda, MD 20814

Prepared for:

Division of Waste Management
Office of Nuclear Material Safety & Safeguards
U.S. Nuclear Regulatory Commission
Washington, D.C. 20555
NRC FIN B6985

8410090201 840917
PDR WMRES EECCORS
B-6985 PDR

NUREG/CR-XXXX

Parameters and Variables Appearing in Computer Codes for Waste Package Structural and Thermal Analysis

Draft Report

Manuscript Completed:
Date Published:

Prepared by:
W. Coffman, M. Mills, D. Vogt

CorSTAR Research, Inc.
7315 Wisconsin Avenue
Suite 702 North
Bethesda, MD 20814

Prepared for:
Division of Waste Management
Office of Nuclear Material Safety and Safeguards
U.S. Nuclear Regulatory Commission
Washington, D.C. 20555
NRC FIN B6985

ABSTRACT

This report defines the parameters and variables appearing in computer codes that can be used for thermal and structural analysis of a high-level waste package. Typical values and ranges of data values are presented. The data in this report were compiled to help guide the selection of values of parameters and variables to be used in code benchmarking. The report also presents the underlying theory of waste package analysis.

CONTENTS

	Page
ABSTRACT	iii
LIST OF FIGURES	viii
LIST OF TABLES	x
ACKNOWLEDGEMENTS	xviii
1.0 INTRODUCTION	1
1.1 Background	1
1.2 Scope of This Report	2
1.3 Processes Considered	3
1.4 Data Limitations and Inadequacies	4
2.0 THERMAL ANALYSIS	7
2.1 Heat Transfer Phenomena	7
2.1.1 Conduction	8
2.1.1.1 Radial Steady-State Conduction with Heat Generation and Constant Thermal Conductivity in a Solid Cylinder	11
2.1.1.2 Radial Steady-State Conduction without Heat Generation and with Constant Thermal Conductivity in a Hollow Cylinder	12
2.1.1.3 Two-Dimensional Conduction	13
2.1.2 Convection	14
2.1.2.1 Forced Convection	15
2.1.2.2 Free or Natural Convection	22
2.1.3 Radiation	27
2.1.3.1 Ideal Radiation Emission	27
2.1.3.2 Material Radiation Properties	31
2.1.3.3 Geometric Aspects of Radiative Heat Transfer	33
2.1.3.4 Grey Body Radiation Heat Transfer	34
2.1.4 Finite Increment Mathematical Models	40
2.1.5 Thermal Loads and Constraints	44
2.1.6 Conservation Equations	45
2.1.7 Simulated Thermal Responses	49
2.2 Thermal System Variables and Parameters	49

CONTENTS (continued)

Page

2.2.1.1 Thermal Conductivity 51
2.2.1.2 Specific Heat 52
2.2.1.3 Mass Density 55
2.2.1.4 Latent Heat 60
2.2.1.5 Material Conduction Properties 63

2.2.2 Convection Parameters 103

2.2.2.1 Dimensionless Parameters 104
2.2.2.2 Forced Convection 107
2.2.2.3 Natural Convection 113
2.2.2.4 Fluid Convection Properties 115

2.2.3 Radiation Parameters 127

2.2.3.1 Stefan-Boltzmann Constant 127
2.2.3.2 Emissivity Data 127
2.2.3.3 View Factors 127

3.0 STRUCTURAL MECHANICS 130

3.1 Analytical Techniques 130

3.1.1 Objectives of Analysis 130
3.1.2 Structural Analysis Approaches 130

3.2 Mechanics Principles 132

3.2.1 Displacement, Deformation, and Strain 132
3.2.2 Internal Loads and Stresses 140
3.2.3 Constitutive Relationships 152

3.2.3.1 Types of Constitutive Relationships and Their Uses 152
3.2.3.2 Generalized Linear Elastic Mechanical and Thermal Constitutive Relationships ... 156
3.2.3.3 Yield Strength, Ultimate Tensile Strength, and Ultimate Compressive Strength 161
3.2.3.4 Plastic Constitutive Relationships 179
3.2.3.5 Creep Constitutive Relationships 197

3.3 Mechanical Properties of Packing Materials 214

3.3.1 Plasticity 220
3.3.2 Strength 222

CONTENTS (continued)

	Page
3.4 Loads and Constraints	226
3.5 Equations of Motion	227
3.6 Equilibrium Relationships	231
3.7 Analytical Responses	233
4.0 REFERENCES	236
APPENDIX A	A 1
APPENDIX B	B 1
APPENDIX C	C 1
APPENDIX D	D 1

LIST OF FIGURES

Number	Legend	Page
2.1	Control Volume in the Laminar Boundary Layer on a Flat Plate	17
2.2	Natural Convection Boundary Layer along Outside Surface of a Warm Pane of Glass in Cold Ambient Air	23
2.3	Velocity and Temperature Profiles in Natural Convection	24
2.4	Incident Thermal Radiation Being Absorbed, Reflected, and Transmitted	32
2.5	Angles, Area Elements, and Separation Distance Terms Used in Evaluating Radiation View Vectors	35
2.6	Plate Consisting of Five Cubic Elements of Unit Dimension on a Side with One Node per Element Located at Its Center	46
2.7	Heat Transfer as a Function of Distance along a Plate	109
3.1	Strain Components Related Geometrically to Displacements	134
3.2	Two of the Possible Six Shear Components Acting on (a) 3D Element; (b) 2D Element; and (c) the Deformed Shape Due to Strain (Angles α and β)	144
3.3	General State of Stress of a Point Defined in Terms of Three Traction Components and Six Shear Components. The Back Faces Have Oppositely Directed Traction and Shear Components Which Are Not Shown.	146
3.4	Conceptual Structural Criteria Application Procedure	154
3.5	Plot Showing Instantaneous Elastic Strain A, Instantaneous Plastic Strain B Plus Primary, Secondary and Tertiary Creep Ranges for Constant Stress and Constant Temperature Controlled Uniaxial Tensile Loading	199
3.6	Creep Strain Versus Time Curves for the Same Temperature but Different Stress Levels $\sigma_1 > \sigma_2 > \sigma_3 > \sigma_4$ The Instanteous Strain Is the Value of Time = 0.	200
3.7	Isochronal Stress Versus Strain Behavior for a Given Temperature	201
3.8	Strain Versus Time Curve Which Includes Instantaneous and Creep Strains	203
3.9	Creep Rate Versus Time Plotted from Figure 3.6 Data	204

List of Figures (continued)

Number	Legend	Page
3.10	Curves of Constant Creep Strain and Rupture on Stress Versus Time-Temperature Parameter (TTP)	212
3.11	Effect of Clay Content and Clay Mineralogy on the Plastic Behavior of Soils	223
3.12	Effect of Clay Content and Clay Mineralogy, Including Hydrous Micas, on the Residual Friction Angle of Soil Under Shear Stress	225
3.13	Simple Two Degree of Freedom System (Two Translations u_1 and u_2) with Mass, Damping and Stiffness, and Transient Forcing Functions	228
B-1	Infinitesimal Cube Used to Define the State of Stress at a Point in a Structure. Stress Components Are Shown Only on the Positive Axis Faces. Components of Equal Magnitude but Opposite Direction Act on the Faces Which Project along the Negative Axes.	B 2
B-2	Mohr's Circles for Stress with Principal Stress σ_1, σ_2, σ_3 and Maximum Shear Stress $\tau_{max} = {}^1/_2 \max\{\lvert\sigma_1-\sigma_2\rvert, \lvert\sigma_2-\sigma_3\rvert, \lvert\sigma_1-\sigma_3\rvert\}$	B 3
B-3	Two Dimensional x-y Plane View of Infinitesimal Cube Used to Define State of Stress at Point p.	B 4
B-4	Sign Convention for Stress Components Used in Constructing Mohr's Circle in the Generalized p-q Plane. Components Are Shown in the Positive Direction.	B 5
B-5	Mohr's Circle for Stress Components Directed as Defined in Figure B-3. An Angle of θ in the xy Plane of the Structure Corresponds to 2 θ on the Mohr's Circle Plot	B 7
B-6	Mohr's Circle of Stress in x-y Plane When Y Directed Normal Stress Is Compressive Rather Than Tensile. An Angle of θ in the xy Plane of the Structure Corresponds to 2 θ on the Mohr's Circle Plot.	B 10
B-7	Mohr's Circle for a Simple Uniaxial Tension Specimen without Shear on the Cube Two of the Mohr's Circles Can Be Considered as Points at (0,0).	B 12
B-8	Mohr's Circle for Strain	B 14
C-1	Von Mises Yield Surfaces Projected on a Plan Normal to the Line Intersection Points Where $\sigma_1 = \sigma_2 = \sigma_3$.	C 4

LIST OF TABLES

Number	Legend	Page
2.1	Cast Iron Conduction Properties Including Thermal Conductivity (k), Mass Density (ρ), Specific Heat (c), and Thermal Diffusivity (a=k/ρc) in English Units	65
2.2	Cast Iron Conduction Properties Including Thermal Conductivity (k), Mass Density (ρ), Specific Heat (c), and Thermal Diffusivity (a=k/ρc) in Metric Units	66
2.3	Carbon Steel Conduction Properties Including Thermal Conductivity (k), Mass Density (ρ), Specific Heat (c), and Thermal Diffusivity (a=k/ρc) in English Units	67
2.4	Carbon Steel Conduction Properties Including Thermal Conductivity (k), Mass Density (ρ), Specific Heat (c), and Thermal Diffusivity (a=k/ρc) in Metric Units	68
2.5	304 Stainless Steel Conduction Properties Including Thermal Conductivity (k), Mass Density (ρ), Specific Heat (c), and Thermal Diffusivity (a=k/ρc) in English Units	69
2.6	304 Stainless Steel Conduction Properties Including Thermal Conductivity (k), Mass Density (ρ), Specific Heat (c), and Thermal Diffusivity (a=k/ρc) in Metric Units	70
2.7	Ticode 12 Conduction Properties Including Thermal Conductivity (k), Mass Density (ρ), Specific Heat (c), and Thermal Diffusivity (a=k/ρc) in English Units	71
2.8	Ticode 12 Conduction Properties Including Thermal Conductivity (k), Mass Density (ρ), Specific Heat (c), and Thermal Diffusivity (a=k/ρc) in Metric Units	72
2.9	Zircaloy 2 Conduction Properties Including Thermal Conductivity (k), Mass Density (ρ), Specific Heat (c), and Thermal Diffusivity (a=k/ρc) in English Units	73
2.10	Zircaloy 2 Conduction Properties Including Thermal Conductivity (k), Mass Density (ρ), Specific Heat (c), and Thermal Diffusivity (a=k/ρc) in Metric Units	74
2.11	Zircaloy 4 Conduction Properties Including Thermal Conductivity (k), Mass Density (ρ), Specific Heat (c), and Thermal Diffusivity (a=k/ρc) in English Units	75

TABLES (continued)

Number	Legend	Page
2.12	Zircaloy 4 Conduction Properties Including Thermal Conductivity (k), Mass Density (ρ), Specific Heat (c), and Thermal Diffusivity (a=k/ρc) in Metric Units	76
2.13	Bentonite Conduction Properties Including Thermal Conductivity (k), Mass Density (ρ), Specific Heat (c), and Thermal Diffusivity (a=k/ρc) in English Units	77
2.14	Bentonite Conduction Properties Including Thermal Conductivity (k), Mass Density (ρ), Specific Heat (c), and Thermal Diffusivity (a=k/ρc) in Metric Units	78
2.15	Defense High-Level Waste Glass Conduction Properties Including Thermal Conductivity (k), Mass Density (ρ), Specific Heat (c), and Thermal Diffusivity (a=k/ρc) in English Units	79
2.16	Defense High-Level Waste Glass Conduction Properties Including Thermal Conductivity (k), Mass Density (ρ), Specific Heat (c), and Thermal Diffusivity (a=k/ρc) in Metric Units	80
2.17	Commercial High-Level Glass Conduction Properties Including Thermal Conductivity (k), Mass Density (ρ), Specific Heat (c), and Thermal Diffusivity (a=k/ρc) in English Units	81
2.18	Commercial High-Level Glass Conduction Properties Including Thermal Conductivity (k), Mass Density (ρ), Specific Heat (c), and Thermal Diffusivity (a=k/ρc) in Metric Units	82
2.19	Uranium Dioxide Conduction Properties Including Thermal Conductivity (k), Mass Density (ρ), Specific Heat (c), and Thermal Diffusivity (a=k/ρc) in English Units	83
2.20	Uranium Dioxide Conduction Properties Including Thermal Conductivity (k), Mass Density (ρ), Specific Heat (c), and Thermal Diffusivity (a=k/ρc) in Metric Units	84
2.21	Air Thermal Conduction Properties at One Atmosphere Pressure Including Thermal Conductivity (k), Mass Density (ρ), Specific Heat (c_p), and Thermal Diffusivity ($a=k/\rho c_p$) in English Units	85

TABLES (continued)

Number	Legend	Page
2.22	Air Thermal Conduction Properties at One Atmosphere Pressure Including Thermal Conductivity (k) Mass Density (ρ), Specific Heat (c_p), and Thermal Diffusivity ($a=k/\rho c_p$) in Metric Units	86
2.23	Helium Thermal Conduction Properties at One Atmosphere Pressure Including Thermal Conductivity (k), Mass Density (ρ), Specific Heat (c_p), and Thermal Diffusivity ($a=k/\rho c_p$) in English Units	87
2.24	Helium Thermal Conduction Properties at One Atmosphere Pressure Including Thermal Conductivity (k), Mass Density (ρ), Specific Heat (c_p), and Thermal Diffusivity ($a=k/\rho c_p$) in Metric Units	88
2.25	Saturated Liquid Water Thermal Conduction Properties Including Thermal Conductivity (k), Mass Density (ρ), Specific Heat (c_p), and Thermal Diffusivity ($a=k/\rho c_p$) in English Units	89
2.26	Saturated Liquid Water Thermal Conduction Properties Including Thermal Conductivity (k), Mass Density (ρ), Specific Heat (c_p) and Thermal Diffusivity ($a=k/\rho c_p$) in Metric Units	90
2.27	Dry Superheated Steam at Atmospheric Pressure Thermal Conduction Properties Including Thermal Conductivity (k), Mass Density (ρ), Specific Heat (c_p), and Thermal Diffusivity ($a=k/\rho c_p$) in English Units	91
2.28	Dry Superheated Steam at Atmospheric Pressure Thermal Conduction Properties Including Thermal Conductivity (k), Mass Density (ρ), Specific Heat (c_p), and Thermal Diffusivity ($a=k/\rho c_p$) in Metric Units	92
2.29	Saturated Liquid and Saturated Steam Properties Including Pressure (P_{sat}), Temperature (T_{sat}), Saturated Liquid Enthalpy (h_f), Saturated Dry Steam Enthalpy (h_g), Saturated Liquid Specific Volume (v_f), and Saturated Dry Steam Specific Volume (v_g) in English Units	93
2.30	Saturated Liquid and Saturated Steam Properties Including Pressure (P_{sat}), Temperature (T_{sat}), Saturated Liquid Enthalpy (h_f), Saturated Dry Steam Enthalpy (h_g), Saturated Liquid Specific Volume (v_f), and Saturated Dry Steam Specific Volume (v_g) in Metric Units	94

TABLES (continued)

Number	Legend	Page
2.31	Thermal Conductivity (k) of Subcooled Liquid Water and Superheated Steam as a Function of Temperature and Pressure in English Units (Btu/hr-ft-^{o}F)	95
2.32	Thermal Conductivity (k) of Subcooled Liquid Water and Superheated Steam as a Function of Temperature and Pressure in Metric Units (milliwatts/meter-^{o}K)	96
2.33	Specific Volume (v) of Subcooled Liquid Water and Superheated Steam as a Function of Temperature and Pressure in English Units (ft^3/lb_m)	97
2.34	Specific Volume (v) of Subcooled Liquid Water and Superheated Steam as a Function of Temperature and Pressure in Metric Units (cm^3/g)	99
2.35	Specific Enthalpy (h) of Subcooled Liquid Water and Superheated Steam as a Function of Temperature and Pressure in English Units (Btu/lb_m)	100
2.36	Specific Enthalpy (h) of Subcooled Liquid Water and Superheated Steam as a Function of Temperature and Pressure in Metric Units (Joules/g)	102
2.37	Air Thermal Convection Properties at Atmospheric Pressure Including Dynamic Viscosity (μ), Mass Density (ρ), Volumetric Coefficient of Thermal Expansion (β), and Kinematic Viscosity (ν) in English Units	116
2.38	Air Thermal Convection Properties at Atmospheric Pressure Including Dynamic Viscosity (μ), Mass Density (ρ), Volumetric Coefficient of Thermal Expansion (β), and Kinematic Viscosity (ν) in Metric Units	117
2.39	Helium Thermal Convection Properties at Atmospheric Pressure Including Dynamic Viscosity (μ), Mass Density (ρ), Volumetric Coefficient of Thermal Expansion (β), and Kinematic Viscosity (ν) in English Units	118
2.40	Helium Thermal Convection Properties at Atmospheric Pressure Including Dynamic Viscosity (μ), Mass Density (ρ), Volumetric Coefficient of Thermal Expansion (β), and Kinematic Viscosity (ν) in Metric Units	119

TABLES (continued)

Number	Legend	Page
2.41	Saturated Liquid Water Thermal Convection Properties Including Dynamic Viscosity (μ), Mass Density (ρ), Volumetric Coefficient of Thermal Expansion (β), and Kinematic Viscosity (ν) in English Units	120
2.42	Saturated Liquid Water Thermal Convection Properties Including Dynamic Viscosity (μ), Mass Density (ρ), Volumetric Coefficient of Thermal Expansion (β), and Kinematic Viscosity (ν) in Metric Units	121
2.43	Dry Superheated Steam at Atmospheric Pressure Thermal Convection Properties Including Dynamic Viscosity (μ), Mass Density (ρ), Volumetric Coefficient of Thermal Expansion (β), and Kinematic Viscosity (ν) in English Units	122
2.44	Dry Superheated Steam at Atmospheric Pressure Thermal Convection Properties Including Dynamic Viscosity (μ), Mass Density (ρ), Volumetric Coefficient of Thermal Expansion (β), and Kinematic Viscosity (ν) in Metric Units	123
2.45	Dynamic Viscosity (μ) of Subcooled Liquid Water and Superheated Steam as a Function of Temperature and Pressure in English Units (lb_m/ft-hr)	124
2.46	Dynamic Viscosity (μ) of Subcooled Liquid Water and Superheated Steam as a Function of Temperature and Pressure in Metric Units (micropoise)	126
2.47	Values of Surface Emissivity for Solid Materials	128
3.1	Relationships between Isotropic Elastic Constants	162
3.2	Zircaloy 2 Tubing Mechanical Properties as a Function of Temperature in English Units	163
3.3	Zircaloy 2 Mechanical Properties as a Function of Temperature in Metric Units	164
3.4	Zircaloy 4 Mechanical Properties as a Function of Temperature in English Units	165
3.5	Zircaloy 4 Mechanical Properties as a Function of Temperature in Metric Units	166

TABLES (continued)

Number	Legend	Page
3.6	Carbon Steel Mechanical Properties as a Function of Temperature in English Units	167
3.7	Carbon Steel Mechanical Properties as a Function of Temperature in Metric Units	168
3.8	304 Stainless Steel Mechanical Properties as a Function of Temperature in English Units	169
3.9	304 Stainless Steel Mechanical Properties as a Function of Temperature in Metric Units	170
3.10	Defense HLW Glass Mechanical Properties as a Function of Temperature in English Units	171
3.11	Defense HLW Glass Mechanical Properties as a Function of Temperature in Metric Units	172
3.12	Commercial HLW Glass Mechanical Properties as a Function of Temperature in English Units	173
3.13	Commercial HLW Glass Mechanical Properties as a Function of Temperature in Metric Units	174
3.14	Cast Iron Mechanical Properties as a Function of Temperature in English Units	175
3.15	Cast Iron Mechanical Properties as a Function of Temperature in Metric Units	176
3.16	Ticode 12 Mechanical Properties as a Function of Temperature in English Units	177
3.17	Ticode 12 Mechanical Properties as a Function of Temperature in Metric Units	178
3.18	Carbon Steel Yield Strength as a Function of Temperature in English Units	180
3.19	Carbon Steel Yield Strength as a Function of Temperature in Metric Units	181
3.20	304 Stainless Steel Yield Strength as a Function of Temperature in English Units	182
3.21	304 Stainless Steel Yield Strength as a Function of Temperature in Metric Units	183

TABLES (continued)

Number	Legend	Page
3.22	Zircaloy 4 Strength Including ULtimate Tensile Strength (σ_u), 0.2 Percent Offset Yield Strength (σ_y), and Linear Elastic (Proportional) Limit (σ_p) in English Units	184
3.23	Zircaloy 4 Strength Including Ultimate Tensile Strength (σ_u), 0.2 Percent Offset Yield Strength (σ_y), and Linear Elastic (Proportional) Limit (σ_p) in Metric Units	185
3.24	Zircaloy 2 Ultimate Strength (σ_u) and Yield Strength (σ_y) as a Function of Temperature in English Units	186
3.25	Zircaloy 2 Ultimate Strength (σ_u) and Yield Strength (σ_y) as a Function of Temperature in Metric Units	187
3.26	Ticode 12 Strength Including Minimum Tensile Strength ($\sigma_u\|_{min}$), Minimum 0.2 Percent Offset Yield Strength (σ_y), and Room Temperature Typical Ultimate Strength (σ_u) and Typical Yield Strength (σ_y) in English Units	188
3.27	Ticode 12 Strength Including Minimum Tensile Strength ($\sigma_u\|_{min}$), Minimum 0.2 Percent Offset Yield Strength (σ_y), and Room Temperature Typical Ultimate Strength (σ_u) and Typical Yield Strength (σ_y) in Metric Units	189
3.28	Cast Iron Yield Data in English Units	190
3.29	Cast Iron Yield Data in Metric Units	191
3.30	Defense Waste Glass (131 TDS) Ultimate Tensile Strength (σ_t) and Ultimate Compressive Strength (σ_c) in English Units	192
3.31	Defense Waste Glass (131 TDS) Ultimate Tensile Strength (σ_t) and Ultimate Compressive Strength (σ_c) in Metric Units	193
3.32	Different Temperature and Load Durations Consistent with a Constant LMP	215
3.33	Carbon Steel Creep Rate	216
3.34	Zircaloy 2 Creep Rate	217

TABLES (continued)

Number	Legend	Page
3.35	304 Stainless Steel Creep Rates	218
3.36	Ticode 12 Creep Rate	219
3.37	Plastic (PW) and Liquid (LW) Limits for Common Clay Minerals	221

ACKNOWLEDGMENTS

We gratefully acknowledge the assistance of Dr. William Harden in reviewing this manuscript. The completion of the manuscript was made possible by the diligent efforts of Ms. Marilyn Singer. This study was performed for the U.S. Nuclear Regulatory Commission under contract NRC-02-81-026. The NRC Project Officers were Dr. Daniel Fehringer and Mrs. Pauline Brooks.

1.0 INTRODUCTION

1.1 Background

The effective management of high-level radioactive wastes is essential to protect the public health and safety. The Department of Energy (DOE), through responsibilities inherited from the Energy Research and Development Administration (ERDA) and the Atomic Energy Commission (AEC), and the authority granted in the Nuclear Waste Policy Act, is charged with the safe disposal of these wastes. The Nuclear Regulatory Commission (NRC), through authority granted by the Energy Reorganization Act of 1974, which created the NRC, and the Nuclear Waste Policy Act, is responsible for the regulation of high-level waste management.

The Environmental Protection Agency (EPA) has the authority and responsibility for setting general standards for radiation in the environment. The NRC is responsible for implementing these standards in its licensing actions and for ensuring that public health and safety are protected. The NRC has promulgated technical criteria for regulating the geologic disposal of HLW which incorporate the EPA standard. (The draft EPA standard was published in the Federal Register dated December 29, 1982.) NRC's technical criteria are intended to be compatible with a generally applicable environmental standard. The performance objectives and criteria address the functional elements of geologic disposal of HLW and the analyses required to provide confidence that these functional elements will perform as intended. These technical criteria are described in 10 CFR Part 60 (Code of Federal Regulations).

In discharging its responsibility, the NRC must review DOE repository performance assessments and independently evaluate the performance of the repositories that the DOE seeks to license. Because of the complexity and multiplicity of these performance assessments, computerized simulation modeling is used. Computer simulation models provide a means to evaluate the most important processes that will be active in a repository, thereby permitting assessment and prediction of repository behavior.

Another factor necessitating the use of models is that the time frames associated with high-level waste management range from decades to tens of thousands of years.

Accordingly, the NRC is developing models and computer codes for use in supporting these regulations and in reviewing proposed nuclear waste management systems. The DOE independently is also developing models and computer codes for use in assessing repository sites and designs. The analytical model and code development effort must include a procedure for independent evaluation of the tools' capability to simulate real processes. Codes must be evaluated to determine their limitations and the adequacy of supporting empirical relations and laboratory tests used for the assessment of long-term repository performance.

1.2 Scope of This Report

This report is one in a series that deals with the independent evaluation of computer codes for analyzing the performance of a high-level radioactive waste repository. The codes used for repository performance assessment have been divided into the following categories: (1) repository siting, (2) radiological assessment, (3) repository design, (4) waste package performance, and (5) overall systems.

Repository siting requires consideration of events at a distance from the repository. Far-field processes include saturated flow, unsaturated flow, surface water flow (flooding routing), solute transport, heat transport, combined solute and heat transport, geochemistry, and geomechanical response.

Radiological assessment includes the development of source terms, the calculation of radionuclide concentrations in the environment, and the analysis of food pathways, dose to man, and expected mortality rates.

Repository design covers areas often called "near field." The processes in the repository design area include heat transport, flow in fractured media, and rock mechanics.

The waste package area deals with the very near field, primarily the interactions that take place within the waste package and the waste package's interactions with the repository host rock. Included are heat transfer, stress analysis, and chemical interactions such as corrosion.

Overall systems include subcategories of the other categories. For example, overall systems codes may consider aspects of radiological assessment, waste package performance, economic cost (e.g., cost/benefit analysis), repository performance, natural multibarrier performance, or probabilistic aspects of repository performance.

This report considers only codes for the thermal and mechanical analysis of a waste package. Parameters associated with corrosion and leaching are being reviewed by others (see Section 1.3 below).

The first step in computer code benchmarking is to select the codes potentially useful for thermal and structural analysis. The next step is to summarize the nature of each selected code and then to prepare benchmark problems for code testing. As a prerequisite to designing benchmark problems, the data that will be used in the problems should be summarized. Thus, three reports will be issued on waste package codes: (1) a model summary report, (2) a data set report, and (3) a report describing the benchmark problems to be used in code testing. This report is the data set report for waste package codes.

1.3 Processes Considered

The major processes that must be considered in the analysis of a high-level waste package are thermal processes, structural mechanics, radiation degradation, and chemical degradation (e.g., corrosion and leaching). Other contractors have summarized the information base relating to waste package radiation and chemical degradation (References DA-82 and DA-82a). Therefore, this report mainly addresses thermal processes and structural mechanics. This report does not address fracture mechanics because the primary structural loading of the waste package will be in

compression, whereas fractures generally grow in materials that are loaded in tension. Compressive loading closes fractures and results in no growth.

In Section 2 of the report, the three heat transfer modes (conduction, convection, and radiation) important to waste package thermal analysis are discussed. Recommended values for material properties and parameters are given, and several important heat transfer correlations are identified.

In Section 3, the basic mechanical principles used for waste package analysis and the values of material properties are identified. Section 3 emphasizes the need for structural criteria that limit the total strain during the service life of the waste package.

Appendices A, B, and C address thermal expansion, Mohr's diagrams, and material yield criteria. The information in these appendices can be found in most engineering texts but is included here to increase the usefulness of this document as a primer providing basic information for thermal and structural analyses. Appendix D presents selected thermal property data from the HEATING code data library.

1.4 Data Limitations and Inadequacies

In addition to providing values of key parameters, this report identifies limitations and inadequacies in the existing data. Some of the more important limitations are summarized below:

- Thermal analyses incorporating phase changes impose the complication of different material properties for the two phases. In order to analyze phase change problems accurately, it is necessary to understand the algorithms used by computer programs to perform phase change calculations. Phase change algorithms are not standardized, and a modeling approach used with one code may not work with another. (See Section 2.1.4)

- Before sealing of a repository, ventilation will be a significant mechanism for heat removal. Ventilation will remove heat primarily by convection with some contribution from radiation. (See Section 2.1.5)

- The thermal properties of bentonite and bentonite rock mixtures are a function of both the density of the material and the moisture content. In general, the thermal conductivity of bentonite rock mixtures increases as density and moisture content increase. Because of the great variation of these properties, it will be necessary to perform thermal measurements on the bentonite or bentonite rock mixtures prior to their use in a repository. (See Section 2.2.1.5)

- Natural convection under geological repository conditions will be a very complex process. While the correlations presented in this report may be useful in repository analysis, additional data and new correlations may be developed to better reflect repository operating conditions. (See Section 2.2.2.3)

- In general, the use of formulas or analytical approaches to solve thermal and mechanical problems is restricted to relatively simple geometries and constant material properties. For detail design analysis, it is likely that more complex finite difference or finite element methods will be required for accurate assessments. (See Section 3.1.2)

- The mechanical loading on waste packages is expected to have a duration that is among the longest of all engineered structures. Since the temperature of the waste package will be elevated for several hundred years, it is important that the adequacy of waste package structures be judged on the basis of total strain. Both creep strains and instantaneous elastic deformation must be considered. Design stress analysis methods based only on instantaneous strains are probably not adequate for estimating waste package mechanical performance. (See Section 3.2.3.1)

- Elastic constants (for example, Young's modulus and Poisson's ratio) can vary depending on whether a material is loaded in tension or compression. Data presented in this report are for materials loaded in tension. (See Section 3.2.3.2)

- Elastic constants and failure parameters for bentonite will be highly dependent on the water content of the bentonite and the ratio of bentonite to host rock. Experimental data should be gathered for specific mixtures under projected repository conditions. (See Section 3.3)

- Creep of materials is generally characterized by the stress level of that material, the temperature of the material, and the time it has been exposed to those environmental conditions. Because of the long time periods of loading for waste package structures, it will be difficult to gather creep data representative of actual repository conditions. Although methods exist for extrapolating creep measurements over short time periods to longer time periods, these methods are not adequate if one must predict the onset of tertiary creep. (See Section 3.2.3.5)

- The creep data presented in this report are for specimens loaded in tension. Creep rates for compressive loading may differ from those reported here. (See Section 3.2.3.5)

2.0 THERMAL ANALYSIS

The two physical sciences used in the analysis of thermal system performance are heat transfer and thermodynamics. Heat transfer is the science that predicts the rate at which thermal energy exchange occurs within bodies and between bodies that may be either in contact or separated by atmospheres or unoccupied space. For regions of space occupied by material substances, heat transfer predicts the spatial temperature distribution associated with the transfer of thermal energy.

Thermodynamic principles apply to energy transformations including heat, work, and the physical properties of materials involved in the transformations. Thermodynamics deals with systems in equilibrium in which processes continue between state points.

2.1 Heat Transfer Phenomena

Engineered systems such as engines, boilers, and compressors frequently rely on the transfer of heat at high rates to prevent excessive temperature increases. High temperatures can cause materials to lose their strength resulting in component failure under imposed service loads.

There are three primary modes of heat transfer:

- Conduction heat transfer occurs when the kinetic energy of molecules (which is proportional to their absolute temperature) is transferred by collisions to portions of the material that are at a lower temperature.

- Convective heat transfer occurs between solid surfaces and a fluid when the solid boundaries are not in temperature equilibrium with the fluid. Mass transport plays a major role in the convective heat exchange process.

- Radiation heat transfer occurs between a body and any other body that can be seen directly from the first body (or indirectly via reflected rays), providing that the intervening medium is

transparent or partially transparent (transmissivity is greater than 0) and the two bodies are at different temperatures. A vacuum is the medium that allows the greatest net radiative heat transfer.

These heat transfer modes act individually or together depending on the physical conditions and the temperature differential that drives them. It is generally recognized that convective heat transfer involves conduction in the fluid region as well as convection. The two processes are treated together and referred to as convection.

2.1.1 Conduction

In 1822, J.B.J. Fourier observed that heat flux is proportional to the temperature difference and inversely proportional to the distance between planes at different temperatures:

$$\phi = \frac{q}{A} \sim \frac{\Delta T}{\Delta x} \tag{2.1}$$

where

ϕ = heat flux $[e/t\ell^2]$*

q = heat flow rate $[e/t]$

A = heat transfer area $[\ell^2]$

T = temperature $[\theta]$

x = direction of heat flow $[\ell]$

* When an equation is presented, the generalized dimensions of the various quantities are given in brackets. They are: ℓ = length or distance; t = time; f = force; m = mass; θ = degree of temperature change or temperature; e = energy (which is equal to the product of $f\ell$).

Fourier stated his law on a differential basis in terms of the quantity

k = thermal conductivity of a material $[e/t\ell\theta]$

such that

$$q = - kA \frac{dT}{dx} \tag{2.2}$$

This law divided the thermal evaluation process into an experimental part, determining the thermal conductivity, and an analytical part, using the thermal conductivity to relate the temperature gradient of the heat flow rate.

The conservation of energy principle can also be applied to a control volume, resulting in:

$$\begin{bmatrix}\text{net heat conducted}\\ \text{to the control}\\ \text{volume per unit}\\ \text{time}\end{bmatrix} + \begin{bmatrix}\text{heat generated in}\\ \text{the control}\\ \text{volume per unit}\\ \text{time}\end{bmatrix} = \begin{bmatrix}\text{increase of}\\ \text{thermal energy}\\ \text{stored in the}\\ \text{control volume}\end{bmatrix}$$

Combining Fourier's law for a cylindrical geometry and the conservation of energy principle yields the following equation:

$$\frac{1}{r}\frac{\partial}{\partial r}\left(kr\frac{\partial T}{\partial r}\right) + \frac{\partial}{\partial z}\left(k\frac{\partial T}{\partial z}\right) + \frac{1}{r^2}\frac{\partial}{\partial \theta}\left(k\frac{\partial T}{\partial \theta}\right) + \dot{q} = \rho c\frac{\partial T}{\partial t} \tag{2.3}$$

where:

T = temperature $[\theta]$

k = thermal conductivity $[e/t\ell\theta]$

r, θ, z = radial, circumferential and longitudinal coordinates for describing the cylindrical geometry $[\ell]$

$\dot{q}$ = volumetric heat generation rate $[e/t\ell^3]$

ρ = material mass density $[m/\ell^3]$

c = material's specific heat $[e/m\theta]$

t = time $[t]$

On the left side of Equation 2.3, the first three terms account for radial, axial, and circumferential conduction, respectively. For waste packages, the first term should predominate in most analysis applications. The second term will be retained in a small portion of the analyses, and the third term will virtually always be negligible. The q term is used to represent the production of thermal energy in the waste package due to decay heat. Generally, in waste package analysis, the heat generation is assumed to be uniform throughout the waste canister's contained volume.

The term on the right side of Equation 2.3 accounts for energy storage, which is associated with an increase in the temperature of the material. This is the sensible heat effect. Latent heat effects associated with additional stored energy if the material were to change to a more volatile phase are not included in Equation 2.3. For most continua, conduction occurs without phase change. It is easier to include latent heat effects associated with phase change in the finite element or finite difference representations of the conduction differential equations than it is to include them on a continuous function basis. The allocation of stored energy between sensible and latent heat in a region generally requires special treatment. For steady-state thermal processes, the right side of Equation 2.3 is zero. For the waste package, the heat will typically be generated in a region represented by a solid, conducting cylinder and transferred radially by conduction to the next annulus.

2.1.1.1 Radial Steady-State Conduction with Heat Generation and Constant Thermal Conductivity in a Solid Cylinder

When circumferential and axial conduction is neglected, Equation 2.3 becomes

$$\frac{k}{r}\frac{d}{dr}\left(r\frac{dT}{dr}\right) + \dot{q} = 0 \tag{2.4}$$

for steady-state, one-dimensional conduction with heat generation in a cylinder with constant thermal conductivity.

Two boundary conditions are:

$$\text{at } r = 0 \quad \frac{dT}{dr} = 0$$

$$\text{at } r = 0 \quad T = T_{max} \tag{2.5}$$

The solution is

$$T = T_{max}\left[1 - \frac{\dot{q}r_o^2}{4k\,T_{max}}\left(\frac{r}{r_o}\right)^2\right] \tag{2.6}$$

where r_o is the outside radius of the solid cylinder. If the outside temperature, T_o (at $r = r_o$), is known from a previous calculation, the centerline temperature T_{max} at $r = 0$ can be determined from

$$T_{max} = T_o + \frac{\dot{q}r_o^2}{4k} \tag{2.7}$$

2.1.1.2 Radial Steady-State Conduction without Heat Generation and with Constant Thermal Conductivity in a Hollow Cylinder

Equation 2.3 reduces to

$$\frac{1}{r}\frac{d}{dr}\left(r\frac{dT}{dr}\right) = 0 \tag{2.8}$$

for radial steady-state conduction without heat generation and with constant thermal conductivity in a region with inside radius r_i and outside radius r_o. Two boundary conditions are:

$$r = r_o \qquad T = T_o \ (T_o \text{ known})$$

$$r = r_i \qquad \frac{dT}{dr} = \frac{-q}{2\pi r_i \ell k} \ (q,\ r_i,\ \ell,\ k \text{ known}) \tag{2.9}$$

The second boundary condition is Fourier's law, and q is the heat flow rate [e/t] through the annular region. The heat generation within the annulus is assumed to be zero.

The solution is

$$T = T_o + \frac{q}{2\pi\ell k}\ \ell n\left(\frac{r_o}{r}\right) \tag{2.10}$$

For waste package analysis, the temperature at the inside surface is usually of interest and is given by

$$T_i = T_o + \frac{q}{2\pi\ell k}\ \ell n\left(\frac{r_o}{r_i}\right) \tag{2.11}$$

The waste package performance assessment programs WAPPA and BARIER assume that the heat flow q (from the waste form) and the outside temperature T_0 are known. They progressively use Equation 2.11 across each barrier until they reach the waste form where they use Equation 2.7 to calculate the maximum waste form temperature at the centerline of the waste package.

2.1.1.3 Two-Dimensional Conduction

The following steps have been used to obtain analytical solutions of two-dimensional transient conduction problems:

(a) Taking the Laplace transform of the time variable

(b) Solving the second-order elliptic differential equation in space by assuming a product solution of two functions in the independent variables (r, z for the radial and axial conduction typical for waste packages)

(c) Taking the inverse Laplace transform of the spatial solution to reenter the time domain

For steady-state, two-dimensional conduction, steps (a) and (c) can be omitted. The difficulty encountered in obtaining analytical solutions increases as heat generation is included and the boundary conditions become more complicated.

It is not practical to attempt to obtain analytical solutions for steady-state or transient two-dimensional conduction in a series of regions (engineered barriers) due to the difficulty in matching temperature solutions at interfaces. It is more convenient to use discrete numerical representations (finite element and finite difference-based algebraic equations) that can handle all of the annuli simultaneously and solve for the temperature distribution in the waste package.

2.1.2 Convection

Convective heat transfer occurs in fluid-occupied regions when a solid boundary and fluid are at different temperatures. This mode of heat transfer is driven by the mass transport of the flowing fluid. The solid boundary and the flowing fluid act as two bodies exchanging heat from the one at higher temperature to the one at lower temperature.

Heat transfer between a solid and a fluid involves a temperature gradient in the fluid near the wall. The region over which this gradient extends is known as the thermal boundary layer or convective film. Outside this boundary layer, the fluid temperature remains at the undisturbed bulk fluid temperature. The temperature gradient in the boundary layer is accompanied by a density gradient. For a quiescent fluid region, the density gradient is acted on by gravity, and the fluid tends to flow, causing mass transfer and heat exchange from a hot wall to the fluid or from the fluid to a cold wall. If the fluid flow past the hot or cold surface is caused only by the density gradient induced by the temperature gradient, the heat transfer is known as natural convection or free convection. If the flow past the hot or cold surface is caused by other means, such as momentum imparted to the fluid by a fan or pump, the heat transfer is known as forced convection.

The basic equation for convective heat transfer was stated by Newton in 1701:

$$q = hA(T_h - T_c) \tag{2.12}$$

where

q = heat flow rate $[e/t]$

h = convective heat transfer coefficient $[e/t\ell^2\theta]$

A = area of heat transfer surface $[\ell^2]$

T_h = representative temperature of hot body [θ]

T_c = representative temperature of cold body (bulk fluid temperature when T_h is wall temperature) [θ]

Newton's equation postulates that, for convective heat transfer, the heat flow rate can be represented by the product of a single coefficient and the temperature difference. Thus, Newton's equation defines a quantity, the convective heat transfer coefficient, h, that must be quantified for particular convection conditions. The heat transfer coefficient depends on the solid surface configuration, fluid type, and flow regime and is often determined empirically. The few analytical solutions that exist suggest functional forms of empirical correlations.

The flow velocity at the solid boundary is zero, and conduction is the primary means of transporting heat through a very thin sublayer region of the boundary layer adjacent to the wall. Except for liquid metals, the thermal conductivity of fluids is relatively low compared to the conductivity of materials that typically are used in solid surfaces of heat transfer equipment. Away from the solid boundary but through most of the boundary layer, convective heat transfer depends primarily on the mass transport mixing currents. In order to transfer heat to or from the boundary layer at a fixed rate, a lower temperature difference (T_h - T_c) is needed if the flow velocity is high. A high velocity promotes turbulence and greater mass transfer between the hot and cold regions of the boundary layer. A low velocity, on the other hand, is compatible with laminar flow and very little transverse mixing.

2.1.2.1 Forced Convection

Forced convection heat transfer theory is based on analytical principles for heat transfer and fluid mechanics. These principles involve the use of control volumes in the fluid region. The principles of mass, momentum, and energy conservation are applied to these control volumes. For laminar

boundary layer flow in the x direction along a flat plate, as shown in Figure 2.1, the mass conservation equation for incompressible, two-dimensional, steady flow is

$$\frac{\partial \bar{u}}{\partial x} + \frac{\partial \bar{v}}{\partial y} = 0 \tag{2.13}$$

where the two terms represent the fluid flow in the control volume in the x and y directions and where

$\bar{u}$ = local fluid velocity in the x direction [ℓ/t]

$\bar{v}$ = local fluid velocity in the y direction [ℓ/t]

The momentum conservation principle applied to steady-state laminar flow yields

$$\bar{u}\frac{\partial \bar{u}}{\partial x} + \bar{v}\frac{\partial \bar{u}}{\partial y} = \nu \frac{\partial^2 \bar{u}}{\partial y^2} \tag{2.14}$$

where

$\nu = \mu/\rho$ = fluid kinematic viscosity [ℓ^2/t]

μ = fluid dynamic viscosity [m/ℓt]

ρ = fluid mass density [m/ℓ^3]

x,y = coordinates as defined in Figure 2.1 [ℓ]

and where the left side represents the net efflux of momentum from the control volume due to exchanges of mass with the surroundings at different velocities, and the right side represents the net viscous shear force exerted on the fluid in the control volume.

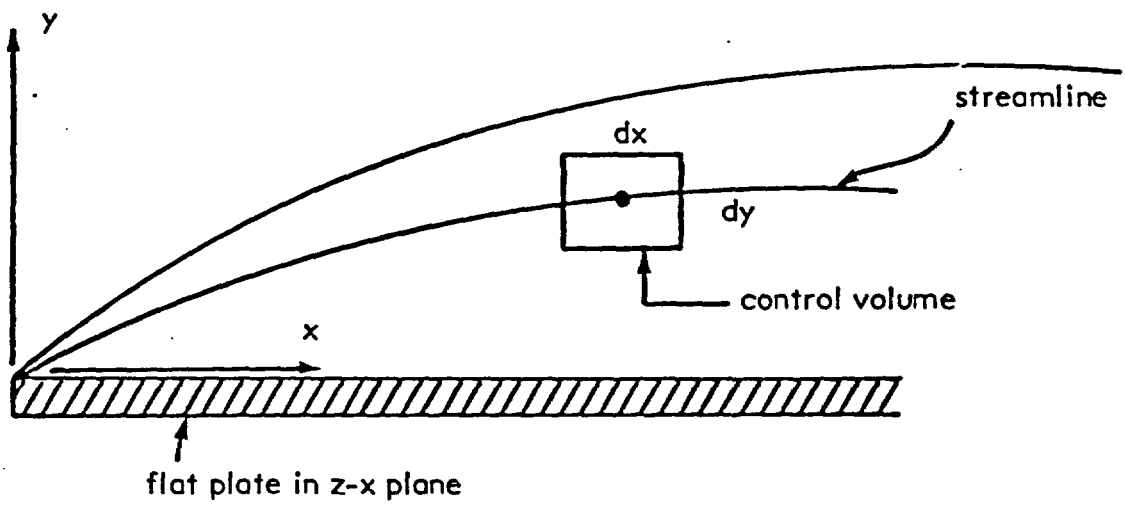

Figure 2.1

Conrol Volume in the Laminar Boundary Layer on a Flat Plate

Applying the conservation of energy principle to steady-state laminar flow yields

$$\bar{u}\,\frac{\partial T}{\partial x} + \bar{v}\,\frac{\partial T}{\partial y} = \alpha\,\frac{\partial^2 T}{\partial y^2} \tag{2.15}$$

where

T = fluid temperature at a point $[\theta]$

$\alpha = k/\rho c$ = fluid thermal diffusivity $[\ell^2/t]$

k = fluid thermal conductivity $[e/t\ell\theta]$

c = fluid specific heat $[e/m\theta]$

ρ = fluid mass density $[m/\ell^3]$

The terms on the left side of Equation 2.15 represent the net rate at which energy leaves the control volume due to fluid mass crossing its boundaries at different temperatures and the right side represents net thermal energy conducted into the control volume.

The momentum and energy differential equations are similar in that both are parabolic, and for $\nu = \alpha$, the temperature and velocity distributions are identical. From this observation, it follows that the transfer of momentum is analogous to the transfer of heat within the laminar boundary layer when the Prandtl number ($Pr = \nu/\alpha$) is unity. Moreover, for a plate with a constant surface temperature T_s, the momentum and energy equations have physically and mathematically similar boundary conditions:

	Boundary Conditions	
	Momentum Equation	Energy Equation
$y = 0$	$\bar{v} = 0$	$\bar{v} = 0$
$y = 0$	$\bar{u} = 0$	$T - T_s = 0$

$$\lim_{y \to \infty} \frac{\partial}{\partial y}\left(\frac{\bar{u}}{u_\infty}\right) = 0, \qquad \frac{\partial}{\partial y}\left(\frac{T-T_s}{T_\infty - T_s}\right) = 0 \tag{2.16}$$

where ∞ reflects the bulk fluid condition outside the boundary layer. Pohlhausen in 1921 published an analytical solution to the temperature distribution in the laminar boundary layer by assuming the same functional form chosen by Blasius in 1908 for the velocities in his momentum equation solution. A derivation of these solutions is given in Reference HO-81.

The solution involves the Nusselt and Reynolds numbers defined on a local basis as

$$Nu_x = \frac{h_x x}{k} \tag{2.17}$$

$$Re_x = \frac{\rho \bar{u} x}{\mu} \tag{2.18}$$

$$Pr_x = \frac{\nu}{\alpha} \tag{2.19}$$

where

Nu_x = local Nusselt number [ ]

Re_x = local Reynolds number [ ]

Pr_x = local Prandtl number [ ]

h_x = local heat transfer coefficient $[e/t\ell^2\theta]$

x = distance along plate in direction of flow to the local region of interest $[\ell]$

k = fluid thermal conductivity $[e/t\ell\theta]$

ρ = fluid mass density $[m/\ell^3]$

$\bar{u}$ = fluid velocity in x direction parallel to plate $[\ell/t]$

μ = dynamic viscosity of fluid $[m/\ell t]$

ν = kinematic viscosity of fluid ($\nu = \mu/\rho$) $[\ell^2/t]$

α = thermal diffusivity of fluid $[\ell^2/t]$

The solution to the laminar thermal boundary layer equations is

$$Nu_x = 0.332\ Re_x^{1/2}\ Pr^{1/3}. \tag{2.20}$$

Typically, it is more convenient to know the average Nusselt number over a length of plate L

$$\overline{Nu} = \frac{\bar{h}L}{k} \tag{2.21}$$

where

L = length of plate in flow direction of interest for convection $[\ell]$

h = average heat transfer coefficient over length of plate L $[e/t\ell^2\theta]$

so the associated average heat transfer coefficient can be evaluated. The average Nusselt number can be evaluated using

$$\overline{Nu} = \frac{1}{k} \int_0^L h_x dx \tag{2.22}$$

where h_x, obtained from Equations 2.17, 2.18, and 2.20, is

$$h_x = 0.332 \frac{k}{x} \left(\frac{\rho u}{\mu}\right)^{1/2} x^{1/2} \; Pr^{1/3} \tag{2.23}$$

The solution to Equation 2.22 is then given by

$$\overline{Nu} = 0.664 \; Re_L^{1/2} \; Pr^{1/3} \tag{2.24}$$

The associated average heat transfer coefficient for the length L of the plate is

$$\bar{h} = 0.664(k/L)Re_L^{1/2} \; Pr^{1/3} \tag{2.25}$$

when the flow in the boundary layer is laminar.

Analytical solutions have been determined for the laminar boundary layer and for simple geometries. For turbulent boundary layer flow, experimentalists have assumed that similar relationships hold between the nondimensional quantities (Nu, Re, and Pr) such that

$$Nu = C \;\; Re^m \;\; Pr^n \tag{2.26}$$

The values of C, m, and n can be evaluated for sets of laboratory data to develop empirical correlations. Alternatively, the empirical process has also suggested modifications in the functional forms that have been used in correlating the Nusselt number and heat transfer coefficient.

2.1.2.2 Free or Natural Convection

Consider the pane of glass shown in Figure 2.2, with an outside surface temperature of 16°C and an outside air bulk temperature of -18°C. The heated air moving upward next to the outside surface of the glass forms a region of flow that is known as a boundary layer. At its inner edge, the velocity is zero, and the air temperature is equal to the temperature of the glass pane's outer surface. Within the boundary layer, heat transfer occurs primarily by conduction, but the overall transfer rate process is treated as convection. At the outer edge of the boundary layer, the temperature of the air is equal to the ambient air temperature (T_∞ or the bulk fluid temperature), and the velocity equals zero. This is true because the air at rest at the edge of the boundary layer is not in a forced flow condition and therefore cannot sustain any shear force. If the temperature gradient were not zero at that point, heat would be conducted out of the boundary layer causing an extended density gradient and more upward flow.

The consequence of these temperature and velocity profiles is that no heat flows from the glass through the boundary layer to the air at ambient temperature. All of the heat goes into the moving boundary layer which has temperature and velocity profiles as depicted in Figure 2.3 and a mean temperature intermediate to that of the glass pane and the ambient air. Note that the temperature of the boundary layer, which is one of the heat exchange media, is not used in Newton's equation. Rather, the ambient air temperature outside the boundary layer is used. The reason for this choice is simply that the ambient fluid has a unique temperature value while the boundary layer has an unquantified temperature distribution.

The same assumptions apply in the application of the mass and energy conservation principles to natural convection as for forced convection, yielding the same mathematical relationships. However, the momentum conservation principle includes a net force resulting from the pressure gradient and a gravitational force term which must be retained. For

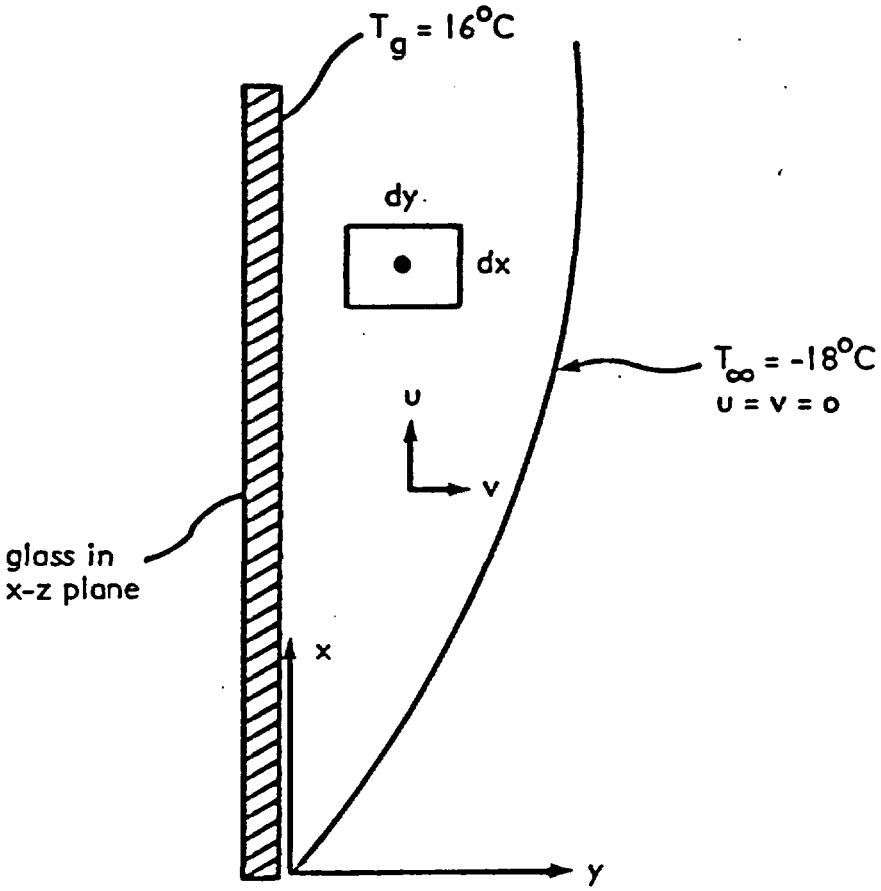

Figure 2.2

Natural Convection Boundary Layer along Outside Surface of a Warm Pane of Glass in Cold Ambient Air

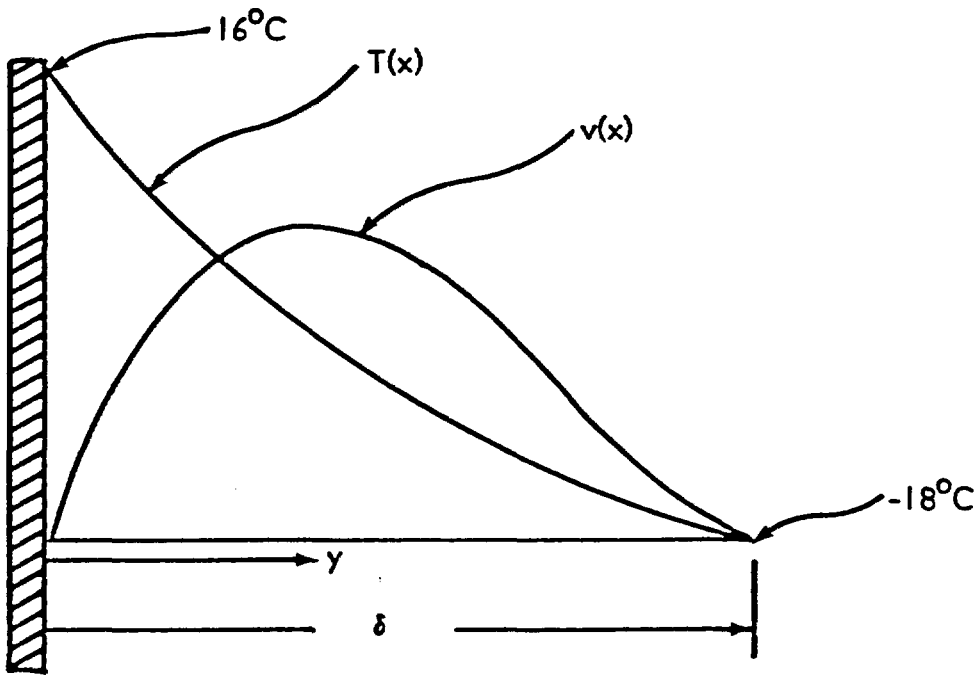

Figure 2.3

Velocity and Temperature Profiles
in Natural Convection

forced convection, these forces were neglected since they are much smaller than the viscous force term. Thus, the equations resulting from the mass, momentum, and energy conservation principles are:

$$\frac{\partial \bar{u}}{\partial x} + \frac{\partial \bar{v}}{\partial y} = 0 \tag{2.27}$$

$$\bar{u}\,\frac{\partial \bar{u}}{\partial x} + \bar{v}\,\frac{\partial \bar{u}}{\partial y} = [g\beta(T-T_\infty)] + \nu\,\frac{\partial^2 \bar{u}}{\partial y^2} \tag{2.28}$$

$$\bar{u}\,\frac{\partial T}{\partial x} + \bar{v}\,\frac{\partial T}{\partial y} = \alpha\,\frac{\partial^2 T}{\partial y^2} \tag{2.29}$$

for the conditions

	Fluid momentum	Thermal energy
$y = 0$	$\bar{u} = \bar{v} = 0$	$T = T_w$
$y = \delta$	$\bar{u} = \bar{v} = 0$	$T = T_\infty$
$y = \delta$	$\frac{\partial \bar{u}}{\partial y} = 0$	$\frac{\partial T}{\partial y} = 0$

(2.30)

where δ is the boundary layer thickness.

Solutions for laminar flow are

$$\frac{T-T_\infty}{T_w-T_\infty} = \left(1 - \frac{y}{\delta}\right)^2 \tag{2.31}$$

$$\frac{\bar{u}}{\bar{u}_x} = \frac{\beta\delta^2 g(T_w - T_\infty)}{4\bar{u}_x \nu} \frac{y}{\delta}\left(1 - \frac{y}{\delta}\right)^2 \tag{2.32}$$

where $\bar{u}_x$ is a representative axial velocity which varies with x, and the heat transfer expressed in terms of Nusselt number is

$$Nu_x = 0.508\, Gr_x^{1/4} \frac{Pr^{1/2}}{(0.952 + Pr)^{1/4}} \tag{2.33}$$

where Gr and β are the Grashof number and the volumetric coefficient of thermal expansion

$$Gr_x = g\beta x^3 \frac{(T_w - T_\infty)}{\nu^2} \tag{2.34}$$

$$\beta = \frac{1}{v}\left(\frac{\partial v}{\partial T}\right)_p \tag{2.35}$$

where

Gr_x = Grashof number [ ]

g = local acceleration of gravity [ℓ/t^2]

β = volumetric coefficient of thermal expansion [θ^{-1}]

x = distance along plate in direction of flow to point of interest [ℓ]

T = temperature [θ]

ν = fluid kinematic viscosity [ℓ^2/t]

v = fluid specific volume [ℓ^3/m]

By integrating h_x over the interval from 0 to L and dividing by L, the average heat transfer coefficient, $\bar{h}$, over that region is determined to be

$$\bar{h} = \frac{4}{3} h_{x=L} \tag{2.36}$$

From Equations 2.33 and 2.36, the average Nusselt number is

$$\overline{Nu}_L = 0.677\ Gr_L^{1/4} \frac{Pr^{1/2}}{(0.952 + Pr)^{1/4}} \tag{2.37}$$

and from Equations 2.21 and 2.37, the average heat transfer coefficient can be expressed as

$$\bar{h}_L = 0.677\ \frac{k}{L}\ Gr_L^{1/4} \frac{Pr^{1/2}}{(0.952 + Pr)^{1/4}} \tag{2.38}$$

The analytical solutions given above suggest the functional form of experimental correlations for other geometric configurations.

2.1.3 Radiation

2.1.3.1 Ideal Radiation Emission

Electromagnetic energy is radiated from the surfaces of all bodies as a result of their temperature. Thermal radiation has an energy corresponding to electromagnetic wavelengths over the range of about 10^{-4} to 10^{-7} meters. Statistical mechanics theory developed by Planck in 1900

yielded an expression for the energy density of radiation per unit volume and per unit wavelength as a continuous function of the wavelength

$$U_\lambda = \frac{8\pi hc\lambda^{-5}}{\exp\left(\frac{hc}{\lambda kT}\right) - 1} \tag{2.39}$$

where

T = temperature of body (^oK) [θ]

h = Planck's constant = 6.625×10^{-34}(J·sec) [et]

k = Boltzmann's constant = 1.381×10^{-23}(J/molecule -^oK) [e/molecule θ]

c = velocity of light = 3.0×10^{10} (cm/sec) [ℓ/t]

λ = radiant energy wavelength (cm) [ℓ]

U_λ = radiant energy density per unit volume per unit wavelength (J/cm^4) [e/ℓ^4]

In 1900, Boltzmann integrated this function over the spectrum from 0 to ∞ (all possible wavelengths) and determined the total radiant energy emitted by a body that will not transmit or reflect any incident radiation (a black body) to be

$$E_b = \sigma T^4 \tag{2.40}$$

where

E_b = total radiant thermal energy flux [e/tℓ^2]

σ = Stefan-Boltzmann constant [e/t$\ell^2\theta^4$]

T = surface absolute temperature [θ]

Earlier, in 1879, Stefan had deduced experimentally that this was the functional form of the total radiant energy emitted by a black body. Statistical mechanics and laboratory observations were in agreement in yielding a simple expression for the radiant thermal energy flux involving a single constant.

Once this functional form for the total energy leaving a body has been established, other engineering questions must be answered before net radiation heat transfer between two real bodies can be quantified. They include:

(1) How much of the radiation emitted by body 1 is incident on body 2 and vice versa?

(2) Of the energy incident on real surfaces (non black bodies), how much is absorbed, reflected, and transmitted?

(3) If there is a partially absorbing medium, such as a gas or glass, between the principal hot and cold surfaces, what effect does it have on the net radiative heat transfer?

Radiation properties of the materials and the geometry of the radiating surfaces must be described and used along with the total radiant energy flux expression for a black body to quantify the net radiant energy transfer rate between real bodies.

A grey surface is one that emits only a fraction of the radiation emitted by a black body. For the grey surface,

$$E = \varepsilon\sigma T^4 \tag{2.41}$$

where $\varepsilon < 1.0$, and for a black body

$$E_b = \sigma T^4 \tag{2.42}$$

giving

$$\varepsilon = \frac{E}{E_b} \tag{2.43}$$

The quantity ε is the emissivity, a material surface property. For a black body, $\varepsilon = 1$ and for a grey body, $0 < \varepsilon < 1$. For a grey body, ε can be treated as a function of temperature. In some cases, it is acceptable to consider ε as a constant.

If a black body, p, exchanges heat only by radiation and only with another body at the same temperature,

$$\begin{bmatrix}\text{Rate incident radiant energy} \\ \text{is being absorbed by body p}\end{bmatrix} = \begin{bmatrix}\text{Rate of energy loss by} \\ \text{radiation from body p}\end{bmatrix}$$

$$\phi A = E_b A \tag{2.44}$$

If the black body, p, is replaced with a grey body, q, at temperature equilibrium, then

$$\phi A \alpha' = EA \tag{2.45}$$

where

ϕ = the radiation energy flux incident on either body $[e/t\ell^2]$

α' = the absorbtivity of body q

Equations 2.44 and 2.45 yield

$$\alpha' = \frac{E}{E_b} \tag{2.46}$$

Equations 2.43 and 2.46 indicate

$$\varepsilon = \alpha' \tag{2.47}$$

for all temperatures.

2.1.3.2 Material Radiation Properties

Of the total radiation incident on a body, a fraction can be absorbed; another fraction reflected; and the remainder transmitted through the body, indicated in Figure 2.4, such that

$$\alpha' + \rho' + \tau' = 1 \tag{2.48}$$

where

α' = absorbtivity [ ]

ρ' = reflectivity [ ]

τ' = transmissivity [ ]

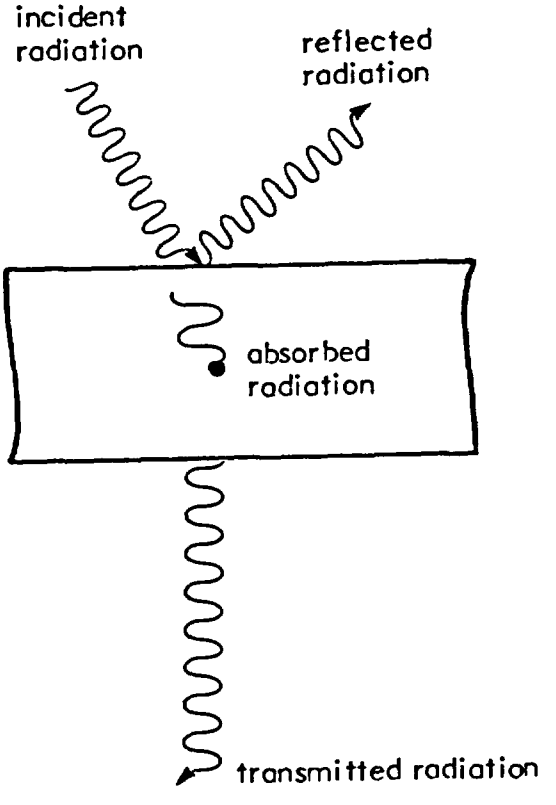

Figure 2.4

Incident Thermal Radiation Being Absorbed, Reflected, and Transmitted

Most solid materials do not transmit any thermal radiation so

$$\alpha' + \rho' = 1$$

in those cases. For a black body $\rho' = \tau' = 0$.

Energy that is reflected by or transmitted through a body maintains a character (wavelength) associated with the temperature of the body from which it was radiated. After energy has been absorbed by a body, future radiation has a radiant energy flux which is related to the temperature of that body.

2.1.3.3 Geometric Aspects of Radiative Heat Transfer

To quantify net radiative heat exchange, a "view factor" must be determined. The view factor, F_{mn}, is defined as the fraction of radiant energy leaving the surface m that is incident on surface n. The view factor is a nondimensional quantity ($0 \leq F_{mn} \leq 1$).

Consider two black bodies that exchange heat with one another. The net heat transfer from body 1 to body 2 is

$$Q_{12} = E_{b1} A_1 F_{12} - E_{b2} A_2 F_{21} \tag{2.49}$$

When they are in temperature equilibrium with each other ($T_1 = T_2$), $Q_{12} = 0$, and $E_{b1} = \sigma T_1^4 = E_{b2} = \sigma T_2^4$ so that

$$A_1 F_{12} = A_2 F_{21} \tag{2.50}$$

which is a reciprocity relationship. It applies in general to any two surfaces (grey body or black body).

For the two black bodies shown in Figure 2.5, the net energy exchange can be stated as

$$q_{\substack{net \\ 1-2}} = (E_{b1}-E_{b2}) \frac{1}{\pi} \int_{A_2} \int_{A_1} \frac{1}{r^2} \cos \phi_2 \cos \phi_1 \, dA_1 \, dA_2 \tag{2.51}$$

where hemispherical uniformity of radiation emission intensity is assumed, and

$$A_1 F_{12} = A_2 F_{21} = \frac{1}{\pi} \int_{A_2} \int_{A_1} \frac{1}{r^2} \cos \phi_2 \cos \phi_1 \, dA_1 \, dA_2 \tag{2.52}$$

This result is convenient but not precisely accurate because the actual intensity of the radiation emitted is generally non-uniformly rather than uniformly distributed over a hemispherical surface as assumed in the above equation.

2.1.3.4 Grey Body Radiation Heat Transfer

For grey bodies ($0 < \varepsilon = \alpha' < 1$), the radiation heat exchange is more complex because part of the incident energy is always reflected from the surface it reaches. The assumption of spatially uniform radiation intensity from diffuse surfaces used previously for the black body heat transfer description will be retained. To account for the net interaction between two bodies, it is convenient to define:

J = radiation leaving a surface (radiosity) $[e/t\ell^2]$

G = incident radiation on a surface (irradiation) $[e/t\ell^2]$

Assuming typical grey bodies that are opaque ($\tau' = 0$),

$$J = \varepsilon E_b + \rho' G \tag{2.53}$$

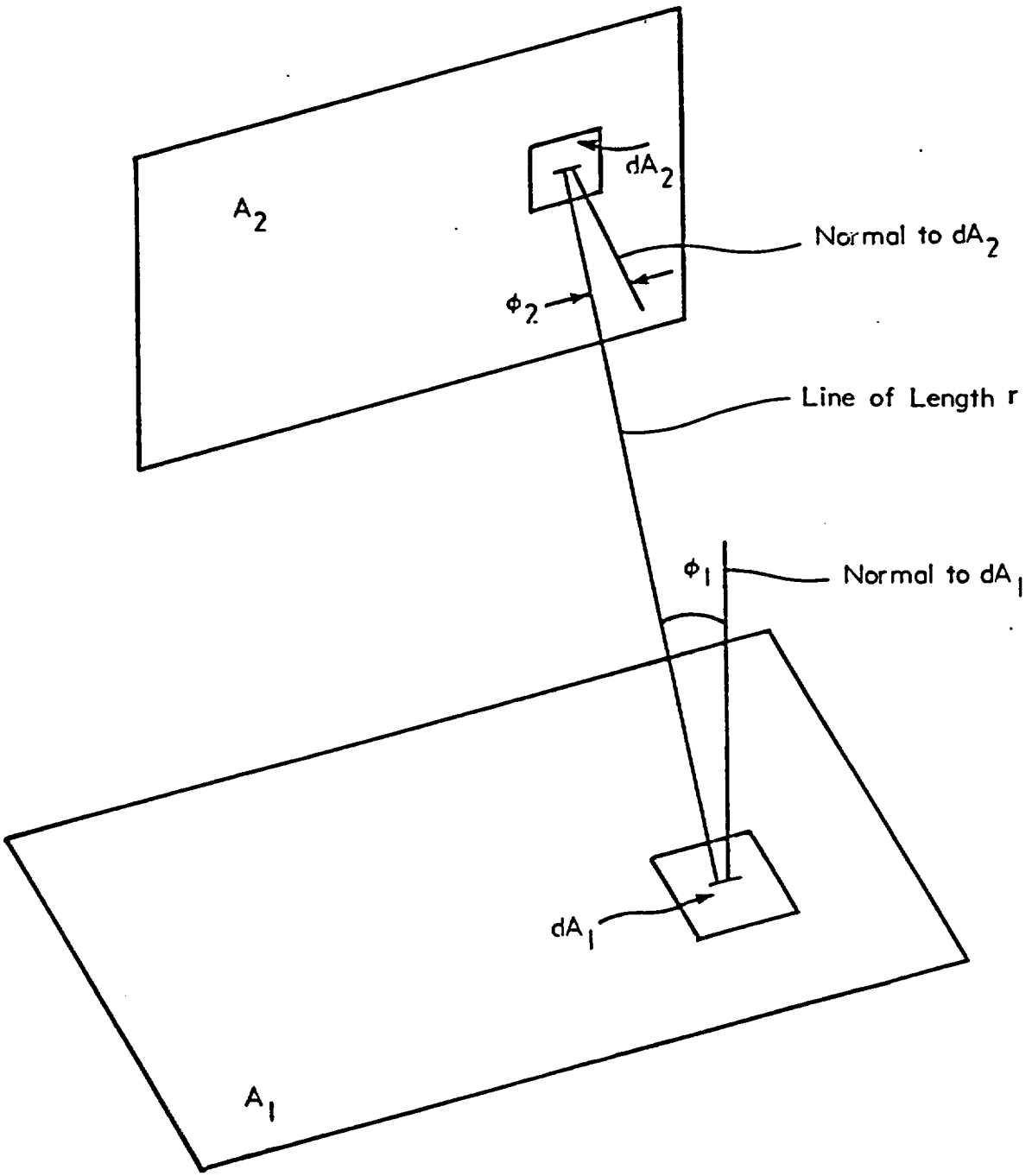

Figure 2.5

Angles, Area Elements, and Separation Distance Terms
Used in Evaluating Radiation View Vectors

where the first term on the right side of Equation 2.53 accounts for energy leaving the grey body, and the second term accounts for surface reflection of incident radiation. Since $\alpha' + \rho' = 1$, this can be written as

$$J = \varepsilon E_b + (1 - \alpha')G \tag{2.54}$$

The net energy leaving the surface is

$$q = A(J-G) = A\left[\varepsilon E_b + (1-\alpha')G - G\right]$$
$$q = A\left[\varepsilon E_b - \alpha' G\right] \tag{2.55}$$

Using Equation 2.54 in conjunction with Equations 2.55 and 2.47,

$$q = \frac{E_b - J}{(1-\varepsilon)/\varepsilon A} \tag{2.56}$$

This is an important relationship as it can be used in the same way as Ohm's law to relate heat flow to potential difference and resistance values. In this relationship, q, which has units of [e/t], is analogous to electrical current; $E_b - J$, which has units of $[e/t\ell^2]$, is analogous to voltage difference; and $(1-\varepsilon)/\varepsilon A$, which has units of $[1/\ell^2]$, is analogous to electrical resistance.

Thus, for two grey bodies that see each other, a radiative heat transfer network is

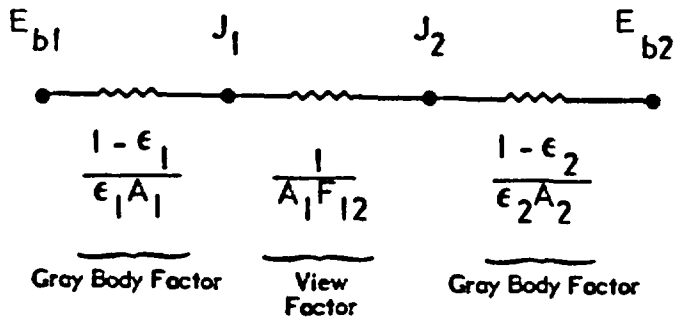

Since $E_{b1} - E_{b2} = \sigma (T_1^4 - T_2^4)$ and letting

$$R_g = \frac{1-\varepsilon_1}{\varepsilon_1 A_1} + \frac{1}{A_1 F_{12}} + \frac{1-\varepsilon_2}{\varepsilon_2 A_2} \tag{2.57}$$

the heat exchange between the two grey bodies is given by

$$q_{\substack{net \\ 1-2}} = \frac{\sigma(T_1^4 - T_2^4)}{R_g} \tag{2.58}$$

For two long concentric cylinders, as shown in the sketch below, $F_{12} = 1$,

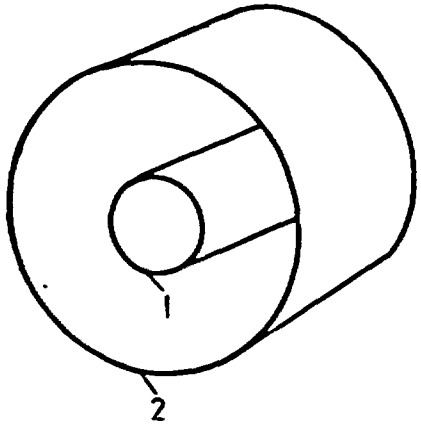

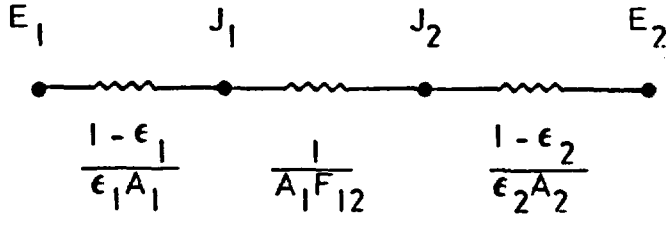

Two Concentric Cylinders Exchanging Heat by Radiation

and Equation 2.58 can be rewritten as

$$q = \frac{\sigma A_1 (T_1^4 - T_2^4)}{\frac{1}{\varepsilon_1} + \frac{A_1}{A_2}\left(\frac{1-\varepsilon_2}{\varepsilon_2}\right)} \tag{2.59}$$

Many cases can be treated in a similar way by developing the appropriate thermal circuit elements for the geometric configuration.

It is sometimes necessary to evaluate heat exchange between two surfaces separated by an absorbing and transmitting medium such as a gas (see sketch below).

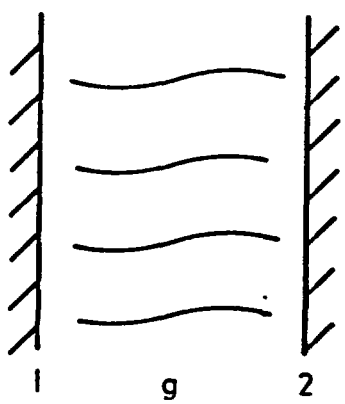

Assuming that the gas does not reflect ($\rho' = 0$), then $\tau' = 1 - \alpha'$.

The direct net exchange between 1 and 2 is

$$q_{1-2} = \frac{J_1 - J_2}{1/[A_1 F_{12}(1-\varepsilon_g)]} \tag{2.60}$$

and from 1 to the gas is

$$q_{1-g} = \frac{J_1 - E_{bg}}{1/(A_1 F_{1g} \varepsilon_g)} \tag{2.61}$$

The radiation network becomes

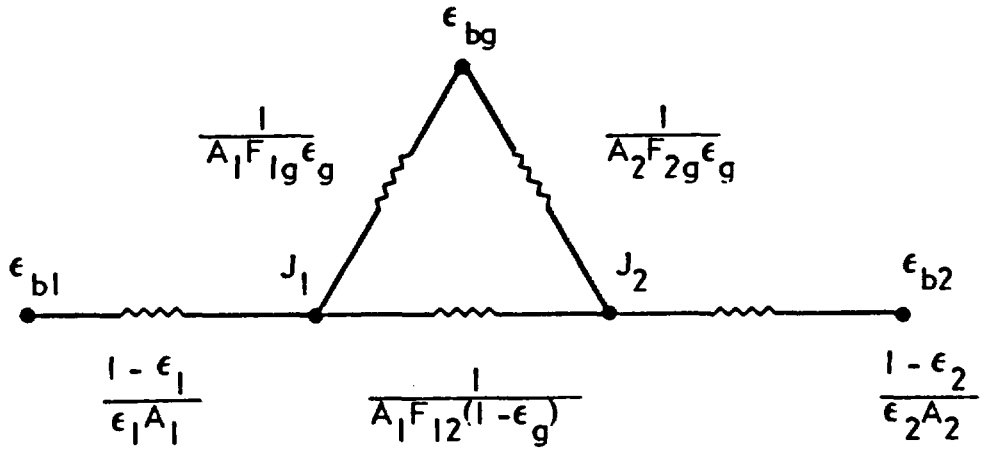

It is usually easier to evaluate the overall resistance R between 1 and 2 after evaluating the individual resistances numerically rather than functionally. For an equivalent network

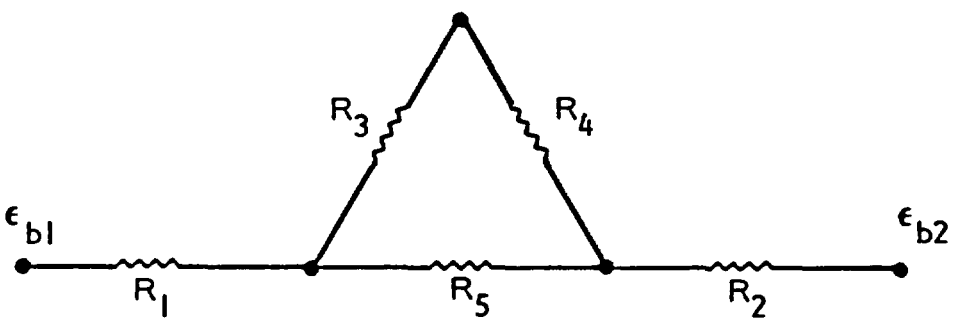

with R_1, R_2, R_3, R_4, and R_5 evaluated numerically, the net heat radiated from surface 1 to 2 is

$$q_{1-2} = \frac{\sigma(T_1^4 - T_2^4)}{R_1 + R_2 + \frac{R_5R_6}{R_5+R_6}} \tag{2.62}$$

where $R_6 = R_3 + R_4$.

2.1.4 Finite Increment Mathematical Models

The finite element and finite difference methods are used to analyze complex heat transfer processes. These methods use a set of algebraic equations to represent the energy conservation principle at discrete intervals of time and space in place of continuous differential equations. The finite increment equations are written in terms of the unknown temperature values at specified node locations. These equations are coupled because each node temperature depends on that of its neighboring nodes with which it directly interacts by exchanging heat. With the finite increment method, a number of regions that have different material property values can be represented, because properties such as thermal conductivity, density, and specific heat are treated numerically. This is a great advantage over continuous differential equations which apply only in regions in which these parameters are continuous. For multiple regions, the analytical effort required to solve the differential equations when two-dimensional temperature variations are involved is so great that this method becomes infeasible. Also, continuous differential equations are much more difficult to solve if the properties are temperature-dependent. With the finite increment methods, material property values can be reevaluated after each solution based on the most recent local temperature values.

The general form of the equations used in finite increment methods to describe dynamic thermal equilibrium is

$$[\bar{C}] \{\dot{T}\} + [\bar{K}] \{\dot{T}\} = \{Q\} \tag{2.63}$$

where $[\bar{C}]$ and $[\bar{K}]$ are the diagonal capacitance and generalized conductance matrices whose elements are determined from

$$\bar{C}_{ij} = \delta_{ij} \rho_i c_i V_i \tag{2.64}$$

$$\bar{K}_{ij} = \frac{k_{ij} A_{ij}}{\Delta x_{ij}} \tag{2.65}$$

where

δ_{ij} = Kronecker delta = 1 for i = j and 0 for i ≠ j

ρ_i = mass density of material associated with node i [m/ℓ^3]

c_i = specific heat of material associated with node i [$e/m\theta$]

V_i = volume of material associated with node i [ℓ^3]

$\bar{C}_{ij}$ = temperature specific energy capacity for node i from diagonal matrix [e/θ]

k_{ij} = thermal conductivity for conduction temperature interactions between nodes i and j [$e/t\ell\theta$]

Δx_{ij} = distance between nodes i and j [ℓ]

A_{ij} = heat transfer area for thermal interaction between nodes i and j [ℓ^2]

$\bar{K}_{ij}$ = thermal conductance between nodes i and j [$e/t\theta$]

Q_i = heat generation in the region associated with node i from heat generation vector $\{Q\}$ [e/t]

T_i = temperature at node i from vector $\{T\}$ [θ]

and where $\{T\}$, $\{\dot{T}\}$, and $\{Q\}$ are the temperature vector for the assemblage of nodes, the time derivative of the temperature vector and the vector of heat generation rates associated with the various nodes, respectively.

This equilibrium relationship is formulated in many finite increment programs by defining $\bar{K}_{ij}$ differently in regions where convection is occurring. This relationship may be expressed as

$$\bar{K}_{ij} = h_{ij} A_{ij} \tag{2.66}$$

where

h_{ij} = convective heat transfer coefficient applicable to exchange between nodes i and j $[e/t\ell^2\theta]$

Similarly, radiation is frequently represented by an equation of a form identical to Newton's equation

$$q_r = h_r A\ (T_h - T_c) \tag{2.67}$$

where

q_r = radiation heat transfer rate $[e/t]$

h_r = equivalent radiative heat transfer coefficient for radiation $[e/t\ell^2]$

T_h = temperature of hot body surface $[\theta]$

T_c = temperature of cold body $[\theta]$

The heat transfer coefficient for radiation is defined as

$$h_r = \sigma F_{12}\ (T_h^2 + T_c^2)_p\ (T_h + T_c)_p \tag{2.68}$$

where the subscript p indicates h_r is evaluated based on the values of T_h and T_c in the previous iterations. When Equation 2.68 is multiplied by the heat transfer area and the current temperature difference $(T_h - T_c)$, the heat flow rate is determined. The thermal conductance representing radiation heat exchange for finite increment models is determined from

$$\bar{K}_{ij} = (h_r)_{ij}\ A_{ij} \tag{2.69}$$

where

$(h_r)_{ij}$ = radiative heat transfer coefficient applicable to thermal radiation exchange between nodes i and j $[e/t\ell^2\theta]$

The dynamic thermal equilibrium equation has another term on the left side when a phase change (assumed to be positive when going from a less volatile phase 1 to a more volatile phase 2) is occurring. The equation would be of the form

$$[\bar{C}]\{\dot{T}\} + [\bar{K}]\{T\} + \{U\} = \{Q\}$$

where

$$U_{ij} = \begin{cases} \delta_{ij}\,\rho_i\,V_i\,u_{fg}\,R_i & \text{liquid-gas} \\ \delta_{ij}\,\rho_i\,V_i\,u_{if}\,R_i & \text{solid-liquid} \end{cases} \tag{2.70}$$

where ρ_i, V_i, and the vectors $\{\dot{T}\}$, $\{T\}$, and $\{Q\}$ are as previously defined and where

u_{fg} = internal energy to gasify a unit mass of liquid $[e/m]$

u_{is} = internal energy to liquify a unit mass of solid $[e/m]$

R_i = rate at which finite spatial region associated with node i is experiencing phase change $[1/t]$

U_{ij} = rate of energy increase causing phase change in spatial region associated with node i $[e/t]$

The quantities R_i are generally not specified directly. They may be calculated on the basis of algorithms that allocate stored energy between sensible and latent heat. Phase changes impose the complication of different material properties for the two phases. It is necessary to understand the procedures involved in various programs that allow phase change as these procedures are not standardized.

2.1.5 Thermal Loads and Constraints

Thermal loads are typically specified in terms of a volumetric heat generation rate in a particular region of space. For a waste package, this is likely to be a uniform heat generation rate for the inside of the canister in its initial undeformed condition. The heat generation is a consequence of the nuclear decay reactions. The parameters required for the calculation of this decay heat generation as a function of time are discussed in an earlier report in this series (Reference MI-83).

Two methods are commonly used for calculating the decay heat. The first is a semi-empirical method which requires a knowledge of the fuel irradiation history; the recoverable energy per fission of U^{235}, Pu^{239}, and U^{238}; and the number of fissions per initial fissile atom. The second method is more detailed and case specific. It involves the use of a depletion code like ORIGEN (Reference OR-77). In addition to the composition of the fuel and its irradiation history, ORIGEN requires the input of the following parameters: spectrum averaged cross sections; fission product yields; radioactive decay constants, decay modes, and branching coefficients; radioactive chain decay information; and photon yields. Calculations are made to describe the decay heat rates for the actual waste geometry and then re-expressed as a spatially uniform rate based on the canister internal volume.

An important thermal load that must be considered in conjunction with repository operation is the loss of heat associated with ventilation. Ventilation will be required both for the initial burial of the waste and its possible retrieval from the repository at a later time. The primary

mechanism for ventilation heat transfer is convection. The important convection parameters such as the Reynolds number, Prandtl number, and Nusselt number have been discussed in Section 2.1.2.1 of this report. If temperature differences exist between different parts of a repository, such as the waste package and repository walls, then the overall heat loss should include thermal radiation heat exchange. Heat loss from ventilation is discussed in an earlier report in this series (Reference CU-83).

Thermal constraints are temperature conditions that the temperature distribution solution must satisfy. The temperature at various locations can be fixed or specified as a function of time. Similarly, thermal gradients can be specified at planes. Alternately, since the thermal conductivity is generally known, the constraint can be specified as a heat flux for the particular plane.

2.1.6 Conservation Equations

The conservation of energy principle applies throughout a heat exchange medium. The finite element method applies the principle only at each of the nodes used to describe the medium.

For conduction in the geometry shown in Figure 2.6, the energy conservation principle applies to each of the five degrees of freedom - the five nodes located at the center of the elements.

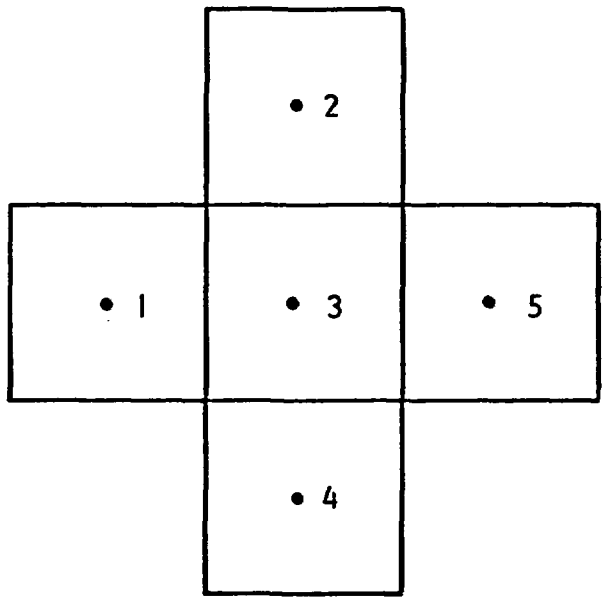

Figure 2.6

Plate Consisting of Five Cubic Elements of Unit Dimension on a Side with One Node per Element Located at Its Center

$$\begin{bmatrix}\text{Rate of increase}\\ \text{of sensible heat}\\ \text{of the element}\end{bmatrix} + \begin{bmatrix}\text{Rate energy is conducted}\\ \text{from the element to an}\\ \text{adjacent element}\end{bmatrix} = \begin{bmatrix}\text{Rate thermal energy}\\ \text{is generated in}\\ \text{the element}\end{bmatrix}$$

$$\begin{bmatrix} C_1 & 0 & 0 & 0 & 0 \\ 0 & C_2 & 0 & 0 & 0 \\ 0 & 0 & C_3 & 0 & 0 \\ 0 & 0 & 0 & C_4 & 0 \\ 0 & 0 & 0 & 0 & C_5 \end{bmatrix} \begin{Bmatrix} T_1 \\ T_2 \\ T_3 \\ T_4 \\ T_5 \end{Bmatrix} + \begin{bmatrix} K & 0 & -K & 0 & 0 \\ 0 & K & -K & 0 & 0 \\ -K & -K & 4K & -K & -K \\ 0 & 0 & -K & K & 0 \\ 0 & 0 & -K & 0 & K \end{bmatrix} \begin{Bmatrix} T_1 \\ T_2 \\ T_3 \\ T_4 \\ T_5 \end{Bmatrix} = \begin{Bmatrix} Q_1(t) \\ Q_2(t) \\ Q_3(t) \\ Q_4(t) \\ Q_5(t) \end{Bmatrix} \tag{2.71}$$

where the material has a spatially uniform and isotropic conductivity and where:

$$C_i = L^3 c\rho \tag{2.72}$$

$$K = Lk \tag{2.73}$$

$$Q_i(t) = L^3 q_i(t) \tag{2.74}$$

where:

L = side dimension of cubic element $[\ell]$

c = specific heat of the material $[e/m\theta]$

k = material isentropic thermal conductivity $[e/t\ell\theta]$

$q_i(t)$ = transient heat generation rate per unit volume for the ith element $[e/\ell^3 t]$

ρ = material mass density $[m/\ell^3]$

In matrix notation, the energy conservation equations become

$$[C] \left\{\dot{T}\right\} + [K] \left\{T\right\} = Q(t) \tag{2.75}$$

The quantities C_i and K_i can also be functions of time because they can be re-evaluated (just as $Q_i(t)$) at the end of each time step at which Equation 2.75 is solved. The set of simultaneous differential equations represented by Equation 2.75 is sometimes known as the temperature equilibrium equation in that it represents the dynamic relationship between temperature values and heat generation.

For steady state analyses, Equations 2.71 and 2.75 reduce to

$$\begin{bmatrix} K & 0 & -K & 0 & 0 \\ 0 & K & -K & 0 & 0 \\ -K & -K & 4K & -K & -K \\ 0 & 0 & -K & K & 0 \\ 0 & 0 & -K & 0 & K \end{bmatrix} \begin{Bmatrix} T_1 \\ T_2 \\ T_3 \\ T_4 \\ T_5 \end{Bmatrix} = \begin{Bmatrix} Q_1 \\ Q_2 \\ Q_3 \\ Q_4 \\ Q_5 \end{Bmatrix} \tag{2.76}$$

and

$$[K] \left\{T\right\} = \left\{Q\right\} \tag{2.77}$$

Various elements used in the finite element method are defined in terms of several nodes. Procedures contained in the computer software allocate portions of the element properties such as volume, area, etc., to each node.

Equation 2.77 can be solved by matrix methods. The general matrix Equation 2.75 can be solved by direct integration, starting with some known initial state of the system.

After the temperature distribution has been determined consistent with the particular temperature boundary and initial conditions, the solution can be checked at each node using the individual equations of Equation 2.75. These equations are no longer coupled since the temperature values have been determined. The purpose of the check is to determine whether thermal equilibrium exists; that is, does the left side of Equation 2.75 equal the right within an acceptable tolerance at each node? The equilibrium check need not be performed after each solution to Equation 2.75. If the equilibrium check is not satisfied, the temperature distribution should be modified and the check re-performed until satisfied.

2.1.7 Simulated Thermal Responses

When sufficient boundard conditions are applied (along with initial conditions for transients), a unique spatial temperature distribution can be obtained as the solution to Equation 2.75. This temperature distribution is the fundamental response of a thermal analysis. From the temperature distribution, gradients and heat fluxes can be calculated for various planes. From these temperatures, the sensible heat storage and heat conduction can be evaluated.

2.2 Thermal System Variables and Parameters

This section of the report presents a collection of data that will quantify the physical properties of the thermal system that affect the conduction, convection, and radiation thermal energy transfer. These data are provided here to aid waste package performance analysts by reducing the effort involved in analytical modeling of the waste package physical characteristics. The following materials are considered:

- Cast iron
- Low carbon steel
- Stainless steel
- Zircaloy

- Titanium alloy - Ticode-12
- High-level waste glass
- Uranium dioxide
- Bentonite
- Air
- Helium
- H_2O - liquid
- H_2O - steam

These data were compiled during an investigation of limited scope and are not always completely defined over the expected range of interest for waste package design. Analysts may need to augment the data presented here with their own investigations in various areas, particularly if material compositions differ from those chosen for the data summaries in this report. The data are taken from published sources believed to be reliable. The data are empirical, and different observers disagree with regard to quantifying various physical parameters. For example, in 1967 an international conference presented more complete steam (and liquid) properties for H_2O. Much attention was devoted to differences that stemmed from different observations, which were probably the result of both imprecise observation techniques and differences in the design and control of the experiment.

2.2.1 Conduction Parameters

Three independent quantities must be defined in order to perform conduction analyses. They are:

k - thermal conductivity $[e/t\ell\theta]$

c - specific heat $[e/m\theta]$

ρ - mass density $[m/\ell^3]$

Thermal diffusivity depends on the values of these three independent quantities:

$$\alpha = \frac{k}{\rho c} = \text{thermal diffusivity} \left[\frac{\ell^2}{t} \right] \tag{2.78}$$

The thermal conductivity of gases is dependent on their pressure and temperature. For liquids and solids, the thermal conductivity is dependent on the material temperature. In some cases, this dependency can be neglected and the conductivity considered as constant. For example, if a steady-state analysis is being performed in which the temperatures can be estimated to within 25°C, it is usually acceptable when dealing with solids to treat the thermal conductivity values as constants evaluated at the estimated average temperature.

2.2.1.1 Thermal Conductivity

Thermal conduction is the flow of thermal energy from one region at a high temperature to an adjoining region at a lower temperature. It is a result of energy transferred through a substance by its free electron migration and kinetic energy exchange due to molecular collisions in which the molecules have vibrational kinetic energies proportional to their temperature. Fourier's law provides a functional definition of thermal conductivity of a substance by relating it to other observable quantities:

$$q = -kA \frac{dT}{dx} \tag{2.79}$$

and

$$\phi = \frac{q}{A} \tag{2.80}$$

where

ϕ = heat flux [$e/t\ell^2$]

q = heat transfer rate [e/t]

A = heat transfer area [ℓ^2]

k = thermal conductivity [$e/t\ell\theta$]

T = temperature [θ]

x = distance along heat transfer direction [ℓ]

The SI unit for thermal conductivity is watt per meter degree celsius, W/(m-^{o}C). Conversions for thermal conductivity units are:

1 cal/(cm-s-^{o}C) = 418.68 W/(m-^{o}C)

1 cal/(cm-s-^{o}C) = 241.9 Btu/(hr-ft-^{o}F)

1 Btu/(hr-ft-^{o}F) = 1.731 W/(m-^{o}C)

1 Btu/(hr-ft-^{o}F) = 0.2162 (lb_f/sec-^{o}F)

2.2.1.2 Specific Heat

Sensible heat manifests itself inside a material as the sum of molecular, kinetic, and potential energies. The sensible heat term describes the change in stored energy in terms of temporal change in a material's temperature:

$$Q_{ss} = \rho c \frac{dT}{dt} \tag{2.81}$$

where

Q_{ss} = increase in stored energy in the form of sensible heat [$e/t\ell^3$]

ρ = material mass density [m/ℓ^3]

c = material specific heat [$e/m\ell$]

T = material temperature [θ]

t = time [t]

This sensible heat term appears in the general (transient) conduction equation developed from the energy conservation principle. The specific heat is the thermal energy addition to a unit mass of material necessary to raise its temperature by one degree.

For finite element and finite difference programs, it is frequently advantageous to deal with the energy storage on a unit volume basis rather than a unit mass basis. This is done by replacing the specific heat (c) with the product of the specific heat and the mass density:

$$\hat{c} = \rho c \tag{2.82}$$

The sensible heat storage term becomes

$$Q_{ss} = \hat{c} \frac{dT}{dt} \tag{2.83}$$

where $\hat{c}$ is the volumetric heat capacity. The volumetric heat capacity is the additional thermal energy that will raise the temperature of a unit volume of material by one degree. Specific heats that are a material property (c) will be presented in this report. If an analyst needs volumetric heat capacities, they can be computed using Equation 2.82.

The general thermodynamic definition of specific heat is

$$c_p = \left(\frac{\partial h}{\partial T}\right)_p \tag{2.84}$$

$$c_v = \left(\frac{\partial u}{\partial T}\right)_v \tag{2.85}$$

where

c_p = specific heat evaluated during a constant pressure polytropic process [e/mθ]

c_v = specific heat evaluated during a constant volume polytropic process [e/mθ]

h = specific enthalpy [e/m]

u = specific internal energy [e/m]

T = temperature [θ]

The SI unit for specific heat is a joule per kilogram degree celsius J/(kg-°C). Another typical unit is kcal/(kg-°C). Conversion factors are:

1 kcal/(kg-°C) = 4186.8 J/(kg-°C)

1 cal/(g-°C) = 4186.8 J/(kg-°C)

1 Btu/(lb-°F) = 4186.8 J/(kg-°C)

For an ideal gas, the difference between c_p and c_v is a constant, R_u:

$$R_u = c_p - c_v \tag{2.86}$$

For real gases, a similar difference is noted in the specific heat terms. The ideal gas law constant R_u is given by

$$R_u = 1.987 \text{ (cal/g-mole } ^oK)$$

$$R_u = 8.314 \times 10^7 \text{ (g cm}^2\text{/sec}^2 \text{ g-mole } ^oK)$$

$$R_u = 1544. \text{ (ft - lb}_f\text{/lb-mole } ^oR)$$

$$R_u = 1.987 \text{ (Btu/lb-mole } ^oR)$$

The gas constant for a specific gas is obtained by

$$R = R_u/M_w \tag{2.87}$$

where M_w is the molecular weight. Values are:

Substance	M_w (lb/lb-mole)	R (ft-lb$_f$/lb$_m$ ^oR)
Air	28.967	53.35
Helium	4.003	386.20

For liquids and solids, there is a very small difference in the two specific heat terms. Liquids and solids are usually treated as incompressible.

2.2.1.3 Mass Density

The mass density of a material, ρ, is defined as the mass per unit volume. For gases, the mass density is a function of both pressure and temperature. For an ideal gas,

$$\rho = \frac{P}{RT} \tag{2.88}$$

where

ρ = mass density [m/ℓ^3]

P = pressure [f/ℓ^2]

R = gas constant [$e/m\theta$]

R_u = 1.987 [$e/(m\text{-mole}\ \theta$]

M_w = gas molecular weight [m/m-mole]

T = absolute temperature [θ]

For a liquid or solid, the mass density varies with temperature but usually doesn't vary significantly with pressure so that

$$\rho = \rho(T) \tag{2.89}$$

For a solid, the equation describing this density change (derived in Appendix A) is:

$$-\frac{\Delta\rho}{\rho} = 3\bar{\alpha}\Delta T \tag{2.90}$$

where

$\bar{\alpha}$ = mean temperature coefficient of thermal expansion [$1/\theta$]

For liquids, the data are usually tabulated in terms of either the mass density or the specific volume versus temperature at fixed values of pressure.

For virtually all substances, the mass density increases with decreases in temperature. For gases, the mass density also increases with increasing pressure.

The specific volume of a substance is the volume required to contain a unit mass of the material at a given thermodynamic state, such as a specific temperature and pressure. The specific volume is the reciprocal of the mass density:

$$v = \frac{1}{\rho} \tag{2.91}$$

where

v = specific volume $[\ell^3/m]$

ρ = mass density $[m/\ell^3]$

Thus, only one of these two properties needs to be known.

When a substance is heated and is free to expand, it experiences a thermal strain,

$$d\varepsilon = \alpha dT \tag{2.92}$$

without experiencing any stress. Over limited ranges of temperature change, the elongation of a specimen can be described by

$$\Delta L = \varepsilon L \tag{2.93}$$

where

ε = strain [ ]

L = original length $[\ell]$

ΔL = incremental length $[\ell]$

For this same limited temperature change,

$$\Delta L = \alpha L \Delta T \tag{2.94}$$

and the thermal strain is

$$\varepsilon = \frac{\Delta L}{L} = \alpha \Delta T \tag{2.95}$$

where

α = coefficient of thermal expansion [$1/\theta$]

$\Delta T = T_2 - T_1$ = temperature increase from state 1 to state 2 [θ]

The term $\alpha\Delta T$ has a limited range of application in the calculations of Equations 2.94 and 2.95 because α is a physical characteristic of a material which varies with temperature. A mean value can be determined by

$$\bar{\alpha} = \frac{1}{\Delta T} \int_{T_1}^{T_2} \alpha dT \tag{2.96}$$

where

$\bar{\alpha}$ = mean coefficient of thermal expansion over the range $T_1 \leq T \leq T_2$

When the temperature of a substance is increased, the substance experiences a fractional volume change according to

$$\frac{\Delta V}{V} \simeq 3\bar{\alpha}\Delta T \tag{2.97}$$

and for constant mass

$$\frac{\Delta V}{V} \simeq -\frac{\Delta \rho}{\rho} \tag{2.98}$$

so that the fractional change in mass density is

$$-\frac{\Delta \rho}{\rho} \simeq 3\bar{\alpha}\Delta T \tag{2.99}$$

where

$\bar{\alpha}$ = mean coefficient of thermal expansion [1/θ]

ΔT = temperature increase [θ]

These relationships are developed in Appendix A. They can be used to determine approximately how the mass density varies with temperature for a solid when the thermal expansion coefficient data are known.

The SI unit for mass density is g/m^3. Other typical units are kg/m^3 and lb_m/ft^3. Conversion factors are:

$1\ kg/m^3 = 1000\ g/m^3$

$1\ kg/m^3 = 0.0624\ lb_m/ft^3$

Since specific volume is the inverse of mass density, these conversion factors can be used for specific volume.

2.2.1.4 Latent Heat

Within a heat transfer region, a phase change can occur when the pressure and temperature have a particular combination of values so that two phases of a substance coexist in equilibrium. The heat transfer can continue without temperature change and with the material changing phase either giving up energy when going to a less volatile phase or absorbing energy when going to a more volatile phase.

Latent heat derives its name from the fact that the internal energy of a substance can change without a change of temperature. This occurs when a material gradually changes phase with a step function difference in internal energies between the two phases.

The science of calorimetry, which preceded the development of the thermodynamic laws, devised the concept of latent heat. This early work involved important physical observations, but some were not stated as precisely as needed for consistency with the thermodynamic laws and principles that were developed later. In its early definition, latent heat was considered the amount of heat which must be added to a unit mass of a substance to cause it to change phase in a constant pressure, constant temperature, frictionless process. The definition is expressed as follows:

$$Q = mq_L = m\Delta u + W \tag{2.100}$$

where

Q = total heat added [e]

m = mass of substance changing phase [m]

q_L = latent heat per unit mass [e/m]

Δu = change in specific internal energy of material [e/m] .

W = work done by volume change by the entire system of mass m without friction [e]

Latent heat can also be defined as a material property rather than heat flow during a process. For an open system, the stream flowing into the system can do work on the system, and the stream flowing out of the system can have work done on it by the system.

The work in either stream is

$$W = FL = pAL = pV \tag{2.101}$$

where

W = flow work per unit time [e/t]

F = total force exerted on the quantity of fluid flowing across boundary (inlet or outlet) per unit time [f/t]

L = length of fluid mass flowing across boundary in unit time [ℓ]

p = pressure at inlet (or outlet) [f/ℓ^2]

A = area of flow into or out of system [ℓ^2]

V = volume of fluid flowing across boundary in unit time [ℓ^3/t]

Equation 2.101 can be written on a per unit mass basis

$$w = pv \tag{2.102}$$

where

v = specific volume of fluid crossing boundary $[\ell^3/m]$

w = work per unit mass $[e/m]$

Pressure and specific volume are properties of the fluid. Thus, the flow work is a property of the fluid. The enthalpy is a fluid property defined as

$$h = u + pv \tag{2.103}$$

where

h = specific enthalpy per unit mass $[e/m]$

u = specific internal energy per unit mass $[e/m]$

p = pressure $[f/\ell^2]$

v = specific volume $[\ell^3/m]$

Latent heat is defined as the difference between the specific enthalpy of one phase of a pure substance at saturation conditions and the specific enthalpy of another phase of the pure substance at the same pressure and temperature.

The latent heat terms are

$$h_{fg} = h_g - h_f \tag{2.104}$$

$$h_{if} = h_f - h_i \tag{2.105}$$

$$h_{ig} = h_g - h_i \tag{2.106}$$

where g, f, and i represent the gas, liquid, and solid phases. Equations 2.104, 2.105, and 2.106 represent the latent heat associated with liquid-gas, solid-liquid, and solid-gas transformations respectively.

2.2.1.5 Material Conduction Properties

Tables in this section present the conduction properties, thermal conductivity (k), mass density (ρ), specific heat (c), and thermal diffusivity (a), for each of the following solid materials:

- Cast iron (Tables 2.1 and 2.2)
- Carbon steel (Tables 2.3 and 2.4)
- 304 stainless steel (Tables 2.5 and 2.6)
- Ticode 12 (Tables 2.7 and 2.8)
- Zircaloy 2 (Tables 2.9 and 2.10)
- Zircaloy 4 (Tables 2.11 and 2.12)
- Bentonite (Tables 2.13 and 2.14)
- High-level waste glass (Tables 2.15, 2.16, 2.17, and 2.18)
- Uranium dioxide (Tables 2.19 and 2.20)

The thermal properties of bentonite and bentonite-rock mixtures are a function of both the density of the material and the moisture content. In general, the thermal conductivity of bentonite-rock mixtures increases as density and moisture content increase.

These same properties are also presented as a function of pressure and temperature for air and helium at low pressure, saturated liquid water,

and dry saturated steam (Tables 2.21 - 2.28). For water and steam, saturation properties including specific volume (reciprocal of mass density) and specific enthalpy are presented in Tables 2.29 and 2.30.

Thermal conductivity, specific volume, and specific enthalpy are presented in Tables 2.31 - 2.36 as a function of pressure and temperature for

- Subcooled liquid water
- Superheated steam
- Saturated liquid water
- Saturated steam

Table 2.1

Cast Iron Conduction Properties
Including Thermal Conductivity (k), Mass Density (ρ),
Specific Heat (c), and Thermal Diffusivity ($a = k/\rho c$)
in English Units

T (^oF)	k (Btu/hr-ft^oF)	ρ (lb_m/ft^3)	c (Btu/$lb_m{}^oF$)	a (ft^2/hr)
32	33.0	474	0.110	0.633
212	31.8	472	0.110	0.612
572	27.7	469	0.110	0.537
932	24.8	466	0.110	0.483

Source: KR-61 (k,c)
BA-78 (ρ)

Table 2.2

Cast Iron Conduction Properties
Including Thermal Conductivity (k), Mass Density (ρ),
Specific Heat (c), and Thermal Diffusivity (a = k/ρc) in Metric Units

T (^oC)	k (watts/m^oC)	ρ (kg/m^3)	c (watt-hr/kg^oC)	a (m^2/hr)
0	57.1	7593	0.128	0.0588
100	55.0	7561	0.128	0.0569
300	47.9	7513	0.128	0.0499
500	42.9	7465	0.128	0.0449

Source: Derived from data in Table 2.1

Table 2.3

Carbon Steel Conduction Properties
Including Thermal Conductivity (k), Mass Density (ρ),
Specific Heat (c), and Thermal Diffusivity ($a = k/\rho c$)
in English Units

T (^oF)	k (Btu/hr-ft^oF)	ρ (lb_m/ft^3)	c (Btu/$lb_m$$^oF$)	a (ft^2/hr)
70	36.0	490.3	0.113	0.651
100	36.6	490.0	0.114	0.656
150	35.7	489.5	0.115	0.635
200	34.9	489.0	0.117	0.609
250	34.0	488.6	0.119	0.585
300	33.2	488.1	0.121	0.562
350	32.3	487.5	0.123	0.539
400	31.6	487.0	0.125	0.519
450	30.6	486.5	0.127	0.495
500	29.8	485.9	0.129	0.475
550	29.0	485.3	0.131	0.456
600	28.3	484.7	0.133	0.439
650	27.5	484.1	0.136	0.417
700	26.8	483.5	0.139	0.399
750	26.0	482.8	0.142	0.379
800	25.4	482.2	0.146	0.361
850	24.6	481.5	0.150	0.340
900	23.8	480.9	0.155	0.319
950	23.2	480.2	0.160	0.302
1000	22.6	479.5	0.165	0.286

Source: ASME-71 (k, a, ρ)
$c = k/\rho a$

Table 2.4

Carbon Steel Conduction Properties
Including Thermal Conductivity (k), Mass Density (ρ),
Specific Heat (c), and Thermal Diffusivity (a = k/ρc)
in Metric Units

T (^oC)	k (watts/m^oC)	ρ (kg/m^3)	c (watt-hr/kg^oC)	a (m^2/hr)
21.1	62.3	7853	0.131	0.0605
37.8	63.3	7849	0.132	0.0609
65.6	61.7	7842	0.133	0.0590
93.3	60.4	7834	0.136	0.0566
121.1	58.8	7826	0.138	0.0544
148.9	57.4	7818	0.140	0.0523
176.7	55.9	7809	0.143	0.0501
204.4	54.7	7801	0.145	0.0482
232.2	52.9	7792	0.148	0.0460
260.0	51.5	7783	0.150	0.0441
287.8	50.2	7774	0.152	0.0424
315.6	48.9	7764	0.154	0.0408
343.3	47.6	7754	0.158	0.0387
371.1	46.4	7744	0.162	0.0371
398.9	45.0	7734	0.165	0.0352
426.7	43.9	7723	0.170	0.0335
454.4	42.5	7713	0.174	0.0316
482.2	41.2	7702	0.181	0.0296
510.0	40.1	7691	0.186	0.0281
537.8	39.1	7680	0.191	0.0266

Source: Derived from data in Table 2.3

Table 2.5

304 Stainless Steel Conduction Properties
Including Thermal Conductivity (k), Mass Density (ρ),
Specific Heat (c), and Thermal Diffusivity ($a = k/\rho c$)
in English Units

T (^oF)	k (Btu/hr-ft^oF)	ρ (lb_m/ft^3)	c (Btu/$lb_m$$^oF$)	a (ft^2/hr)
70	8.38	501.5	0.111	0.150
100	8.40	501.1	0.111	0.150
150	8.67	500.4	0.113	0.153
200	8.90	499.7	0.115	0.155
250	9.12	499.0	0.116	0.157
300	9.35	498.3	0.118	0.159
350	9.56	497.5	0.120	0.160
400	9.80	496.8	0.121	0.163
450	10.0	496.1	0.123	0.164
500	10.2	495.3	0.124	0.166
550	10.5	494.6	0.126	0.169
600	10.7	493.8	0.127	0.171
650	10.9	493.0	0.129	0.172
700	11.1	492.2	0.130	0.174
750	11.4	491.5	0.132	0.176
800	11.6	490.7	0.133	0.178
850	11.8	489.9	0.134	0.180
900	12.0	489.1	0.136	0.181
950	12.2	488.3	0.137	0.183
1000	12.4	487.5	0.137	0.185

Source: ASME-71 (k, ρ, a)
$c = k/\rho a$

Table 2.6

304 Stainless Steel Conduction Properties
Including Thermal Conductivity (k), Mass Density (ρ),
Specific Heat (c), and Thermal Diffusivity ($a = k/\rho c$)
in Metric Units

T (^oC)	k (watts/m^oC)	ρ (kg/m^3)	c (watt-hr/kg^oC)	a (m^2/hr)
21.1	14.49	8030	0.130	0.0139
37.8	14.53	8023	0.130	0.0139
65.6	15.00	8012	0.132	0.0142
93.3	15.39	8001	0.134	0.0144
121.1	15.77	7990	0.135	0.0146
148.9	16.17	7978	0.136	0.0148
176.7	16.53	7966	0.139	0.0149
204.4	16.95	7955	0.141	0.0151
232.2	17.30	7943	0.143	0.0152
260.0	17.64	7931	0.144	0.0154
287.8	18.16	7919	0.146	0.0157
315.6	18.51	7907	0.147	0.0159
343.3	18.85	7894	0.149	0.0160
371.1	19.20	7882	0.150	0.0162
398.9	19.72	7869	0.153	0.0164
426.7	20.06	7856	0.155	0.0165
454.4	20.41	7844	0.156	0.0167
482.2	20.75	7831	0.158	0.0168
510.0	21.10	7818	0.159	0.0170
537.8	21.45	7805	0.160	0.0172

Source: Derived from data in Table 2.5

Table 2.7

Ticode 12 Conduction Properties
Including Thermal Conductivity (k), Mass Density (ρ),
Specific Heat (c), and Thermal Diffusivity ($a = k/\rho c$)
in English Units

T (^oF)	k (Btu/hr-ft^oF)	ρ (lb_m/ft^3)	c (Btu/$lb_m{}^oF$)	a (ft^2/hr)
32	-	282	-	-
75	-	282	0.13	-
-	11.0	-	-	-
600	-	282	-	

Source: TI

Table 2.8

Ticode 12 Conduction Properties
Including Thermal Conductivity (k), Mass Density (ρ),
Specific Heat (c), and Thermal Diffusivity ($a = k/\rho c$)
in Metric Units

T (^oC)	k (watts/m^oC)	ρ (kg/m^3)	c (watt-hr/kg^oC)	a (m^2/hr)
0.0	-	4510	-	-
23.9	-	4510	0.151	-
-	19.03	-	-	-
315.6	-	4510	-	

Source: Derived from data in Table 2.7

Table 2.9

Zircaloy 2 Conduction Properties
Including Thermal Conductivity (k), Mass Density (ρ),
Specific Heat (c), and Thermal Diffusivity (a = k/ρc)
in English Units

T (^oF)	k (Btu/hr-ft^oF)	ρ (lb_m/ft^3)	c (Btu/$lb_m$$^oF$)	a (ft^2/hr)
212	7.74	409.1	0.0731	0.259
392	8.38	408.3	0.0774	0.265
572	9.02	407.5	0.0817	0.271
752	9.83	406.7	0.0860	0.281
932	10.6	405.9	0.0903	0.289
1112	11.5	405.1	0.0946	0.300

Source: SC-65

Table 2.10

Zircaloy 2 Conduction Properties
Including Thermal Conductivity (k), Mass Density (ρ),
Specific Heat (c), and Thermal Diffusivity ($a = k/\rho c$)
in Metric Units

T (^oC)	k (watts/m^oC)	ρ (kg/m^3)	c (watt-hr/kg^oC)	a (m^2/hr)
100	13.39	6551	0.0850	0.0240
200	14.49	6538	0.0900	0.0246
300	15.60	6525	0.0950	0.0252
400	17.00	6512	0.1000	0.0261
500	18.33	6499	0.1050	0.0269
600	19.89	6486	0.1100	0.0279

Source: Derived from data in Table 2.9

Table 2.11

Zircaloy 4 Conduction Properties
Including Thermal Conductivity (k), Mass Density (ρ),
Specific Heat (c), and Thermal Diffusivity (a = k/ρc)
in English Units

T (^oF)	k (Btu/hr-ft^oF)	ρ* (lb_m/ft^3)	c (Btu/$lb_m$$^oF$)	a (ft^2/hr)
70	8.19	409.7	0.0840	0.238
212	8.64	409.1	0.0714	0.296
392	9.21	408.3	0.0638	0.354
572	9.78	407.5	0.0576	0.417
752	10.35	406.7	0.0556	0.458
932	10.92	405.9	0.0538	0.500
1112	11.48	405.1	0.0546	0.519

* Assumed to be equal to Zircaloy 2 density.

Source: SC-65

Table 2.12

Zircaloy 4 Conduction Properties
Including Thermal Conductivity (k), Mass Density (ρ),
Specific Heat (c), and Thermal Diffusivity (a = k/ρc)
in Metric Units

T (^oC)	k (watts/m^oC)	ρ (kg/m^3)	c (watt-hr/kg^oC)	a (m^2/hr)
21	14.17	6560	0.0976	0.0221
100	14.94	6551	0.0830	0.0275
200	15.92	6538	0.0742	0.0328
300	16.90	6525	0.0670	0.0387
400	17.89	6512	0.0646	0.0425
500	18.87	6499	0.0625	0.0465
600	19.86	6486	0.0635	0.0482

Source: Derived from data in Table 2.11

Table 2.13

Bentonite Conduction Properties
Including Thermal Conductivity (k), Mass Density (ρ),
Specific Heat (c), and Thermal Diffusivity (a = k/ρc)
in English Units

T (^oF)	k (Btu/hr-ft^oF)	ρ* (lb_m/ft^3)	c** (Btu/$lb_m$$^oF$)	a (ft^2/hr)
Bentonite				
68	0.058	83.65	0.22	0.0030
140	0.075	83.65	0.22	0.0042
248	0.110	83.65	0.22	0.0059
Bentonite				
68	0.064	92.39	0.22	0.0032
140	0.093	92.39	0.22	0.0046
248	0.127	92.39	0.22	0.0068
Bentonite expanded with water				
68	0.075	78.03	0.46	0.0022
140	0.133	78.03	0.46	0.0038
248	0.214	78.03	0.46	0.0061
Bentonite expanded with water				
68	0.116	76.79	0.46	0.0032
140	0.168	76.79	0.46	0.0048
248	0.249	76.79	0.46	0.0071

* Note different densities

** Calculated c = k/ρa

Source: Derived from data in Table 2.14

Table 2.14

Bentonite Conduction Properties
Including Thermal Conductivity (k), Mass Density (ρ),
Specific Heat (c), and Thermal Diffusivity (a = k/ρc)
in Metric Units

T (^oC)	k (watts/m^oC)	ρ* (kg/m^3)	c** (watt-hr/kg^oC)	a (m^2/hr)
Bentonite				
20	.10	1340	0.26	0.00028
60	.13	1340	0.26	0.00039
120	.19	1340	0.26	0.00055
Bentonite				
20	.11	1480	0.25	0.00030
60	.16	1480	0.25	0.00043
120	.22	1480	0.25	0.00063
Bentonite expanded with water				
20	.13	1250	0.53	0.00020
60	.23	1250	0.53	0.00035
120	.37	1250	0.53	0.00057
Bentonite expanded with water				
20	.20	1230	0.53	0.00030
60	.29	1230	0.53	0.00045
120	.43	1230	0.53	0.00066

* Note different densities

** Calculated c = k/ρa

Source: SI-83

Table 2.15

Defense High-Level Waste Glass Conduction Properties Including Thermal Conductivity (k), Mass Density (ρ), Specific Heat (c), and Thermal Diffusivity ($a = k/\rho c$) in English Units

T (^oF)	k (Btu/hr-ft^oF)	ρ (lb_m/ft^3)	c (Btu/$lb_m$$^oF$)	a (ft^2/hr)
68	0.504	171.7	0.196	0.0150
212	0.562	171.2	0.237	0.0139
392	0.634	170.7	0.271	0.0137
572	0.707	170.2	0.296	0.0140
752	0.779	169.7	0.314	0.0146
932	0.851	169.4	0.328	0.0153
1112	0.924	166.8	0.338	0.0164

Source: Derived from data in Table 2.16

Table 2.16

Defense High-Level Waste Glass Conduction Properties Including Thermal Conductivity (k), Mass Density (ρ), Specific Heat (c), and Thermal Diffusivity ($a = k/\rho c$) in Metric Units

T (^oC)	k (watts/m^oC)	ρ (kg/m^3)	c (watt-hr/kg^oC)	a (m^2/hr)
20	0.872	2750	0.228	0.00139
100	0.972	2743	0.276	0.00128
200	1.097	2735	0.315	0.00127
300	1.222	2726	0.344	0.00130
400	1.347	2718	0.365	0.00136
500	1.472	2713	0.381	0.00142
600	1.598	2672	0.393	0.00152

Source: WE-83

Table 2.17

Commercial High-Level Waste Glass Conduction Properties Including Thermal Conductivity (k), Mass Density (ρ), Specific Heat (c), and Thermal Diffusivity (a = k/ρc) in English Units

T (^oF)	k (Btu/hr-ft^oF)	ρ (lb_m/ft^3)	c (Btu/$lb_m$$^oF$)	a (ft^2/hr)
32	0.46	-	-	-
68	0.47	193.5	.17	.014
212	0.52	-	-	-
392	0.58	-	-	-
572	0.64	-	-	-
752	0.69	-	-	-
932	0.75	-	-	-

NOTE: These are estimated values

Source: Derived from data in Table 2.18

Table 2.18

Commercial High-Level Waste Glass Conduction Properties Including Thermal Conductivity (k), Mass Density (ρ), Specific Heat (c), and Thermal Diffusivity ($a = k/\rho c$) in Metric Units

T (^oC)	k (watts/m^oC)	ρ (kg/m^3)	c (watt-hr/kg^oC)	a (m^2/hr)
0	0.8	-	-	-
20	0.82	3100	0.2	0.0013
100	0.9	-	-	-
200	1.0	-	-	-
300	1.1	-	-	-
400	1.2	-	-	-
500	1.3	-	-	-

NOTE: These are estimated values

Source: WE-83

Table 2.19

Uranium Dioxide Conduction Properties Including Thermal Conductivity (k), Mass Density (ρ), Specific Heat (c), and Thermal Diffusivity ($a = k/\rho c$) in English Units

T (^{o})	k (Btu/hr-ft^{o}F)	ρ (lb_m/ft^3)	c (Btu/lb_m^{o}F)	a (ft^2/hr)
68	4.71	683.9	7.45	0.00924
212	4.07		6.16	
392	3.49		6.48	
572	3.07		5.41	
752	2.71		5.08	
932	2.44		4.76	
1112	2.21		4.60	
1292	2.10		4.43	
1472	1.87		4.47	
1652	1.73			
1832	1.63			

Source: Derived from data in Table 2.20

Table 2.20

Uranium Dioxide Conduction Properties Including Thermal Conductivity (k), Mass Density (ρ), Specific Heat (c), and Thermal Diffusivity ($a = k/\rho c$) in Metric Units

T (^oC)	k (watts/m^oC)	ρ (kg/m^3)	c (watt-hr/kg ^oC)	a (m^2/hr)
20	8.15	10,960	8.66	0.000859
100	7.05		7.16	
200	6.04		7.53	
300	5.31		6.28	
400	4.69		5.90	
500	4.22		5.53	
600	3.83		5.34	
700	3.64		5.15	
800	3.24		5.19	
900	3.00			
1000	2.82			

Source: WE-73

Table 2.21

Air Thermal Conduction Properties at One Atmosphere Pressure Including Thermal Conductivity (k), Mass Density (ρ), Specific Heat (c_p), and Thermal Diffusivity ($a = k/\rho c_p$) in English Units

T (^oF)	k (Btu/hr-ft^oF)	ρ (lb_m/ft^3)	c_p (Btu/$lb_m$$^oF$)	a (ft^2/hr)
0	0.0133	0.086	0.239	0.646
32	0.0140	0.081	0.240	0.720
100	0.0154	0.071	0.240	0.905
200	0.0174	0.060	0.241	1.20
300	0.0193	0.052	0.243	1.53
400	0.0212	0.046	0.245	1.88
500	0.0231	0.0412	0.247	2.27
600	0.0250	0.0373	0.250	2.68
700	0.0268	0.0341	0.253	3.10
800	0.0286	0.0314	0.256	3.56
900	0.0303	0.0291	0.259	4.02
1000	0.0319	0.0271	0.262	4.50

Source: KR-61

Table 2.22

Air Thermal Conduction Properties at One Atmosphere Pressure Including Thermal Conductivity (k), Mass Density (ρ), Specific Heat (c_p), and Thermal Diffusivity ($a = k/\rho c_p$) in Metric Units

T (^oC)	k (watts/m^oC)	ρ (kg/m^3)	c_p (watt-hr/kg^oC)	a (m^2/hr)
-17.8	0.0225	1.38	0.28	0.060
0.0	0.0242	1.30	0.28	0.067
37.8	0.0259	1.14	0.28	0.084
93.3	0.0294	0.961	0.28	0.111
148.9	0.0329	0.833	0.28	0.142
204.4	0.0363	0.737	0.29	0.175
260.0	0.0398	0.657	0.29	0.211
315.6	0.0432	0.593	0.29	0.249
371.1	0.0467	0.545	0.29	0.288
426.7	0.0502	0.497	0.30	0.331
482.2	0.0519	0.465	0.30	0.373
537.8	0.0553	0.432	0.30	0.418

Source: Derived from data in Table 4.21

Table 2.23

Helium Thermal Conduction Properties at One Atmosphere Pressure Including Thermal Conductivity (k), Mass Density (ρ), Specific Heat (c_p), and Thermal Diffusivity ($a = k/\rho c_p$) in English Units

T (^oF)	k (Btu/hr-ft^oF)	ρ (lb_m/ft^3)	c_p (Btu/lb_m ^oF)	a (ft^2/hr)
0	0.078	0.01200	1.24	5.25
200	0.097	0.00835	1.24	9.36
400	0.115	0.00640	1.24	14.5
600	0.129	0.00520	1.24	20.0
800	0.138	0.00436	1.24	25.5

Source: KR-61

Table 2.24

Helium Thermal Conduction Properties at One Atmosphere Pressure Including Thermal Conductivity (k), Mass Density (ρ), Specific Heat (c_p), and Thermal Diffusivity ($a = k/\rho c_p$) in Metric Units

T (^oC)	k (watts/m^oC)	ρ (kg/m^3)	c_p (watt-hr/kg^oC)	a (m^2/hr)
-17.8	0.135	0.192	1.44	0.488
93.3	0.168	0.134	1.44	0.870
204.4	0.199	0.103	1.44	1.35
315.6	0.223	0.0833	1.44	1.86
426.7	0.239	0.0698	1.44	2.37

Source: Derived from data in Table 2.23

Table 2.25

Saturated Liquid Water Thermal Conduction Properties Including Thermal Conductivity (k), Mass Density (ρ), Specific Heat (c_p), and Thermal Diffusivity ($a = k/\rho c_p$) in English Units

T (^oF)	k (Btu/hr-ft^oF)	ρ (lb_m/ft^3)	c_p (Btu/lb_m ^oF)	a (ft^2/hr)
32	0.319	62.4	1.01	5.07×10^{-3}
50	0.332	62.4	1.00	5.33×10^{-3}
100	0.364	62.0	0.998	5.88×10^{-3}
150	0.384	61.2	1.00	6.27×10^{-3}
200	0.394	60.1	1.00	6.55×10^{-3}
250	0.396	58.8	1.01	6.69×10^{-3}
300	0.395	57.3	1.03	6.70×10^{-3}
350	0.391	55.6	1.05	6.69×10^{-3}
400	0.381	53.6	1.08	6.57×10^{-3}
450	0.367	51.6	1.12	6.34×10^{-3}
500	0.349	49.0	1.19	5.99×10^{-3}
550	0.325	45.9	1.31	5.05×10^{-3}
600	0.292	42.4	1.51	4.57×10^{-3}

Source: KR-61

Table 2.26

Saturated Liquid Water Thermal Conduction Properties Including Thermal Conductivity (k), Mass Density (ρ), Specific Heat (c_p), and Thermal Diffusivity ($a = k/\rho c_p$) in Metric Units

T (^oC)	k (watts/m^oC)	ρ (kg/m^3)	c_p (watt-hr/kg^oC)	a (m^2/hr)
0.0	0.552	1000	1.17	4.72×10^{-4}
10.0	0.575	1000	1.16	4.96×10^{-4}
37.8	0.630	993	1.16	5.47×10^{-4}
65.6	0.665	980	1.16	5.85×10^{-4}
93.3	0.682	963	1.16	6.11×10^{-4}
121.1	0.685	942	1.17	6.22×10^{-4}
148.9	0.683	918	1.20	6.20×10^{-4}
176.7	0.676	891	1.22	6.22×10^{-4}
204.4	0.659	859	1.26	6.02×10^{-4}
232.2	0.635	827	1.30	5.91×10^{-4}
260.0	0.604	785	1.38	5.58×10^{-4}
287.8	0.562	735	1.52	5.03×10^{-4}
315.6	0.505	679	1.76	4.23×10^{-4}

Source: Derived from data in Table 2.25

Table 2.27

Dry Superheated Steam at Atmospheric Pressure Thermal Conduction Properties Including Thermal Conductivity (k), Mass Density (ρ), Specific Heat (c_p), and Thermal Diffusivity ($a = k/\rho c_p$) in English Units

T (^oF)	k (Btu/hr-ft^oF)	ρ (lb_m/ft^3)	c_p (Btu/lb_m ^oF)	a (ft^2/hr)
212	0.0145	0.0372	0.451	0.864
300	0.0171	0.0328	0.456	1.14
400	0.0200	0.0288	0.462	1.50
500	0.0228	0.0258	0.470	1.88
600	0.0257	0.0233	0.477	2.31
700	0.0288	0.0213	0.485	2.79
800	0.0321	0.0196	0.494	3.32
900	0.0355	0.0181	0.500	3.93
1000	0.0388	0.0169	0.510	4.50

Source: KR-61

Table 2.28

Dry Superheated Steam at Atmospheric Pressure Thermal Conduction Properties Including Thermal Conductivity (k), Mass Density (ρ), Specific Heat (c_p), and Thermal Diffusivity ($a = k/\rho c_p$) in Metric Units

T (^oC)	k (watts/m^oC)	ρ (kg/m^3)	c_p (watt-hr/kg^oC)	a (m^2/hr)
100.0	0.0251	0.596	0.524	0.0804
148.9	0.0296	0.525	0.530	0.106
204.4	0.0346	0.461	0.537	0.140
260.0	0.0394	0.413	0.546	0.175
315.6	0.0444	0.373	0.554	0.215
371.1	0.0498	0.341	0.564	0.259
426.7	0.0555	0.314	0.574	0.308
482.2	0.0614	0.290	0.581	0.364
537.8	0.0671	0.271	0.593	0.418

Source: Derived from data in Table 2.27

Table 2.29

Saturated Liquid and Saturated Steam Properties Including Pressure (P_{sat}), Temperature (T_{sat}), Saturated Liquid Enthalpy (h_f), Saturated Dry Steam Enthalpy (h_g), Saturated Liquid Specific Volume (v_f), and Saturated Dry Steam Specific Volume (v_g) in English Units

P_{sat} (lb_f/in^2)	T_{sat} (^oF)	h_f (Btu/lb_m)	h_g (Btu/lb_m)	v_f (ft^3/lb_m)	v_g (ft^3/lb_m)
0.0886	32.00	-0.018	1075.28	0.016021	3304.320000
0.0886	32.02	0	1075.28	0.016021	3301.980000
0.1780	50.00	18.053	1083.03	0.016024	1704.670000
0.3389	68.00	36.055	1091.20	0.016047	926.417000
0.6152	86.00	54.027	1098.93	0.016088	527.457000
1.0697	104.00	72.003	1106.67	0.016145	313.088000
1.7891	122.00	89.987	1114.41	0.016212	192.937000
2.8890	140.00	107.960	1121.72	0.016292	122.980000
4.5195	158.00	125.970	1129.03	0.016383	80.815600
6.8687	176.00	143.990	1136.34	0.016483	54.594100
10.1690	194.00	162.050	1143.65	0.016593	37.816900
14.6960	212.00	180.190	1150.53	0.016715	26.789100
20.7800	230.00	198.330	1156.96	0.016843	19.383400
28.7960	248.00	216.560	1163.43	0.016984	14.283400
39.1760	266.00	234.880	1169.44	0.017134	10.705100
52.4110	284.00	253.280	1175.46	0.017296	8.147720
69.0340	302.00	271.810	1181.05	0.017469	6.288190
89.6390	320.00	290.430	1185.78	0.017653	4.915120
114.8700	338.00	309.170	1190.51	0.017850	3.886290
145.4300	356.00	328.090	1194.38	0.018060	3.105090
182.0700	374.00	347.180	1197.88	0.018284	2.504410
225.5300	392.00	366.480	1200.83	0.018525	2.037330
276.7300	410.00	385.960	1202.98	0.018783	1.670120
336.5200	428.00	405.740	1204.70	0.019065	1.378540
405.8000	446.00	425.770	1205.13	0.019361	1.144840
485.5900	464.00	446.110	1205.13	0.019688	0.955858
576.9000	482.00	466.830	1204.29	0.020042	0.801797
680.8200	500.00	487.980	1202.12	0.020431	0.675143
798.4600	518.00	509.570	1199.54	0.020860	0.570225
931.0100	536.00	531.750	1195.24	0.021338	0.482670
1079.8000	554.00	554.630	1189.22	0.021873	0.409052
1246.1000	572.00	578.270	1181.91	0.022483	0.346678
1431.4000	590.00	602.780	1172.45	0.023186	0.293386
1637.3000	608.00	628.580	1160.85	0.024014	0.247494
1865.8000	626.00	656.090	1146.23	0.025020	0.207705
2118.7000	644.00	686.190	1127.74	0.026254	0.172658
2398.5000	662.00	718.870	1120.80	0.027887	0.141038
2708.4000	680.00	757.560	1066.68	0.030338	0.111213
3053.5000	698.00	813.450	1002.20	0.035560	0.078969
3090.2000	699.80	822.480	991.02	0.036681	0.074964
3127.5000	701.60	832.800	977.25	0.038123	0.070479
3164.7000	703.40	846.560	958.77	0.040205	0.064873
3203.9000	705.20	873.640	922.66	0.044850	0.055583
3208.2490	705.47	900.730	900.73	0.050777	0.050777

Source: CO-66

Table 2.30

Saturated Liquid and Saturated Steam Properties Including Pressure (P_{sat}), Temperature (T_{sat}), Saturated Liquid Enthalpy (h_f), Saturated Dry Steam Enthalpy (h_g), Saturated Liquid Specific Volume (v_f), and Saturated Dry Steam Specific Volume (v_g) in Metric Units

Temperature(°C)	p Pressure (Bar)	v - Specific Volume (cm^3/g) Water	Steam	h - Specific Enthalpy (Joules/g)* Water	Steam
0	0.006108	1.00021	206,288	-0.0416	2501
0.01	0.006112	1.00021	206,146	0.000611	2501
10	0.012271	1.0004	106,422	41.99	2519
20	0.023368	1.0018	57,836	83.86	2538
30	0.042418	1.0044	32,929	125.66	2556
40	0.073750	1.0079	19,546	167.47	2574
50	0.12335	1.0121	12,045	209.3	2592
60	0.19919	1.0171	7,677.6	251.1	2609
70	0.31161	1.0228	5,045.3	293.0	2626
80	0.47358	1.0290	3,408.3	334.9	2643
90	0.70109	1.0359	2,360.9	376.9	2660
100	1.01325	1.0435	1,673.0	419.1	2676
110	1.4327	1.0515	1,210.1	461.3	2691
120	1.9854	1.0603	891.71	503.7	2706
130	2.7011	1.0697	668.32	546.3	2720
140	3.6136	1.0798	508.66	589.1	2734
150	4.7597	1.0906	392.57	632.2	2747
160	6.1804	1.1021	306.85	675.5	2758
170	7.9202	1.1144	242.62	719.1	2769
180	10.027	1.1275	193.85	763.1	2778
190	12.553	1.1415	156.35	807.5	2786
200	15.550	1.1565	127.19	852.4	2793
210	19.080	1.1726	104.265	897.7	2798
220	23.202	1.1900	86.062	943.7	2802
230	27.979	1.2087	71.472	990.3	2803
240	33.480	1.2291	59.674	1037.6	2803
250	39.776	1.2512	50.056	1085.8	2801
260	46.941	1.2755	42.149	1135.0	2796
270	55.052	1.3023	35.599	1185.2	2790
280	64.191	1.3321	30.133	1236.8	2780
290	74.449	1.3655	25.537	1290	2766
300	85.917	1.4036	21.643	1345	2749
310	98.694	1.4475	18.316	1402	2727
320	112.89	1.4992	15.451	1462	2700
330	128.64	1.562	12.967	1526	2666
340	146.08	1.639	10.779	1596	2623
350	165.37	1.741	8.805	1672	2565
360	186.74	1.894	6.943	1762	2481
370	210.53	2.22	4.93	1892	2331
371	213.06	2.29	4.68	1913	2305
372	215.63	2.38	4.40	1937	2273
373	218.2	2.51	4.05	1969	2230
374	220.9	2.80	3.47	2032	2146
374.15 ±0.10	221.2	3.17	3.17	2095	2095

* To convert to watt-hours/g, divide by 3600.
Source: CO-66

Table 2.31

Thermal Conductivity (k) of Subcooled Liquid Water and Superheated Steam as a Function of Temperature and Pressure in English Units (Btu/hr-ft-°F)

Pressure, psia	Temperature, °F															
	32.000	122.000	212.000	302.000	392.000	482.000	572.000	662.000	705.470	752.000	797.000	842.000	887.000	932.000	1022.000	1112.000
14.504	0.32010	0.37615	0.01404	0.01652	0.01924	0.02213	0.02513	0.02837	0.02999	0.03178	0.03351	0.03525	0.03698	0.03929	0.04333	0.04738
72.519	0.32022	0.37632	0.39770	0.39833	0.01965	0.02253	0.02542	0.02831	0.02999	0.03178	0.03351	0.03525	0.03698	0.03929	0.04333	0.04738
145.038	0.32033	0.37649	0.39787	0.39857	0.02080	0.02311	0.02542	0.02889	0.03056	0.03236	0.03409	0.03582	0.03756	0.03987	0.04391	0.04738
362.596	0.32074	0.37696	0.39845	0.39920	0.38557	0.02542	0.02658	0.02947	0.03114	0.03293	0.03467	0.03640	0.03813	0.04045	0.04449	0.04796
725.191	0.32137	0.37777	0.39937	0.40036	0.38695	0.35997	0.03062	0.03120	0.03232	0.03409	0.03582	0.03756	0.03929	0.04102	0.04507	0.04911
1087.790	0.32201	0.37857	0.40030	0.40145	0.38834	0.36170	0.03756	0.03467	0.03467	0.03582	0.03756	0.03929	0.04045	0.04218	0.04622	0.05004
1450.380	0.32264	0.37938	0.40117	0.40261	0.38973	0.36344	0.31640	0.03929	0.03817	0.03813	0.03929	0.04102	0.04218	0.04391	0.04796	0.05142
1812.980	0.32328	0.38019	0.40215	0.40377	0.39111	0.36517	0.31900	0.04680	0.04345	0.04218	0.04218	0.04276	0.04449	0.04565	0.04969	0.05258
2175.570	0.32391	0.38100	0.40307	0.40436	0.39244	0.36690	0.32166	0.06067	0.05062	0.04680	0.04565	0.04565	0.04680	0.04796	0.05142	0.05431
2538.170	0.32455	0.38181	0.40400	0.40481	0.39383	0.36864	0.32426	0.23574	0.06014	0.05258	0.05027	0.04911	0.04911	0.05027	0.05316	0.05605
2900.760	0.32519	0.38262	0.40492	0.40712	0.39521	0.37037	0.32686	0.24383	0.07458	0.06182	0.05547	0.05316	0.05258	0.05258	0.05489	0.05778
3208.250	0.32573	0.38330	0.40571	0.40810	0.39639	0.37184	0.32956	0.24775	0.13369	0.07260	0.06135	0.05708	0.05552	0.05503	0.05636	0.05925

Source: CO-66

Table 2.32

Thermal Conductivity (k) of Subcooled Liquid Water and Superheated Steam as a Function of Temperature and Pressure in Metric Units (milliwatts/meter-^{o}K)

Pressure Bar	Temperature, ^{o}C 0	50	100	150	200	250	300	350	375	400	425	450	475	500	550	600
1	569*	643	24.8	28.7	33.2	38.2	43.4	49.0	51.9	54.9	58.0	61.1	64.2	67.4	73.9	80.6
5	569	644	681	687	33.8	38.6	43.8	49.4	52.3	55.3	58.3	61.4	64.5	67.7	74.3	80.9
10	570	644	681	687	35.1	39.3	44.4	49.9	52.8	55.7	58.8	61.8	65.0	68.2	74.7	81.4
25	571	645	682	688	665	42.9	46.5	51.6	54.3	57.2	60.2	63.3	66.4	69.6	76.1	82.7
50	573	647	684	690	668	618	52.5	55.4	57.6	60.2	63.0	65.9	68.9	72.0	78.4	85.0
75	575	649	686	691	670	622	63.7	60.8	62.0	63.9	66.3	68.9	71.7	74.7	80.9	87.4
100	577	651	688	693	672	625	545	68.8	67.9	68.6	70.2	72.4	74.9	77.6	83.5	89.8
125	579	653	689	695	674	629	552	81.3	75.9	74.5	74.9	76.4	78.4	80.8	86.3	92.4
150	581	655	691	696	676	633	559	104	87.5	82.2	80.7	81.0	82.4	84.3	89.3	95.1
175	583	657	693	698	679	636	565	442	106	92.6	87.9	86.5	86.9	88.3	92.5	98.0
200	585	659	695	700	681	639	571	454	126	107	96.9	93.1	92.1	92.6	96.0	101

* Non-stable phase

Source: CO-66

Table 2.33

Specific Volume (v) of Subcooled Liquid Water and Superheated Steam as a Function of Temperature and Pressure in English Units (ft^3/lb_m)

Pressure psia	Temperature, °F 32.000	122.000	212.000	302.000	392.000	482.000	572.000	662.000
14.504	0.01602	0.01621	27.166	31.011	34.807	38.53930	42.27150	45.98770
72.519	0.01602	0.01621	0.01671	0.01747	6.809	7.598	8.36941	9.13186
145.038	0.01601	0.01620	0.01671	0.01746	3.300	3.727	4.13104	4.52348
362.596	0.01600	0.01619	0.01670	0.01745	0.01851	1.394	1.584	1.75717
725.191	0.01598	0.01618	0.01667	0.01742	0.01847	0.02001	0.726	0.832
1087.790	0.01596	0.01616	0.01665	0.01740	0.01843	0.01995	0.428	0.520
1450.380	0.01594	0.01614	0.01664	0.01737	0.01839	0.01988	0.02238	0.359
1812.980	0.01592	0.01612	0.01662	0.01735	0.01836	0.01981	0.02222	0.258
2175.570	0.01590	0.01611	0.01660	0.01732	0.01832	0.01974	0.02207	0.184
2538.170	0.01588	0.01609	0.01657	0.01730	0.01828	0.01968	0.02193	0.02749
2900.760	0.01586	0.01607	0.01656	0.01727	0.01823	0.01962	0.02178	0.02667
3208.250	0.01585	0.01606	0.01654	0.01725	0.01821	0.01958	0.02168	0.02619

Source: CO-66

(continued)

Table 2.33 (continued)

Pressure psia	Temperature, °F 705.470	752.000	797.000	842.000	887.000	932.000	1022.000	1112.000
14.504	47.78260	49.70390	51.54590	53.40400	55.26210	57.10420	60.82030	64.52050
72.519	9.49703	9.88631	10.26110	10.63760	11.00920	11.38560	12.13200	12.87690
145.038	4.71071	4.90631	5.10013	5.29075	5.48136	5.67037	6.04359	6.42332
362.596	1.83764	1.92216	2.00225	2.08234	2.16243	2.24092	2.39629	2.55007
725.191	0.87777	0.92520	0.96957	1.01298	1.05543	1.09723	1.17908	1.25934
1087.790	0.55537	0.59122	0.62406	0.65562	0.68605	0.71584	0.77335	0.82909
1450.380	0.39178	0.42287	0.45043	0.47621	0.50072	0.52475	0.57040	0.61381
1812.980	0.29118	0.32052	0.34535	0.36809	0.38940	0.41631	0.44834	0.48470
2175.570	0.221	0.25068	0.27455	0.29553	0.31475	0.33317	0.36697	0.39853
2538.170	0.168	0.19958	0.22313	0.24331	0.26125	0.27807	0.30883	0.33702
2900.760	0.120	0.15938	0.18373	0.20359	0.22089	0.23675	0.26510	0.29089
3208.250	0.05078	0.13099	0.15710	0.17710	0.19399	0.20931	0.23617	0.26046

Table 2.34

Specific Volume (v) of Subcooled Liquid Water and Superheated Steam as a Function of Temperature and Pressure in Metric Units (cm^3/g)

Temperature, °C

Pressure Bar	0	50	100	150	200	250	300	350	375	400	425	450	475	500	550	600
1	1.0002	1.0121	1696	1936	2173	2406	2639	2871	2987	3103	3218	3334	3450	3565	3779	4028
5	0.9999	1.0119	1.0433	1.0906	425.1	474.4	522.5	570.1	593.7	617.2	640.6	664.1	687.5	710.8	757.4	803.9
10	0.9997	1.0117	1.0431	1.0903	206.0	232.7	257.9	282.4	294.5	306.5	318.4	330.3	342.2	354.0	377.5	401.0
25	0.9989	1.0110	1.0423	1.0894	1.1556	87.0	98.9	109.7	114.9	120.0	125.0	130.0	135.0	139.9	149.6	159.2
50	0.9976	1.0099	1.0410	1.0878	1.1531	1.2495	45.34	51.93	54.90	57.76	60.53	63.24	65.89	68.50	73.61	78.62
75	0.9964	1.0088	1.0398	1.0862	1.1507	1.2452	26.71	32.44	34.75	36.91	38.96	40.93	42.83	44.69	48.28	51.76
100	0.9952	1.0077	1.0386	1.0846	1.1483	1.2409	1.397	22.44	24.53	26.40	28.12	29.73	31.26	32.76	35.61	38.32
125	0.9940	1.0066	1.0373	1.0830	1.1460	1.2367	1.387	16.14	18.25	20.01	21.56	22.98	24.31	25.59	27.99	30.26
150	0.9928	1.0055	1.0361	1.0813	1.1436	1.2327	1.378	11.49	13.91	15.65	17.14	18.45	19.65	20.80	22.91	24.88
175	0.9915	1.0044	1.0348	1.0798	1.1414	1.2288	1.369	1.716	10.57	12.46	13.93	15.19	16.31	17.36	19.28	21.04
200	0.9904	1.0033	1.0336	1.0782	1.1391	1.2251	1.360	1.665	7.68	9.95	11.47	12.71	13.79	14.78	16.55	18.16

Source: CO-66

Table 2.35

Specific Enthalpy (h) of Subcooled Liquid Water and Superheated Steam as a Function of Temperature and Pressure in English Units (Btu/lb_m)

Pressure, psia	Temperature, °F							
	32.000	122.000	212.000	302.000	392.000	482.000	572.000	662.000
14.504	0.026	89.987	1150.53	1193.95	1236.52	1279.080	1321.640	1365.070
72.519	0.202	90.116	180.318	271.810	1228.35	1273.06	1317.350	1362.060
145.038	0.421	90.331	180.447	271.896	1216.74	1265.32	1311.760	1357.760
362.596	1.075	90.847	181.006	272.326	366.655	1238.67	1293.70	1344.000
725.191	2.171	91.793	181.780	272.971	367.085	466.832	1257.58	1319.07
1087.790	3.259	92.739	182.597	273.659	367.601	466.875	1209.86	1291.12
1450.380	4.342	93.685	183.414	274.347	368.074	466.918	577.413	1257.15
1812.980	5.417	94.587	184.231	275.035	368.547	466.961	576.124	1215.02
2175.570	6.492	95.490	185.047	275.722	369.020	467.047	575.264	1157.41
2538.170	7.567	96.436	185.864	276.410	369.536	467.133	574.404	714.995
2900.760	8.642	97.382	186.681	277.098	370.009	467.262	573.544	707.686
3208.250	9.553	98.148	187.374	277.682	370.446	467.444	572.815	702.946

Source: CO-66

(continued)

Table 2.35 (continued)

Pressure, psia	Temperature, °F 705.470	752.000	797.000	842.000	887.000	932.000	1022.000	1112.000
14.504	1386.670	1409.350	1431.710	1454.500	1476.850	1499.640	1546.080	1592.080
72.519	1383.660	1406.770	1429.560	1451.920	1474.700	1497.920	1544.360	1591.650
145.038	1379.770	1403.330	1426.120	1449.340	1472.550	1495.340	1542.210	1589.930
362.596	1368.090	1393.020	1416.660	1440.310	1464.390	1488.460	1536.620	1584.770
725.191	1346.480	1374.100	1400.320	1426.120	1451.060	1476.420	1526.300	1576.170
1087.790	1322.680	1353.890	1382.700	1410.210	1436.870	1463.530	1515.980	1567.140
1450.380	1295.780	1331.960	1364.640	1393.880	1422.680	1450.630	1505.230	1558.540
1812.980	1264.860	1307.460	1343.570	1376.250	1408.060	1437.300	1494.480	1549.510
2175.570	1227.60	1280.370	1321.210	1357.330	1390.870	1423.110	1483.300	1540.060
2538.170	1180.48	1248.980	1297.140	1337.550	1374.100	1408.920	1471.690	1530.600
2900.760	1112.42	1212.010	1270.480	1316.490	1356.470	1393.450	1460.090	1521.140
3208.250	900.731	1174.090	1244.960	1297.160	1340.790	1380.320	1449.880	1512.750

Table 2.36

Specific Enthalpy (h) of Subcooled Liquid Water and Superheated Steam as a Function of Temperature and Pressure in Metric Units (Joules/g)*

Pressure Bar	Temperature, °C															
	0	50	100	150	200	250	300	350	375	400	425	450	475	500	550	600
0	2502	2595	2689	2784	2880	2978	3077	3178	3229	3280	3332	3384	3436	3489	3597	3706
1	0.06	209.3	2676	2777	2876	2975	3074	3175	3227	3278	3330	3383	3435	3488	3596	3705
5	0.47	209.6	419.4	632.2	2857	2961	3064	3168	3220	3272	3325	3377	3430	3484	3592	3702
10	0.98	210.1	419.7	632.4	2830	2943	3051	3158	3211	3264	3317	3371	3425	3478	3587	3698
25	2.50	211.3	421.0	633.4	852.8	2881	3009	3126	3184	3240	3295	3350	3406	3462	3574	3686
50	5.05	213.5	422.8	634.9	853.8	1085.8	2925	3068	3134	3196	3257	3317	3375	3434	3550	3666
75	7.58	215.7	424.7	636.5	855.0	1085.9	2814	3003	3079	3149	3216	3280	3342	3404	3526	3645
100	10.1	217.9	426.6	638.1	856.1	1086.0	1343	2924	3017	3098	3172	3242	3309	3374	3501	3625
125	12.6	220.0	428.5	639.7	857.2	1086.1	1340	2826	2946	3041	3125	3201	3273	3343	3476	3604
150	15.1	222.1	430.4	641.3	858.3	1086.3	1338	2692	2861	2978	3073	3157	3235	3310	3450	3582
175	17.6	224.3	432.3	642.9	859.5	1086.5	1336	1663	2755	2905	3017	3111	3196	3277	3423	3560
200	20.1	226.5	434.2	644.5	860.6	1086.8	1334	1646	2605	2819	2955	3062	3155	3241	3396	3538

*To convert to watt-hours/g, divide by 3600

Source: CO-66

2.2.2 Convection Parameters

Convection data are presented for the following fluids: helium, air, water, and steam. These data may be used to calculate the convective heat transfer coefficient, h, so that the rate of heat exchange between a solid boundary and the fluid in the boundary layer can be evaluated. The convection heat transfer equation is

$$q = h\,A(T - T_\infty) \tag{2.12}$$

and

$$\phi = q/A \tag{2.107}$$

where:

ϕ = heat flux $[e/t\ell^2]$

q = rate of heat transfer from surface to fluid $[e/t]$

A = surface area over which heat transfer is being described $[\ell^2]$

h = heat transfer coefficient $[e/t\theta^2]$

T = surface temperature of the solid boundary $[\theta]$

T_∞ = fluid temperature outside the boundary layer $[\theta]$

The convective heat transfer coefficient depends on a variety of parameters related to flow conditions, fluid properties, and solid boundary configurations. In addition, the coefficient will vary with position on the solid surface. Equations 2.12 and 2.107 prescribe how the heat flux can be calculated, but the calculation is predicated on the hypothesis that the heat transfer coefficient can be evaluated. Because the heat transfer coefficient varies with position, it is convenient to evaluate and use the areal average heat transfer coefficient. Equation 2.22 can be used to obtain the areal average Nusselt number and Equation 2.21 to obtain the areal average heat transfer coefficient. Experimentally, heat transfer

coefficients are often given on an areal average basis. The heat transfer rate can then be determined from Equation 2.12.

This section describes the parameters required for the evaluation of convective heat transfer coefficients.

2.2.2.1 Dimensionless Parameters

For some conditions, the thermal boundary layer equations can be solved but an analytic solution is typically not attempted when natural or forced convection is encountered. The principal value of available solutions is that they can be used to suggest the functional form of the interdependence of system properties including the heat transfer coefficient, thermal conductivity, position along convecting surface, fluid thermodynamic and transport properties, and fluid velocity.

When a new geometric configuration is encountered, convection heat transfer coefficients can be described by a previously used general correlation. The general correlation is tailored to the new configuration by the assignment of appropriate values to the constants which appear as coefficient and exponential terms in the correlation. The empirical data are used to quantify these constants by fitting the data to the correlation. Alternatively, some investigators prefer to alter the algebraic form of the correlation to be fitted to the experimental data.

For convective heat transfer, four dimensionless groups are commonly used:

$$\text{Nusselt Number} = Nu = \frac{hL}{k} \; [\;] \tag{2.108}$$

$$\text{Reynolds Number} = Re = \frac{\rho u L}{\mu} \; [\;] \tag{2.109}$$

$$\text{Grashof Number} = Gr = \frac{g\beta L^3 \Delta T}{\nu^2} \quad [\ ] \tag{2.110}$$

$$\text{Prandtl Number} = Pr = \frac{\nu}{\alpha} \quad [\ ] \tag{2.111}$$

where

L = characteristic dimension of the solid boundary (L = diameter for pipe and duct flow) $[\ell]$

h = boundary layer heat transfer coefficient $[e/t\ell^2]$

k = fluid thermal conductivity $[e/t\ell\theta]$

ρ = fluid mass density $[m/\ell^3]$

u = velocity of fluid $[\ell/t]$

μ = fluid dynamic viscosity $[m/\ell t]$

g = local gravitational acceleration $[\ell/t^2]$

β = volumetric coefficient of thermal expansion $[1/\theta]$

ΔT = absolute value of the temperature difference between the wall and the temperature of the fluid at the outside edge of the boundary layer $(= |T - T_\infty|)$ $[\theta]$

ν = fluid kinematic viscosity $(\nu = \mu/\rho)$ $[\ell^2/t]$

α = fluid thermal diffusivity ($\alpha = k/\rho c_p$ where c_p = fluid specific heat at constant pressure) $[\ell^2/t]$

Physically, the Nusselt number is the ratio of convective heat transfer capability (which involves some conduction) of the moving fluid in the boundary layer to the conduction heat transfer capability of the fluid next to the solid boundary. The Reynolds number is the ratio of fluid inertial force to fluid viscous force in the boundary layer. The Grashof number is used in natural or free convection analogous to the way the

Reynolds number is used in forced convection. The Grashof number is the ratio of buoyant forces to viscous forces in the boundary layer. The Prandtl number is a property of the fluid. It is the ratio of the kinematic viscosity to the thermal diffusivity.

The volumetric coefficient of thermal expansion is defined as

$$\beta = \rho \left[\frac{\partial(\frac{1}{\rho})}{\partial T}\right]_p$$

$$= \frac{1}{v}\left(\frac{\partial v}{\partial T}\right)_p$$

$$= \frac{1}{T} \text{ for an ideal gas} \tag{2.112}$$

where

β = volumetric coefficient of thermal expansion [$1/\theta$]

v = specific volume [ℓ^3/m]

For fluids which do not behave as ideal gases, β can be approximated as

$$\beta = \frac{\rho_\infty - \rho}{\rho(T - T_\infty)}$$

$$= \frac{1}{v_\infty}\left(\frac{v - v_\infty}{T - T_\infty}\right) \tag{2.113}$$

in terms of conditions on both edges of the boundary layer, where T, v, and ρ are the fluid temperature, specific volume, and mass density. These properties are evaluated at the film temperature defined as the average between the wall temperature T_w and the free stream temperature T_∞.

Though less common than the four just presented, many other dimensionless groups are used in describing convection. These groups include:

$$\text{Stanton Number} = St = \frac{Nu}{R_e P_r} = \frac{h}{\rho c_p u_\infty} \tag{2.114}$$

$$\text{Peclet Number} = Pe = Re\ Pr = \frac{u_\infty L}{\alpha} \tag{2.115}$$

$$\text{Rayleigh Number} = Ra = GrPr = \frac{g\beta L^3 \Delta T}{\nu_\infty} \tag{2.116}$$

$$\text{Modified Grashof Number} = Gr' = GrNu = \frac{g\beta L^4 \Delta Th}{\nu^2 k} \tag{2.117}$$

2.2.2.2 Forced Convection

Section 2.1.2.1 presented the laminar boundary layer equations for a flat plate with a solution given by Blasius. The work of Nusselt (about 1915) led to the completely non-dimensional form of the forced convection equation, which was stated as

$$Nu = C\ Re^m\ Pr^n \tag{2.118}$$

where C, m, and n are constants.

This general form is common for the turbulent as well as for the laminar boundary layers for both external surfaces (i.e., unconfined flow) such

as walls and for internal surfaces (i.e., confined flow) such as pipes or ducts. For confined flow in ducts or pipes, the diameter is typically used as the characteristic dimension in the Nusselt and Reynolds numbers in place of characteristic length, L, or position, x, measured in the downstream direction.

If the duct is not round, the hydraulic diameter, D_h, is used where

$$D_h = \frac{4\ (\text{flow area})}{(\text{wetted perimeter})} \tag{2.119}$$

Typically, the objective of laboratory experiments is to define the parameters C, m, and n for a given convection configuration and flow conditions.

In a pipe, the transition from laminar flow to turbulent flow occurs when the Reynolds number (based on the areal average flow velocity) reaches a value of about 2,000 to 3,000. A value of 2,300 is commonly used in engineering analyses. For a flat plate, when the Reynolds number is based on a characteristic length equal to the plate dimension in the flow direction, the laminar to turbulent flow transition usually occurs in the range $100{,}000 < Re_L < 1{,}000{,}000$. In engineering analyses, a value of 3.2×10^5 is commonly assumed to be representative.

In the upstream region of the plate, the boundary layer is laminar. The heat transfer is excellent at the leading edge but diminishes rapidly in the downstream direction as shown in Figure 2.7 until the transition to turbulent flow occurs. The heat transfer diminishes because the lamina that are established in this region support a temperature gradient and tend to insulate the plate. In the transition region, the flow lines are broken up by fluid swirl and less temperature gradient can be sustained across the boundary layer. Downstream where turbulence is established, the fluid is well mixed and contacts the surface at a high frequency and thus acts as a colder and/or more accessible sink than in the laminar region. This discussion assumes the plate to be hot and the fluid cold.

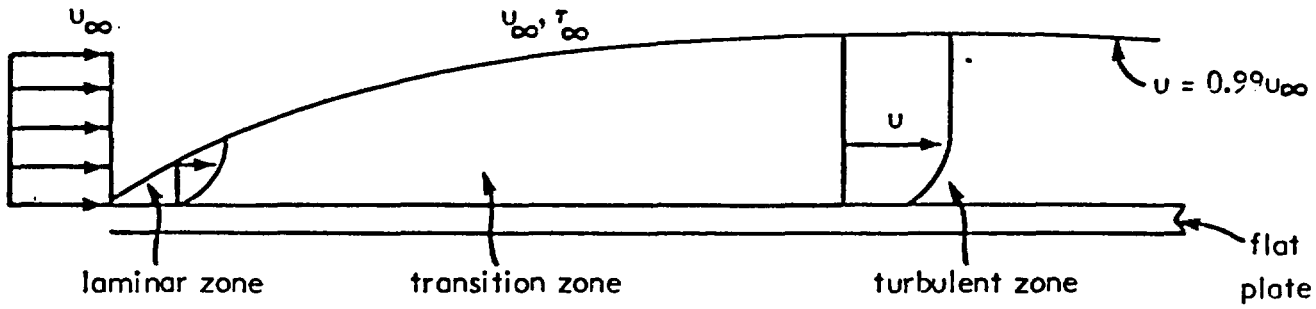

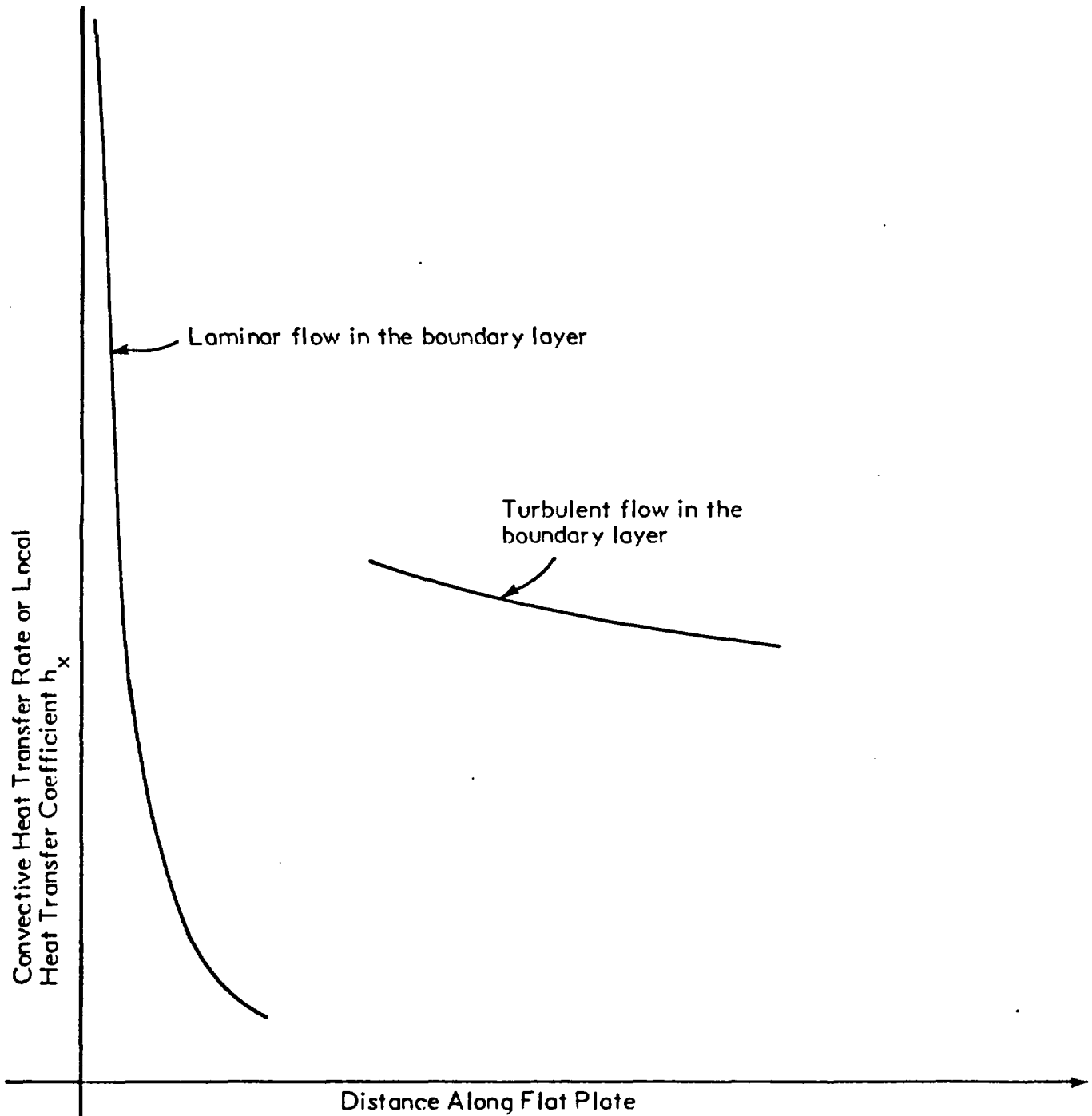

Figure 2.7

Heat Transfer as a Function of Distance along a Plate

The heat transfer rate increases very rapidly in the transition region. Figure 2.7 shows these regions and qualitatively indicates how the heat transfer rate varies with axial position. This figure illustrates the relatively high average heat transfer rate that can be sustained in the turbulent boundary layer region. The laminar region is not very effective for heat transfer because the transfer rate diminishes rapidly with distance along the plate in the flow direction and tends to have a small average value. For these reasons, most heat transfer equipment is designed for turbulent flow and higher heat transfer coefficients with the associated higher convection heat transfer rates.

As the thermal boundary layer increases to equal the inside radius in pipe flow, the free stream no longer exists. Thus, T_∞ is not used in pipe flow as the fluid reference temperature for convection calculations. The fluid reference temperature is based on the average temperature of all the mass flowing past a given cross-section of the pipe and is referred to as the bulk fluid temperature, T_b, given by

$$T_b = \frac{\int_0^R \rho u(r) c_p T r dr}{\int_0^R \rho u(r) c_p r dr} \tag{2.120}$$

where

ρ = fluid mass density [m/ℓ^3]

$u(r)$ = fluid velocity which is a function of radius at any cross-section [ℓ/t]

c_p = constant pressure specific heat of the fluid [$e/m\,\theta$]

T = fluid temperature [θ]

R = inside radius of pipe [ℓ]

r = denotes radial position in the flow stream [ℓ]

A similar relationship would be used for flow channels that are not round. The heat transfer rate between the tube wall and the fluid flowing in the pipe is given by

$$q = hA\,(T_w - T_b) \tag{2.12}$$

In regions where the boundary layer thickness is much smaller than the distance separating solid surfaces, non-planar surfaces are often treated as flat plates.

For laminar flow along a flat plate, the Nusselt number and heat transfer coefficient which resulted from the Blasius-Pohlhausen solution are:

a) For local conditions

$$Nu_x = 0.332\ Re_x^{1/2}\ Pr^{1/3} \tag{2.121}$$

$$h_x = 0.332\ (k/x)\ Re_x^{1/2}\ Pr^{1/3} \tag{2.122}$$

and

b) For the average values over the plate

$$Nu = 0.664\ Re_L^{1/2}\ Pr^{1/3} \tag{2.123}$$

$$h = 0.664\ (k/L)\ Re_L^{1/2}\ Pr^{1/3} \tag{2.124}$$

For turbulent flow along a flat plate, Whittaker has provided the following correlation:

$$\overline{Nu_L} = 0.036\ Pr^{0.43}\ (Re^{0.8} - 9200) \tag{2.125}$$

$$\bar{h}_L = 0.036\ Pr^{0.43}\ (Re^{0.8} - 9200)k/L \tag{2.126}$$

for gases and

$$\overline{Nu_L} = 0.036\ Pr^{0.43}\ (Re^{0.8} - 9200)\ (\mu_\infty/\mu_w)^{1/4} \tag{2.127}$$

$$\bar{h}_L = 0.036\ Pr^{0.43}\ (Re^{0.43} - 9200)\ (\mu_\infty/\mu_w)^{1/4}\ k/L \tag{2.128}$$

for liquids. Except for the viscosity correction term, all fluid properties are evaluated at the film temperature T_f defined as

$$T_f = (T_w + T_\infty)/2 \tag{2.129}$$

where

T_w = wall temperature [θ]

T_∞ = free stream temperature [θ]

For laminar flow in a pipe of diameter d, at low Reynolds numbers, the energy equation can be solved to give an exact solution for the Nusselt number:

$$Nu_d = hd/k \tag{2.130}$$

$$Nu_d = 4.36 \tag{2.131}$$

$$h = 4.36k/d \tag{2.132}$$

In 1930, Dittus and Boelter correlated the heat transfer coefficient for convection with turbulent flow inside automobile radiator tubes. The

correlation is widely accepted and used for flow in ducts, channels, pipes, etc., and is given by

$$\overline{Nu}_d = 0.023\ Re_d^{0.8}\ Pr^{0.4} \tag{2.133}$$

$$\bar{h}_d = 0.023\ Re_d^{0.8}\ Pr^{0.4}(k/d) \tag{2.134}$$

where the fluid properties are based on the fluid bulk temperature given by Equation 2.120.

Numerous correlations are available for various boundary configurations, flow conditions, and parameter ranges. This report presents representative correlations. The waste package thermal analysts will need to consult other sources for comprehensive treatment of forced convection correlations.

2.2.2.3 Natural Convection

Natural convection was described in Section 2.1.2.2. A principal difference between natural and forced convection is that the velocity profile diminishes to zero at the outer edge of the thermal boundary layer in natural convection. In forced convection, it reaches the free stream velocity value at the outer edge of the hydrodynamic boundary layer. The thermal and hydrodynamic boundary layers have the same thickness for natural convection.

The Grashof number plays a role in natural convection heat transfer correlations analogous to that of the Reynolds number in forced convection. The transition from laminar to turbulent boundary layer flow occurs for values of the Grashof number near 4×10^8.

A number of correlations have been presented for various configurations and flow conditions. Fishenden and Saunders (Reference FI-50) suggested

average values of Nusselt numbers and heat transfer coefficients when the Nusselt and Grashof numbers are based on properties evaluated at the film temperature given in Equation 2.129. These correlations for liquids and gases in the range of $10^5 \leq GrPr \leq 10^8$ are:

(1) Vertical plane surfaces and cylinders of large diameter (characteristic dimension is height, L)

$$\overline{Nu_L} = 0.56(Gr_L Pr)^{0.25} \quad (2.135)$$

$$\overline{h_L} = 0.56(k/L)(Gr_L Pr)^{0.25} \quad (2.136)$$

(2) Horizontal or vertical cylinders (characteristic dimension is length, L)

$$\overline{Nu_L} = 0.47(GrPr)^{0.25} \quad (2.137)$$

$$\overline{h_L} = 0.47(k/L)(GrPr)^{0.25} \quad (2.138)$$

(3) Horizontal plane facing upward (characteristic dimension is side length, L)

$$\overline{Nu_L} = 0.54(GrPr)^{0.25} \quad (2.139)$$

$$\overline{h_L} = 0.54(k/L)(GrPr)^{0.25} \quad (2.140)$$

(4) Horizontal plane facing downward (characteristic dimension is side length, L)

$$\overline{Nu} = 0.25(GrPr)^{0.25} \quad (2.141)$$

$$\overline{h_L} = 0.25(k/L)(GrPr)^{0.25} \quad (2.142)$$

For gases where $GrPr \geq 10^8$, the correlations are

(1) Vertical plane surfaces and cylinders of large diameter (characteristic dimension height L)

$$\overline{Nu_L} = 0.12(Gr_L Pr)^{0.33} \quad (2.143)$$

$$\overline{h_L} = 0.12(k/L)(Gr_L Pr)^{0.33} \quad (2.144)$$

(2) Horizontal or vertical cylinders (characteristic dimension is length L)

$$\overline{Nu_L} = 0.10(GrPr)^{0.33} \quad (2.145)$$

$$\overline{h_L} = 0.10(k/L)(GrPr)^{0.33} \quad (2.146)$$

(3) Horizontal plane facing upward (characteristic dimension is side length L)

$$\overline{Nu_L} = 0.14(GrPr)^{0.33} \tag{2.147}$$

$$\overline{h_L} = 0.14(k/L)(GrPr)^{0.33} \tag{2.148}$$

For water in the turbulent region $N_{Gr} > 4 \times 10^8$ where $GrPr > 2 \times 10^9$, Geidt (Reference GE-61) indicates that experimental data are well represented by

$$\overline{Nu} = 0.17(GrPr)^{0.33} \tag{2.149}$$

$$\bar{h} = 0.17\ (k/L)\ \ (GrPr)^{0.33} \tag{2.150}$$

where L is the vertical dimension.

2.2.2.4 Fluid Convection Properties

Fluid properties that are needed to evaluate convection correlation terms include the fluid dynamic viscosity, μ, and the volumetric coefficient of thermal expansion, β. Data are presented in Tables 2.37-2.46 for: air and helium at low pressures, saturated liquid water, dry saturated steam, subcooled water, and superheated steam. The specific volume tables for subcooled water and superheated steam that were presented in Section 2.2.1 can be used to calculate β using

$$\beta = \frac{1}{v}\left(\frac{\partial v}{\partial T}\right)_p \tag{2.151}$$

Table 2.37

Air Thermal Convection Properties at Atmospheric Pressure Including Dynamic Viscosity (μ), Mass Density (ρ), Volumetric Coefficient of Thermal Expansion (β), and Kinematic Viscosity (ν) in English Units

T (^oF)	$\mu \times 10^6$ (lb_m/ft-sec)	ρ (lb_m/ft^3)	β ($1/^oF$)	$\nu \times 10^6$ (ft^2/sec)
0	11.1	0.086	0.00218	130
32	11.7	0.081	0.00203	145
100	12.9	0.071	0.00179	180
200	14.4	0.060	0.00152	239
300	16.1	0.052	0.00132	306
400	17.5	0.046	0.00116	378
500	18.9	0.041	0.00104	455
600	20.0	0.037	0.000943	540
700	21.4	0.034	0.000862	625
800	22.5	0.031	0.000794	717
900	23.6	0.029	0.000735	815
1000	24.7	0.027	0.000685	917

Source: KR-61

Table 2.38

Air Thermal Convection Properties at Atmospheric Pressure Including Dynamic Viscosity (μ), Mass Density (ρ), Volumetric Coefficient of Thermal Expansion (β), and Kinematic Viscosity (ν) in Metric Units

T (^oC)	$\mu \times 10^6$ (kg/m-sec)	ρ (kg/m^3)	β (1/^oC)	$\nu \times 10^6$ (m^2/sec)
-17.8	16.5	1.38	0.00392	12.0
0.0	17.4	1.30	0.00365	13.4
37.8	19.2	1.14	0.00322	16.9
93.3	21.4	0.961	0.00274	22.3
148.9	24.0	0.833	0.00238	28.8
204.4	26.0	0.737	0.00209	35.3
260.0	28.1	0.657	0.00187	42.8
315.6	29.8	0.593	0.00170	50.3
371.1	31.8	0.545	0.00155	58.3
426.7	33.5	0.497	0.00143	67.4
482.2	35.1	0.465	0.00132	75.5
537.8	36.8	0.432	0.00123	85.2

Source: Derived from data in Table 2.37

Table 2.39

Helium Thermal Convection Properties at Atmospheric Pressure Including Dynamic Viscosity (μ), Mass Density (ρ), Volumetric Coefficient of Thermal Expansion (β), and Kinematic Viscosity (ν) in English Units

T (^oF)	$\mu \times 10^6$ (lb_m/ft-hr)	ρ (lb_m/ft^3)	β ($1/^oF$)	$\nu \times 10^6$ (ft^2/hr)
0	11.4	0.0120	0.00218	950
200	14.8	0.00835	0.00152	1770
400	17.8	0.00640	0.00116	2780
600	20.2	0.00520	0.000943	3890
800	22.9	0.00436	0.000794	5240

Source: KR-61

Table 2.40

Helium Thermal Convection Properties at Atmospheric Pressure Including Dynamic Viscosity (μ), Mass Density (ρ), Volumetric Coefficient of Thermal Expansion (β), and Kinematic Viscosity (ν) in Metric Units

T (^oC)	$\mu \times 10^6$ (kg/m-sec)	ρ (kg/m^3)	β ($1/^oC$)	$\nu \times 10^6$ (m^2/sec)
-17.8	17.0	0.192	0.00392	88.3
93.3	22.0	0.134	0.00274	164.4
204.4	26.5	0.103	0.00209	258.3
315.6	30.1	0.0833	0.00169	361.4
426.7	34.1	0.0698	0.00142	486.8

Source: Derived from data in Table 2.39

Table 2.41

Saturated Liquid Water Thermal Convection Properties Including Dynamic Viscosity (μ), Mass Density (ρ), Volumetric Coefficient of Thermal Expansion (β), and Kinematic Viscosity (ν) in English Units

T (^oF)	$\mu \times 10^3$ (lb_m/ft-sec)	ρ (lb_m/ft^3)	β ($1/^oF$)	$\nu \times 10^6$ (ft^2/sec)
32	1.20	62.4	-0.04	19.3
50	0.880	62.4	0.05	14.0
100	0.458	62.0	0.20	7.40
150	0.292	61.2	0.31	4.77
200	0.205	60.1	0.40	3.41
250	0.158	58.8	0.48	2.69
300	0.126	57.3	0.60	2.20
350	0.105	55.6	0.69	1.89
400	0.091	53.7	0.80	1.70
450	0.080	51.6	0.90	1.55
500	0.071	49.0	1.00	1.45
550	0.064	45.9	1.10	1.39
600	0.058	42.4	1.20	1.37

Source: KR-61

Table 2.42

Saturated Liquid Water Thermal Convection Properties Including Dynamic Viscosity (μ), Mass Density (ρ), Volumetric Coefficient of Thermal Expansion (β), and Kinematic Viscosity (ν) in Metric Units

T (^oC)	$\mu \times 10^3$ (kg/m-sec)	ρ (kg/m^3)	β ($1/^oC$)	$\nu \times 10^6$ (m^2/sec)
0.0	1.79	1000	-0.072	1.78
10.0	1.31	1000	0.09	1.31
37.8	0.682	993	0.36	0.681
65.6	0.435	980	0.56	0.443
93.3	0.305	963	0.72	0.317
121.1	0.235	942	0.86	0.250
148.9	0.188	918	1.08	0.204
176.7	0.156	891	1.24	0.176
204.4	0.135	860	1.44	0.157
232.2	0.119	827	1.62	0.144
260.0	0.106	785	1.80	0.135
287.8	0.095	735	1.98	0.129
315.6	0.086	679	2.16	0.127

Source: Derived from data in Table 2.41

Table 2.43

Dry Superheated Steam at Atmospheric Pressure Thermal Convection Properties Including Dynamic Viscosity (μ), Mass Density (ρ), Volumetric Coefficient of Thermal Expansion (β), and Kinematic Viscosity (ν) in English Units

T (^oF)	$\mu \times 10^6$ (lb_m/ft-sec)	ρ (lb/ft^3)	β ($1/^oF$)	$\nu \times 10^6$ (ft^2/sec)
212	8.70	0.0372	0.00149	234
300	10.0	0.0328	0.00132	305
400	11.3	0.0288	0.00116	392
500	12.7	0.0257	0.00104	494
600	14.2	0.0233	0.000943	609
700	15.6	0.0213	0.000862	732
800	17.0	0.0196	0.000794	867
900	18.1	0.0181	0.000735	1000
1000	19.2	0.0169	0.000685	1136

Source: KR-61

Table 2.44

Dry Superheated Steam at Atmospheric Pressure Thermal Convection Properties Including Dynamic Viscosity (μ), Mass Density (ρ), Volumetric Coefficient of Thermal Expansion (β), and Kinematic Viscosity (ν) in Metric Units

T (^oC)	$\mu \times 10^6$ (kg/m sec)	ρ (kg/m^3)	β ($1/^oC$)	$\nu \times 10^6$ (m^2/sec)
100.0	12.9	0.596	0.00268	21.7
148.9	14.9	0.525	0.00238	28.3
204.4	16.8	0.461	0.00209	36.4
260.0	18.9	0.412	0.00187	45.9
315.6	21.1	0.373	0.00170	56.6
371.1	23.2	0.341	0.00155	68.0
426.7	25.3	0.314	0.00143	80.5
482.2	26.9	0.290	0.00132	92.9
537.8	28.6	0.271	0.00123	105.5

Source: Derived from data in Table 2.43

Table 2.45

Dynamic Viscosity (μ) of Subcooled Liquid Water and Superheated Steam as a Function of Temperature and Pressure in English Units (lb_m/ft-hr)

Pressure, psia	Temperature, °F								
	32.000	122.000	212.000	302.000	392.000	482.000	572.000	662.000	705.470
14.504	4.23996	1.31647	0.02929	0.03423	0.03914	0.04408	0.04899	0.05382	0.05628
72.519	4.23657	1.31672	0.67517	0.43834	0.03875	0.04388	0.04894	0.05395	0.05642
145.038	4.23246	1.31720	0.67565	0.43858	0.03834	0.04369	0.04891	0.05416	0.05657
362.596	4.22012	1.31817	0.67662	0.43955	0.32537	0.04301	0.04877	0.05443	0.05705
725.191	4.19932	1.31986	0.67832	0.44076	0.32706	0.26271	0.04853	0.05528	0.05789
1087.790	4.17851	1.32180	0.68001	0.44221	0.32876	0.26441	0.04819	0.05620	0.05888
1450.380	4.15795	1.32349	0.68170	0.44366	0.33021	0.26634	0.22328	0.05719	0.06004
1812.980	4.13714	1.32542	0.68340	0.44511	0.33190	0.26828	0.22449	0.05903	0.06148
2175.570	4.11634	1.32712	0.68509	0.44632	0.33359	0.27021	0.22570	0.06144	0.06331
2538.170	4.09578	1.32881	0.68678	0.44777	0.33529	0.27191	0.22745	0.17853	0.06591
2900.760	4.07497	1.33075	0.68848	0.44923	0.33674	0.27384	0.22836	0.17998	0.07031
3208.250	4.05733	1.33218	0.68991	0.45046	0.33817	0.27548	0.22959	0.18162	0.10402

Source: CO-66

(continued)

Table 2.45 (continued)

Pressure, psia	Temperature, °F 752.000	797.000	842.000	887.000	932.000	1022.000	1112.000	1202.000	1292.000
14.504	0.05883	0.06130	0.06377	0.06621	0.06868	0.07361	0.07852	0.08346	0.08837
72.519	0.05898	0.06142	0.06389	0.06633	0.06880	0.07371	0.07862	0.08356	0.08847
145.038	0.05912	0.06157	0.06401	0.06648	0.06892	0.07383	0.07874	0.08365	0.08856
362.596	0.05956	0.06198	0.06442	0.06686	0.06931	0.07417	0.07906	0.08397	0.08885
725.191	0.06036	0.06275	0.06515	0.06754	0.06996	0.07480	0.07964	0.08450	0.08936
1087.790	0.06128	0.06360	0.06594	0.06829	0.07066	0.07545	0.08024	0.08506	0.08987
1450.380	0.06232	0.06454	0.06682	0.06911	0.07144	0.07613	0.08087	0.08564	0.09043
1812.980	0.06353	0.06561	0.06778	0.07001	0.07226	0.07685	0.08152	0.08624	0.09098
2175.570	0.06498	0.06684	0.06887	0.07100	0.07318	0.07765	0.08222	0.08687	0.09156
2538.170	0.06674	0.06829	0.07011	0.07207	0.07414	0.07848	0.08295	0.08752	0.09217
2900.760	0.06906	0.06998	0.07151	0.07327	0.07521	0.07937	0.08372	0.08822	0.09280
3208.250	0.07183	0.07177	0.07288	0.07442	0.07622	0.08017	0.08442	0.08882	0.09333

Table 2.46

Dynamic Viscosity (μ) of Subcooled Liquid Water and Superheated Steam as a Function of Temperature and Pressure in Metric Units (micropoise)

Pressure Bar	Temperature, °C																	
	0	50	100	150	200	250	300	350	375	400	425	450	475	500	550	600	650	700
1	17500*	5440	121.1	141.5	161.8	182.2	202.5	223	233	243	253	264	274	284	304	325	345	365
5	17500	5440	2790	1810	160.2	181.4	202.3	223	234	244	254	264	274	284	305	325	345	366
10	17500	5440	2790	1810	158.2	180.6	202.2	224	234	244	255	265	275	285	305	326	346	366
25	17500	5440	2800	1820	1340	177.8	201.6	225	236	246	256	266	276	287	307	327	347	367
50	17500	5450	2800	1820	1350	1070	200.6	229	240	250	259	269	279	289	309	329	349	369
75	17500	5450	2800	1830	1350	1080	199.2	232	244	253	263	273	282	292	312	332	352	372
100	17500	5450	2810	1830	1360	1080	905	236	249	258	267	276	286	295	315	334	354	374
125	17500	5460	2810	1840	1360	1090	911	244	254	263	271	280	289	299	318	337	357	376
150	17400	5460	2820	1840	1370	1100	917	254	262	269	276	285	294	302	321	340	359	379
175	17400	5460	2820	1850	1380	1100	924	723	273	276	282	290	298	307	324	343	362	381
200	17400	5460	2830	1860	1380	1100	930	735	291	286	289	296	303	311	328	346	365	384

* The entry shown for 0°C and 1 bar relates to a metastable liquid state. The stable state is solid here.

Source: CO-66

2.2.3 Radiation Parameters

2.2.3.1 Stefan-Boltzmann Constant

The Stefan-Boltzmann constant is:

$$\sigma = 0.1712 \times 10^{-8} \text{ Btu/hr-ft}^2\text{-}^{o}\text{R}^4$$

$$\sigma = 1.355 \times 10^{-12} \text{ cal/sec-cm}^2\text{-}^{o}\text{K}^4$$

$$\sigma = 5.67 \times 10^{-8} \text{ W/m}^2\text{-}^{o}\text{K}^4$$

2.2.3.2 Emissivity Data

Table 2.47 presents surface emissivity data for various solid materials of interest in waste package design.

2.2.3.3 View Factors

For waste package analysis, the most frequently encountered geometry of bodies between which radiation heat exchange occurs is expected to be concentric cylinders. This is fortunate because, if the cylinders can be treated as infinite in length (a treatment compatible with the vast majority of one-dimensional conduction analyses), the view factor for the smaller cylinder is unity. This assumes there is no absorbing medium between the surfaces such as a gas or that the medium has a negligible effect if it is present.

Table 2.47

Values of Surface Emissivity
for Solid Materials

	T (^oF)	ε
Cast Iron		
recently machined	72	0.44
machined and heated	1620	0.6
machined and heated	1810	0.7
smooth, oxidized	130	0.78
smooth, oxidized	520	0.82
Carbon Steel		
oxidized steel	390	0.79
oxidized steel	1100	0.79
Stainless Steel		
304-42 hrs at 530^oF	220	0.62
polished	100	0.13

Sources: GE-61, oxidized steel, smooth oxidized cast iron
BA-78, 304-42 hrs at 530^oF
polished stainless steel
HO-81, machined cast iron, machined and heated cast iron

Analysts who encounter other geometric configurations between which radiative heat transfer is occurring can use Equation 2.52 and Figure 2.5 to evaluate the view factor by performing the double integral. The following references can be consulted for tables and graphs of view factors: BA-78, PE-73, HO-67, and SI-68.

3.0 STRUCTURAL MECHANICS

3.1 Analytical Techniques

3.1.1 Objectives of Analysis

The purpose of analytical structural mechanics, as it relates to waste package performance, is to evaluate conditions in a constrained structure when expected service loads act on that structure. The conditions are monitored as responses, such as displacements, deformations, strains, and stresses. Mechanical analysis is performed and structural conditions are monitored so that the responses for all the anticipated loading cases can be evaluated against responses that have been found to allow acceptable service for the life of the structure.

3.1.2 Structural Analysis Approaches

Structural analysis tends to follow one of two approaches. The first approach is the use of formulas that typically are solutions to continuous differential equations. These formulas are usually taken from strength of materials, mechanics of materials, and theory of elasticity texts for structures whose geometry, loading, constraints, and material properties are well defined. Formulas are available for most problems that can be solved analytically with reasonable resources. The formulas are precise analytical solutions that aid in the understanding of mechanics and complement information gained experimentally. The formulas should be used only for conditions similar to those in the analytical problem for which the solutions were derived. The proper application of formulas is instructive, straightforward, and reliable. However, for complex problems, analytical solutions are often not available.

The second method of analysis is the use of finite increment techniques, including finite element and finite difference methods. The use of finite increment methods requires specifying a structure as an assemblage of discrete interactive parts. This simplification in problem

formulation reduces the differential equations describing structural response to algebraic equations and allows analysis of more intricate structures than does the "formula" method.

These finite increment methods are usually applied using a computer and computer program to order and automate the solution procedure. Such programs typically solve a set of coupled algebraic equations for the displacement of points (nodes) whose coordinates are defined for the structure before application of the loads. The equations are coupled because the nodes are connected to various other nodes by elements with particular stiffness characteristics.

By specifying the stiffness characteristics of each element of the constrained structure and applying displacement compatibility of elements and force equilibrium at a common node, one can evaluate: the deflection of nodes; deformation of structural elements between nodes; the forces and strains in structural elements at various nodes; and finally the stresses in the elements. Adjacent elements with heterogeneous characteristics such as different materials can be represented. This is in contrast to the differential equations which are applicable to a continuum. Thus, the finite increment methods are very adaptable to solving actual problems. This adaptation involves up-front simplifications yielding sets of algebraic equations that can be solved using computer methods. Finite increment methods can generally be applied successfully to most simple and complex engineering mechanics problems.

In general, the use of formulas is restricted to relatively simple geometries (e.g., slabs, cylinders, or spheres) and constant material properties. Since many engineering structures have complex geometries, the use of formulas is often restricted to conceptual design analysis, design tradeoffs, or scoping studies. Geometrically complex structures that undergo inelastic deformation (e.g., plastic deformation due to yielding or creep) generally can not be analyzed using formulas.

By contrast, finite increment methods can be applied to more complex geometries, varying material properties, and inelastic deformation.

Often in the design and analysis of a structure, formulas are used for the initial screening and selection of candidate designs. Candidate designs are then analyzed in more detail using finite increment methods.

3.2 Mechanics Principles

3.2.1 Displacement, Deformation, and Strain

A structure should be able to carry the imposed loading conditions envisioned during its service life without incurring significant distortions. This is necessary to maintain stability and to maintain tolerances with interfacing equipment. Also, the design of the structure must be adequate to prevent instantaneous failure.

Distortion causes common structural materials such as steel to lose ductility.* If large distortions occur, the material may become brittle in local regions and fracture. Theories of failure have been developed for various classes of materials, but ductile structural metals such as steels usually experience shear failure when loaded excessively. Shear failure is described in Appendix C (see the Tresca criterion). Limiting deformation is the most direct means of preventing structural failure.

Many conditions must be specified in order to perform this analysis of a structure. One must specify the location of the structure in space. Geometric deformation conditions due to loading are described in terms of the displacements u, v, and w along the Cartesian coordinates x, y, and z or, along the polar coordinates, r, θ, and z, at a general point in the structure.

*Ductility is the capability of the material to deform without cracking or rupturing. A brittle material is one that has very little ductility. For example, soft copper is a ductile material, while glass has very little ductility.

The state of strain at a point is unique but can be expressed in various coordinate systems, one of which is typically advantageous in offering a simpler analysis of a given structure. Strains are nondimensional deformations, defined in terms of displacements, that have been normalized to the initial dimensions. Strain at a point in a continuous structure is a tensor quantity having a particular plane, direction, and magnitude associated with its various components. One normal strain component is associated with each coordinate direction. The normal strain components are defined mathematically as

$$\varepsilon_x = \frac{\partial u}{\partial x} ; \quad \varepsilon_y = \frac{\partial v}{\partial y} ; \quad \varepsilon_z = \frac{\partial w}{\partial z} \tag{3.1}$$

where

$\varepsilon_x, \varepsilon_y, \varepsilon_z$ are the normal strains and

u, v, w are the displacements from the initial shape in the x, y, and z directions

The differential displacement is the deformation component of the material. The x and y directed components of normal strain are shown in Figure 3.1.

Similarly, there are three components of shear strain. There is one associated with each of the three orthogonal coordinate system planes that intersect at the point (x, y, z). The shear strain due to forces (shear stresses) acting along perpendicular planes is equal to the decrement of an initial right angle drawn on the material that was coincident with the two coordinate system planes before the strain (i.e., prior to the loading being applied). The strain component associated with the xy plane is:

$$\gamma_{xy} = \alpha + \beta \tag{3.2}$$

$u_1 c_1$ 0

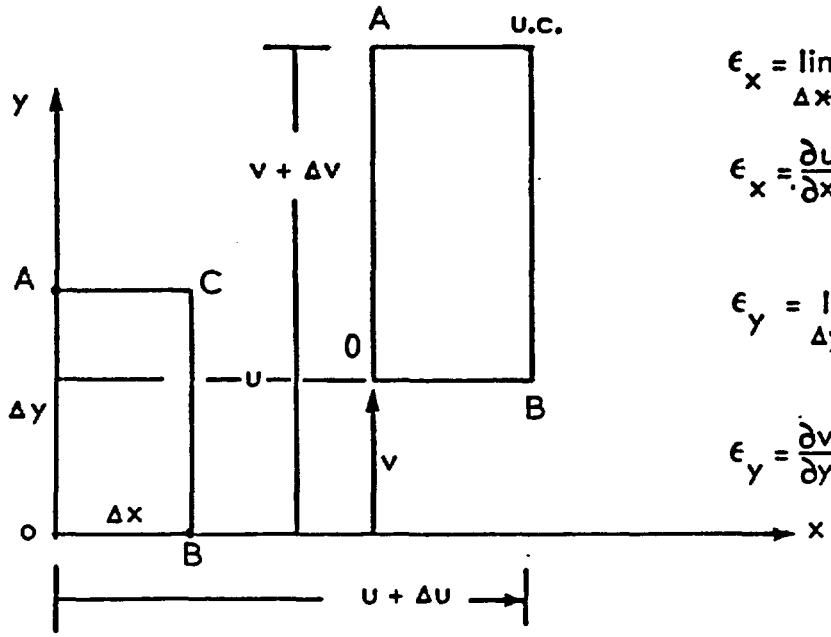

$$\epsilon_x = \lim_{\Delta x \to 0} \frac{u + \frac{\Delta u}{\Delta x} x - u}{\Delta_x}$$

$$\epsilon_x = \frac{\partial u}{\partial x}$$

$$\epsilon_y = \lim_{\Delta y \to 0} \frac{v + \frac{\Delta v}{\Delta y} \Delta_y - v}{\Delta_y}$$

$$\epsilon_y = \frac{\partial v}{\partial y}$$

a) Pure normal strain in x direction and in y direction due to forces (axial stresses) acting in x and in y directions

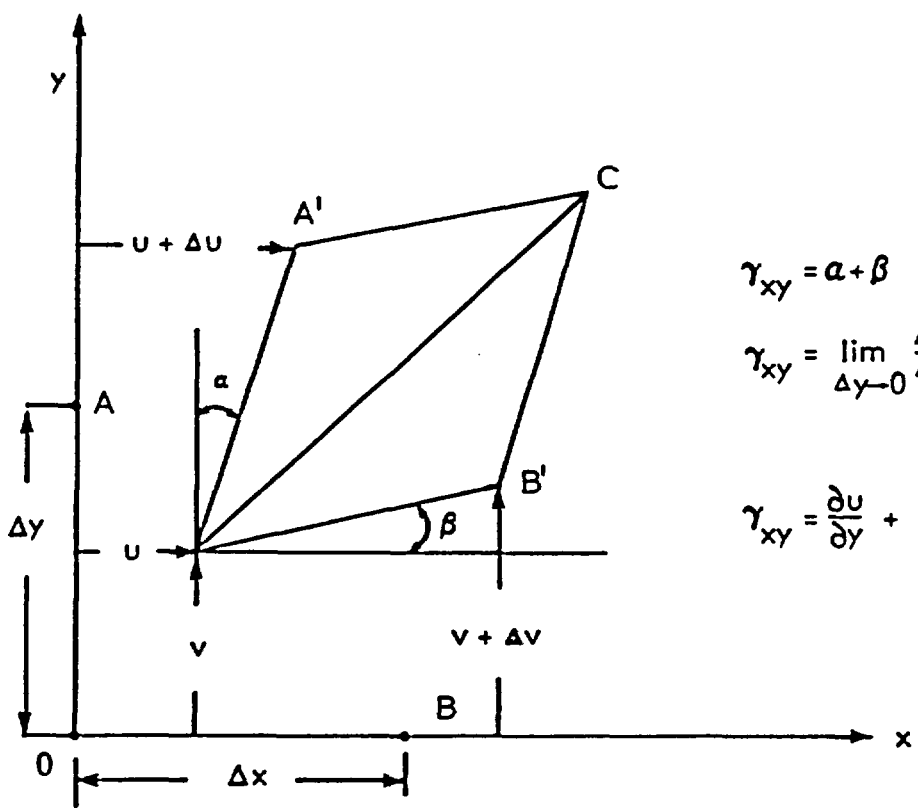

$$\gamma_{xy} = \alpha + \beta$$

$$\gamma_{xy} = \lim_{\Delta y \to 0} \frac{\Delta u}{\Delta y} + \lim_{\Delta x \to 0} \frac{\Delta v}{\Delta x}$$

$$\gamma_{xy} = \frac{\partial u}{\partial y} + \frac{\partial v}{\partial x}$$

b) Pure strain in x - y plane due to forces (shear stresses) acting along x - z and y - z planes

Figure 3.1

Strain Components Related Geometrically to Displacements

Figure 3.1 shows how shear strain components are related geometrically to displacements.

The three shear strain components can be written in terms of the displacements as

$$\gamma_{xy} = \frac{\partial u}{\partial y} + \frac{\partial v}{\partial x} \; ; \quad \gamma_{yz} = \frac{\partial v}{\partial z} + \frac{\partial w}{\partial y} \; ; \quad \gamma_{xz} = \frac{\partial u}{\partial z} + \frac{\partial w}{\partial x} \tag{3.3}$$

where

$\gamma_{xy}, \gamma_{yz}, \gamma_{xz}$ = shear strains

u, v, w = displacements from the initial shape to the strained state in the x, y, and z directions, respectively

The strain matrix consists of six strain components with potentially unique magnitudes* and is used with sign conventions to describe the state of strain at a point. In matrix form, the strain is defined in terms of the component magnitudes as:

$$\varepsilon = \begin{bmatrix} \varepsilon_x & \frac{1}{2}\gamma_{xy} & \frac{1}{2}\gamma_{xz} \\ \frac{1}{2}\gamma_{xy} & \varepsilon_y & \frac{1}{2}\gamma_{yz} \\ \frac{1}{2}\gamma_{xz} & \frac{1}{2}\gamma_{yz} & \varepsilon_z \end{bmatrix} \tag{3.4}$$

*As a consequence of force equilibrium (Section 3.2.2), $\gamma_{xy} = \gamma_{yx}$ $\gamma_{yz} = \gamma_{zy}$, and $\gamma_{xz} = \gamma_{zx}$.

The matrix elements denote the magnitudes of strains. Both the magnitude and direction of the strains are shown in Figure 3.1.

Principal strains at a point in the structure are the normal strains occurring along a set of coordinates which are normal to a set of three intersecting orthogonal planes on which there is no shear strain. These planes will remain fixed in space as strains are induced. The normal vectors may change magnitude but not direction. These planes are the principal planes, and the normals are the principal directions. The strains in the principal directions are the principal strains. Mohr's diagrams for principal strains are discussed in Appendix B. The principal strains ε_1, ε_2, and ε_3 are the three real roots of the equation

$$\varepsilon^3 - I_{\varepsilon 1} \; \varepsilon^2 + I_{\varepsilon 2} \, \varepsilon - I_{\varepsilon 3} = 0 \tag{3.5}$$

where the coefficients $I_{\varepsilon 1}$, $I_{\varepsilon 2}$, and $I_{\varepsilon 3}$ are the strain invariants:

$$I_{\varepsilon 1} = \varepsilon_x + \varepsilon_y + \varepsilon_z = \varepsilon_1 + \varepsilon_2 + \varepsilon_3 \tag{3.6}$$

$$I_{\varepsilon 2} = \varepsilon_x\varepsilon_y + \varepsilon_y\varepsilon_z + \varepsilon_x\varepsilon_z - \frac{\gamma^2_{xy}}{4} - \frac{\gamma^2_{yz}}{4} - \frac{\gamma^2_{xz}}{4} = \varepsilon_1\varepsilon_2 + \varepsilon_2\varepsilon_3 + \varepsilon_1\varepsilon_3 \tag{3.7}$$

$$I_{\varepsilon 3} = \varepsilon_x\varepsilon_y\varepsilon_z - \frac{\varepsilon_x\gamma^2_{yz}}{4} - \frac{\varepsilon_y\gamma^2_{zx}}{4} - \frac{\varepsilon_z\gamma^2_{xy}}{4} + \frac{\gamma_{xy}\gamma_{yz}\gamma_{xz}}{4} = \varepsilon_1\varepsilon_2\varepsilon_3 \tag{3.8}$$

The first strain invariant is equal to the volumetric strain and is often referred to as the dilation. The notation is:

$$\Delta = \frac{\delta V}{V} = I_{\varepsilon 1} \tag{3.9}$$

where

Δ = volumetric strain

V = original volume

δV = change in volume

The direction cosines of the principal plane (ℓ, m, and n) with respect to an arbitrary plane, p, are given by

$$\ell^2 = \frac{\left(\frac{\gamma_p}{2}\right)^2 + (\varepsilon_p-\varepsilon_2)\ (\varepsilon_p-\varepsilon_3)}{(\varepsilon_1-\varepsilon_2)\ (\varepsilon_1-\varepsilon_3)} \tag{3.10}$$

$$m^2 = \frac{\left(\frac{\gamma_p}{2}\right)^2 + (\varepsilon_p-\varepsilon_2)\ (\varepsilon_p-\varepsilon_3)}{(\varepsilon_2-\varepsilon_3)\ (\varepsilon_2-\varepsilon_1)} \tag{3.11}$$

$$n^2 = \frac{\left(\frac{\gamma_p}{2}\right)^2 + (\varepsilon_p-\varepsilon_1)\ (\varepsilon_p-\varepsilon_2)}{(\varepsilon_3-\varepsilon_1)\ (\varepsilon_3-\varepsilon_2)} \tag{3.12}$$

where γ_p and ε_p are the shear strain and normal strain for plane p. The Mohr diagram methods discussed in Appendix B are used to determine the principal strains and their directions.

To aid in envisioning and handling the strain tensor, it is conceptualized in two parts: a spherical part and a deviatoric part. The spherical part is:

$$s_{ij} = \begin{bmatrix} \frac{\Delta}{3} & 0 & 0 \\ 0 & \frac{\Delta}{3} & 0 \\ 0 & 0 & \frac{\Delta}{3} \end{bmatrix} \tag{3.13}$$

where s_{ij} is the spherical strain tensor and represents a dilation (or shrinking) of the original geometry with an associated change in volume. The deviator strain is given by

$$d_{ij} = \begin{bmatrix} \varepsilon_x - \frac{\Delta}{3} & \frac{1}{2}\gamma_{xy} & \frac{1}{2}\gamma_{xz} \\ \frac{1}{2}\gamma_{xy} & \varepsilon_y - \frac{\Delta}{3} & \frac{1}{2}\gamma_{yz} \\ \frac{1}{2}\gamma_{xz} & \frac{1}{2}\gamma_{yz} & \varepsilon_z - \frac{\Delta}{3} \end{bmatrix} = \begin{bmatrix} e_x & \frac{1}{2}\gamma_{xy} & \frac{1}{2}\gamma_{xz} \\ \frac{1}{2}\gamma_{xy} & e_y & \frac{1}{2}\gamma_{yz} \\ \frac{1}{2}\gamma_{xz} & \frac{1}{2}\gamma_{yz} & e_z \end{bmatrix} \tag{3.14}$$

where

d_{ij} = deviatoric strain

e_x, e_y, e_z = deviatoric strain components

$\frac{\Delta}{3}$ = mean strain

The deviatoric strain tensor represents a change in shape without any change in volume. Failure in ductile structural metals is closely related to the state of deviatoric strain and relatively independent of the spherical strain. Deviatoric strain invariants exist but are not commonly used and thus not included here.

The maximum shear strains are given by:

$$\gamma_1 = |\varepsilon_2 - \varepsilon_3| \tag{3.15}$$

$$\gamma_2 = |\varepsilon_1 - \varepsilon_3| \tag{3.16}$$

$$\gamma_3 = |\varepsilon_1 - \varepsilon_2| \tag{3.17}$$

The largest of the three maximum shear strains is the key index of failure for ductile metals.

For some types of analyses, particularly those dealing with energy methods, strain rates are used. The strain rates are defined as:

$$\dot{\varepsilon}_x = \frac{\partial v_x}{\partial x} \; ; \quad \dot{\varepsilon}_y = \frac{\partial v_y}{\partial y} \; ; \quad \dot{\varepsilon}_z = \frac{\partial v_z}{\partial z} \tag{3.18}$$

$$\dot{\gamma}_{xy} = \frac{\partial v_x}{\partial y} + \frac{\partial v_y}{\partial x} \; ; \quad \dot{\gamma}_{yz} = \frac{\partial v_y}{\partial z} + \frac{\partial v_z}{\partial y} \; ; \quad \dot{\gamma}_{xz} = \frac{\partial v_x}{\partial z} + \frac{\partial v_z}{\partial x} \tag{3.19}$$

where

$\dot{\varepsilon}_x, \dot{\varepsilon}_y, \dot{\varepsilon}_z$ = normal axial strain rate components

$\dot{\gamma}_{xy}, \dot{\gamma}_{yz}, \dot{\gamma}_{xz}$ = shear strain rate components

v_x, v_y, v_z = time rate of displacement in x, y, and z directions respectively

All of the preceding relationships given for strains are equally valid for strain rates. Strain rate tensors, deviatoric strain rates, strain rate invariants, principal strain rates, and principal shear strain rates are used in various relationships.

In 1828, Poisson studied material behavior and found that the ratio of the magnitude of strain in a lateral direction (in which there is no applied load) to that in the direction coincident with uniaxial loading

varies with material type. When a tensile load is applied, there is an elongation strain (conventionally positive) in the loading direction and a contraction strain (conventionally negative) in each of two directions which are orthogonal to the loading direction and mutually orthogonal. The Poisson ratio, which is a property of a material, is defined as

$$\mu = \frac{-(\text{lateral strain})}{\text{axial strain}} \tag{3.20}$$

3.2.2 Internal Loads and Stresses

Loads, including forces and moments, are transmitted internally throughout a structure. Both uniform and nonuniform forces may act over a cross-sectional area due to these internal loads. It is necessary to determine the local material loading due to its variation with position. Ultimately, loads must be compared to the load-carrying ability of the material so that conclusions regarding structural adequacy can be made. The structural load and the material's load-carrying capability are specified conveniently on a uniform force per unit area basis. This quantity is called stress or allowable stress for the material. Stress is a convenient basis for judging structural adequacy of low-performance structures (those subject to short term loading, room temperature, and no plastic deformation).

Because internal loads in a cross section vary with position, it is necessary to base the stress on a very small area at a point in the cross section, which can be compared to the material allowable stress. The definition of normal stress component is

$$\sigma_x = \lim_{A \to 0} \left(\frac{F}{A}\right) \tag{3.21}$$

where

F = net traction load on area A in the x direction [f]

A = cross-sectional area [ℓ^2]

σ_x = stress component in x direction (tensile stress is conventionally positive) [f/ℓ^2]

This equation is typically written

$$\sigma_x = \frac{F_x}{A} \tag{3.22}$$

where

F_x = axial force in x direction [f]

A = area in yz plane of cross section [ℓ^2]

It is understood that the force on a small local area must be considered if a nonuniform load distribution is present. The gross cross-sectional quantities can be used if the force is uniformly distributed over the area.

Any force acting on the plane of the cross section can be specified in terms of two orthogonal forces, F_y and F_z, acting on one of the faces parallel to the yz plane. In general, these forces vary with position over the cross section and are specified for the local infinitesimal area at a point to give the following shear stress components at that point:

$$\tau_{xy} = \lim_{A \to 0}\left(\frac{F_y}{A}\right) \tag{3.23}$$

$$\tau_{xz} = \lim_{A \to 0} \left(\frac{F_z}{A} \right) \tag{3.24}$$

where

τ_{xy} = shear stress component perpendicular to the x direction in the y direction $[f/\ell^2]$

τ_{xz} = shear stress component perpendicular to the x direction in the z direction $[f/\ell^2]$

These equations are typically written:

$$\tau_{xy} = \frac{F_y}{A} \tag{3.25}$$

$$\tau_{xz} = \frac{F_z}{A} \tag{3.26}$$

where

F_y = force in y direction $[f]$

F_z = force in z direction $[f]$

A = area in yz plane $[\ell^2]$

The force on a small area at a particular point must be considered when a significant variation of F_y or F_z occurs over A.

For a general point in a structure (where the load components act in all three directions, F_x, F_y, and F_z, and the cross-sectional area does not lie

in a single coordinate system plane), there are three normal stress components (σ_x, σ_y, and σ_z) and six shear stress components (τ_{xy}, τ_{yx}, τ_{xz}, τ_{zx}, τ_{yz}, τ_{zy}). The first subscript of the shear stresses denotes the axis to which the stress is normal and the second the direction of the associated force component causing the stress. Because of the different directions of the shear stresses, in general, the vectors:

$$\tau_{xy} \neq \tau_{yx}$$

$$\tau_{xz} \neq \tau_{zx}$$

$$\tau_{yz} \neq \tau_{zy} \tag{3.27}$$

The τ_{ij} are tensor components that act on different planes and have different directions. The differences in the τ_{xy} and τ_{yx} components can be investigated for a body acted upon by pure shear as shown in Figure 3.2. Moment equilibrium can be applied at point O about the z axis:

$$\circlearrowleft + \sum M_o = 0 = |\tau_{yx}| \ (\Delta x \Delta z)\Delta y - |\tau_{xy}| \ (\Delta y \Delta z)\Delta x \tag{3.28}$$

which indicates

$$|\tau_{xy}| = |\tau_{yx}| \tag{3.29}$$

which means the two components have equal magnitudes. This is also true for

$$|\tau_{yz}| = |\tau_{zy}| \tag{3.30}$$

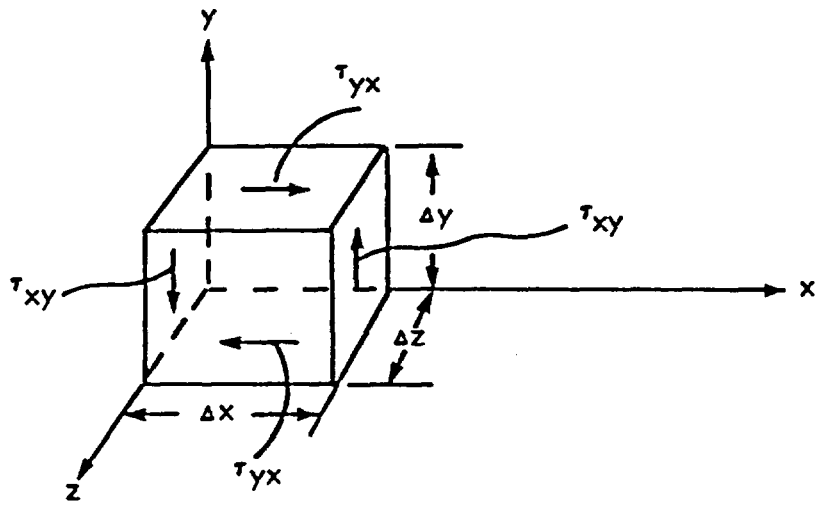

(a) Element in pure shear (no traction stresses) with two of six shear stress components being non-zero

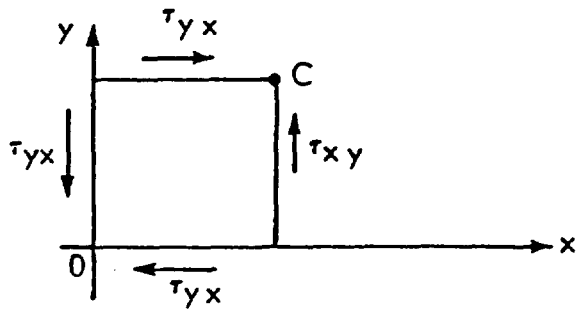

(b) Two dimensional x-y view of the pure shear element of (a).

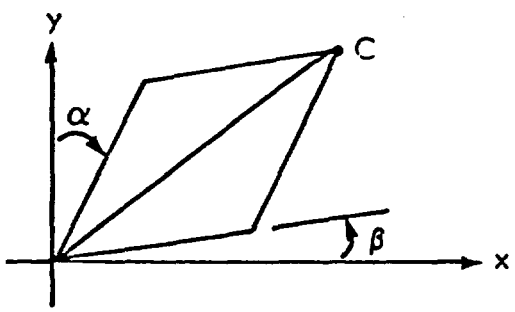

(c) Two dimensional view of deformed shape of pure shear element.

Figure 3.2

Two of the Possible Six Shear Components Acting on (a) 3D Element; (b) 2D Element; and (c) the Deformed Shape Due to Strain Angles (α and β)

$$|\tau_{xz}| = |\tau_{zx}| \tag{3.31}$$

Equation 3.29, which results from moment equilibrium, requires

$$\alpha = \beta \tag{3.32}$$

as shown in Figure 3.2(c) and also in Figure 3.1(b), providing that the material is isotropic. This means the deformation is symmetric about a line through points O and C in these figures.

The general state of stress at a point is defined if the three traction stress components and six shear stress components shown in Figure 3.3 have specified magnitudes. The faces they act on and their conventional positive directions are defined in Figure 3.3. The back faces have normal and shear stress components in opposite directions.

The stress matrix consists of six components with potentially unique magnitudes and is used with our sign conventions of Figures 3.1 and 3.3 to describe the state of stress at a point:

$$[\sigma] = \begin{bmatrix} \sigma_x & \tau_{xy} & \tau_{xz} \\ \tau_{xy} & \sigma_y & \tau_{yz} \\ \tau_{xz} & \tau_{yz} & \sigma_z \end{bmatrix} \tag{3.33}$$

where

σ_x, σ_y, σ_x = traction stress components (negative if compressive)

τ_{xy}, τ_{yz}, τ_{xz} = shear stress components

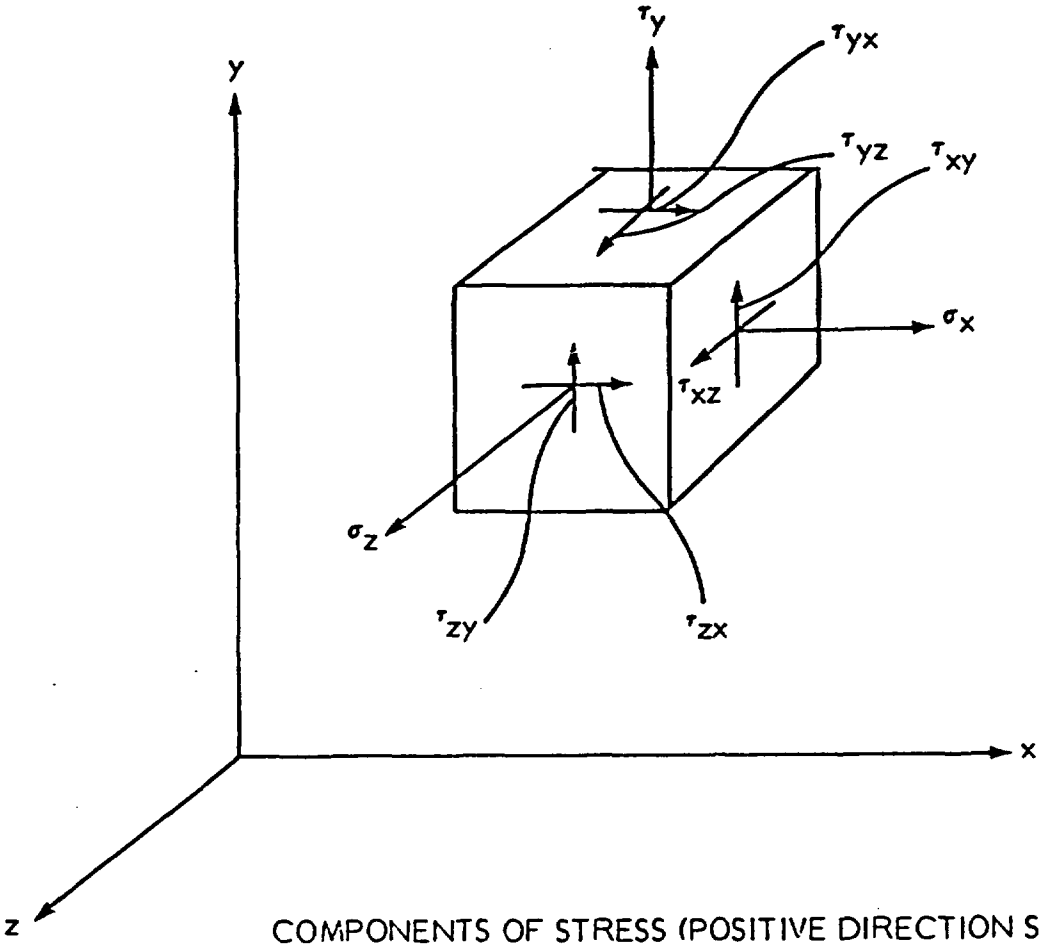

COMPONENTS OF STRESS (POSITIVE DIRECTION SHOWN)

Figure 3.3

General State of Stress at a Point Defined in Terms of Three Traction Components and Six Shear Components. The Back Faces Have Oppositely Directed Traction and Shear Components Which Are Not Shown.

Principal stresses at a point in the structure are the traction (tension or compression) stresses occurring along a set of coordinates which are normal to a set of three mutually orthogonal planes on each of which there is no shear stress. The principal stresses occur normal to the principal planes and are coincident with principal strains. A set of principal stresses can be found for any generalized state of stress. The Mohr diagram method presented in Appendix B illustrates the process graphically.

The principal stresses σ_1, σ_2, and σ_3 are the three real roots of the equation

$$S^3 - I_1 S^2 + I_2 S - I_3 = 0 \tag{3.34}$$

where

$$I_1 = \sigma_x + \sigma_y + \sigma_z \tag{3.35}$$

$$I_2 = \sigma_x\sigma_y + \sigma_y\sigma_z + \sigma_x\sigma_z - \tau_{xy}^2 - \tau_{yz}^2 - \tau_{xz}^2 \tag{3.36}$$

$$I_3 = \sigma_x\sigma_y\sigma_z + 2\tau_{xy}\tau_{yz}\tau_{xz} - \sigma_x\tau_{yz}^2 - \sigma_y\tau_{xz}^2 - \sigma_z\tau_{xy}^2 \tag{3.37}$$

For a particular state of stress, the coefficients in Equation 3.34 are related to a unique set of principal planes and are independent of the initial coordinate system used to specify the structure's geometry and loading. The coefficients are known as the stress invariants and can be defined in terms of the principal stress components as

$$I_1 = \sigma_1 + \sigma_2 + \sigma_3 \tag{3.38}$$

$$I_2 = \sigma_1\sigma_2 + \sigma_2\sigma_3 + \sigma_1\sigma_3 \tag{3.39}$$

$$I_3 = \sigma_1\sigma_2\sigma_3 \tag{3.40}$$

To aid in envisioning and handling the stress tensor, it is conceptualized in two parts: a mean part and a deviatoric part. The mean stress σ_m is defined as:

$$\sigma_m = \frac{1}{3}(\sigma_1 + \sigma_2 + \sigma_3) = \frac{1}{3}(\sigma_x + \sigma_y + \sigma_z) = \frac{I_1}{3} \tag{3.41}$$

The mean stress, also known as the spherical stress, is independent of direction. For the special case of

$$\sigma_x = \sigma_y = \sigma_z = \sigma_m = \frac{I_1}{3} \tag{3.42}$$

the mean stress is defined as the hydrostatic stress. Physically, the hydrostatic state of stress has very little influence on failure. The spherical stress tensor is written

$$S_{ij} = \sigma_m\delta_{ij} = \begin{bmatrix} \sigma_m & 0 & 0 \\ 0 & \sigma_m & 0 \\ 0 & 0 & \sigma_m \end{bmatrix} \tag{3.43}$$

where

δ_{ij} is the Kronecker delta or substitution tensor defined by $\delta_{ij} = 0$ for $i \neq j$ and $\delta_{ij} = 1$ for $i = j$

The stress deviator tensor is given by

$$D_{ij} = \sigma_{ij} - S_{ij} \tag{3.44}$$

or

$$D_{ij} = \begin{bmatrix} \sigma_x - \sigma_m & \tau_{xy} & \tau_{xz} \\ \tau_{yz} & \sigma_y - \sigma_m & \tau_{yz} \\ \tau_{zx} & \tau_{zy} & \sigma_z - \sigma_m \end{bmatrix} . \tag{3.45}$$

The stress deviator tensor in terms of the principal stress is

$$D_{ij} = \begin{bmatrix} \sigma_1 - \sigma_m & 0 & 0 \\ 0 & \sigma_2 - \sigma_m & 0 \\ 0 & 0 & \sigma_3 - \sigma_m \end{bmatrix} \tag{3.46}$$

or from Equation 3.45 for a general state of stress

$$D_{ij} = \begin{bmatrix} S_x^* & \tau_{xy} & \tau_{xz} \\ \tau_{yx} & S_y^* & \tau_{yz} \\ \tau_{zx} & \tau_{zy} & S_z^* \end{bmatrix} \tag{3.47}$$

where S_x^*, S_y^*, and S_z^* are the deviatoric stress components.

Since any state of stress in general has invariants, the deviatoric stress tensor can be shown to have invariants defined as

$$J_1 = S_x^* + S_y^* + S_z^* = 0 \tag{3.48}$$

$$\begin{aligned} J_2 &= \frac{1}{2}\left(S_x^{*2} + S_y^{*2} + S_z^{*2} + 2\tau_{xy}^2 + 2\tau_{yz}^2 + 2\tau_{xz}^2\right) \\ &= \frac{1}{2}\left(S_1^2 + S_2^2 + S_3^2\right) \end{aligned} \tag{3.49}$$

$$J_3 = \begin{vmatrix} S_x & \tau_{xy} & \tau_{xz} \\ \tau_{xy} & S_y & \tau_{yz} \\ \tau_{xz} & \tau_{yz} & S_z \end{vmatrix} = 1/3\left(S_1^3 + S_2^3 + S_3^3\right) \tag{3.50}$$

where S_1, S_2, and S_3 are the principal deviatoric stress components.

Parameters formulated in terms of the stress invariants are used to indicate stress conditions in a structure. Their values can be compared to experimentally determined values at failure for the same material

type to judge structural adequacy. For example, the octahedral normal and octahedral shear stresses are defined as:

$$\sigma_{oct} = \frac{1}{3}(\sigma_1 + \sigma_2 + \sigma_3) = \sigma_m \tag{3.51}$$

$$\tau_{oct} = \sqrt{\frac{1}{3}(S_1^2 + S_2^2 + S_3^2)} = \sqrt{\frac{2}{3} J_2} \tag{3.52}$$

where

σ_{oct} = octahedral normal stress

τ_{oct} = octahedral shear stress

These stresses act on a plane intersecting the principal axes at equal angles. The name of these stresses derives from the fact that the plane surface that they act on makes up one-eighth of a regular octahedron about the origin.

The maximum shear stress is a very important quantity as it is a direct index to the failure of ductile materials. It is given by

$$\tau_{max} = \max(\tau_A, \tau_B, \tau_C) \tag{3.53}$$

where τ_A, τ_B, and τ_C are the maximum shear stress on a two-dimensional basis

$$\tau_A = \frac{1}{2}|\sigma_2 - \sigma_1|$$

$$\tau_B = \frac{1}{2}|\sigma_3 - \sigma_1|$$

$$\tau_C = \frac{1}{2}|\sigma_2 - \sigma_3| \tag{3.54}$$

and where σ_1, σ_2, and σ_3 are the principal stresses.

The maximum shear stresses on a two-dimensional basis, τ_A, τ_B, and τ_C, occur on planes that are at 45° to the principal stress directions determined on a two-dimensional basis.

3.2.3 Constitutive Relationships

3.2.3.1 Types of Constitutive Relationships and Their Uses

Constitutive relationships are mathematical expressions that describe the essence of the primary physical interaction that occurs in a solid body or structure. The relationship is between the response expressed in terms of strain and the stresses that are a direct consequence of the internal loads carried by the structure.

The constitutive relationship is the most basic relationship between the variables in a structural analysis method as it describes the fundamental cause-effect relationship between internal loading per unit area (stress) and the response stated in terms of strain. The relationship is defined in mathematical form and contains parameters whose values pertain to a particular material type. The relationship is usually limited to a particular category of strain. These strain categories are typically:

- Instantaneous linear elastic
- Instantaneous plastic
- Long-term creep

The first two strain categories are instantaneous effects; the third is cumulative over the time of loading. The third method can produce cumulative strains over time along with the instantaneous strains from either of the first two categories. Generally, creep strain increases with higher stress levels and higher material temperatures.

When a tensile specimen fails, the failure for the material is reported in terms of either reduction of area at the point of failure or elongation per unit length in one of several standard gauge length sections in which the failure occurred. These data are closely related to strain. Strain is a more general index from which to judge structural adequacy than is stress. If structural service is such that the instantaneous response is in the linear elastic or plastic range and the loading duration is short and temperatures not excessive (about 30 years and 700°F is acceptable for many structural steels), then creep strain contributions to failure can be neglected. When time of loading and/or temperature values are high, neglecting the creep strain can lead to faulty conclusions regarding structural adequacy. Both instantaneous and creep strains cause the ductility of the material to be consumed. Since the loading on waste packages is expected to have a duration that is among the longest of all engineered structures and the temperature is elevated, it is important that the adequacy of these structures be judged on the basis of total strain. Analysis programs for assessing waste package systems deal with the overall effects of the radiation, corrosion, leaching, and thermal models and attempt to facilitate a waste package barrier structural adequacy evaluation. Stress analysis methods based only on instantaneous strains are not adequate for this determination.

Figure 3.4 outlines some key considerations involved in applying structural criteria. An infrastructure of criteria has not yet been developed for the waste package, so Figure 3.4 should be considered conceptual. At level 1, the structural loading and geometry are reviewed to see if thermal loads are applied. Thermal loads result if the structure is constrained against free expansion and part or all of the structure is at a temperature different from the temperature that existed when no loads were present and the constraints exerted no reaction loads.

If thermal loads do occur, then the thermal strain ε^T occurs compatible with the temperature conditions, T; constraints, c; element stiffnesses, k; and the condition that each node remains in force equilibrium, e.

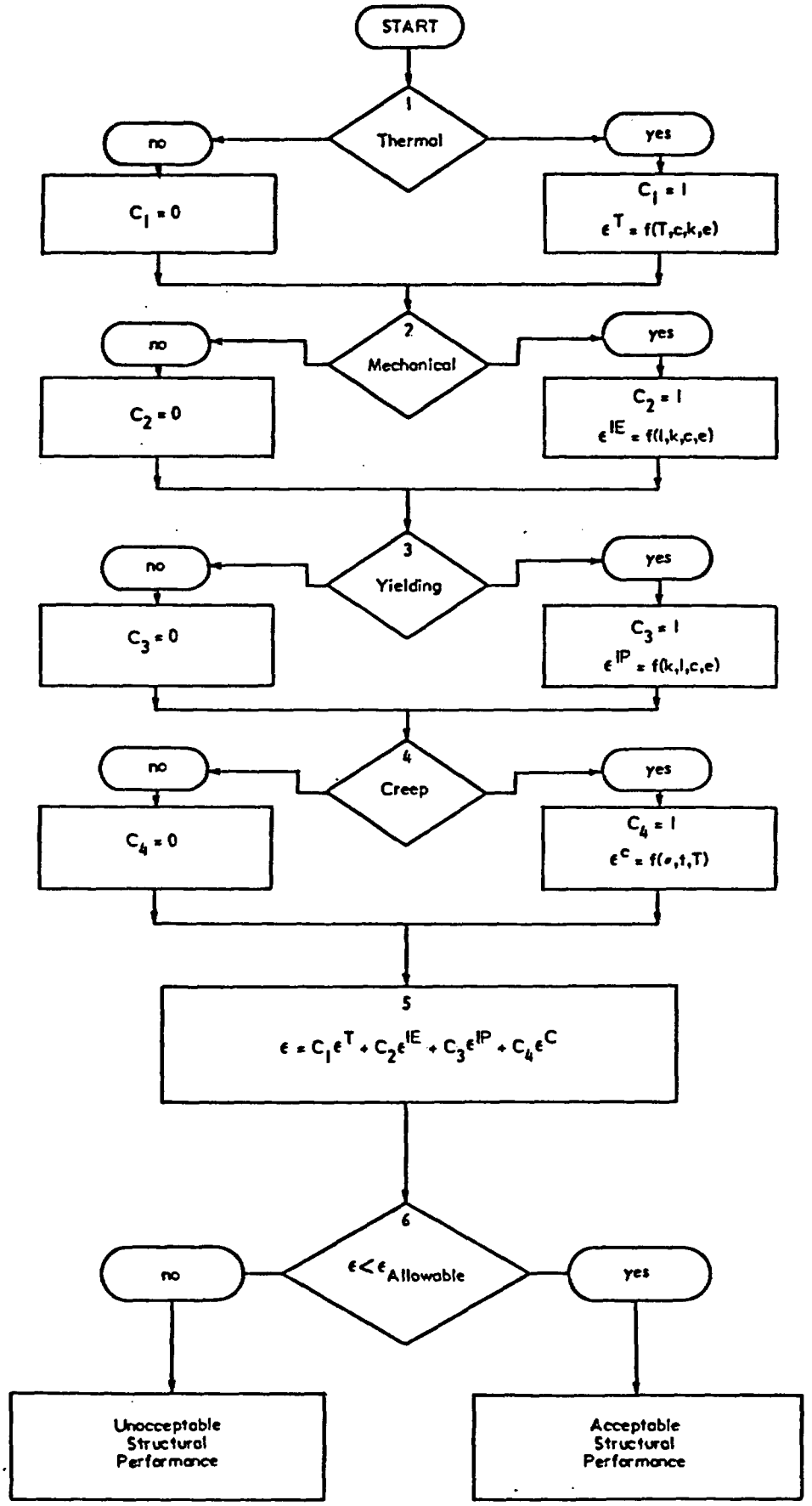

Figure 3.4

Conceptual Structural Criteria Application Procedure

At level 2, the mechanical load case, concurrent with the thermal load, results in a linear-elastic strain response. The instantaneous elastic strain ε^{IE} is a function of the internal loads, ℓ; element stiffness, k; constraints, c; and the condition of force equilibrium, e, is maintained at each node.

At level 3, a stress analysis can be made. The purpose of the stress analysis is to determine whether yielding has occurred for the concurrent instantaneous thermal and mechanical load cases or individually if there is no concurrency. This check could be made for metals with either the Tresca or von Mises yield criteria as presented in Appendix C. If yielding has not occurred and creep effects are known to be negligible, a stress analysis may be adequate as an overall structural analysis approach. If plastic deformation has occurred, strain limits are appropriate and best suited to judging structural adequacy. For a yielded structure, the instantaneous plastic strain ε^{IP} can be evaluated for ductile metals using the Prandtl-Reuss equations with the von Mises yield criterion. The procedure is similar to evaluating the instantaneous elastic strain ε^{IE} except that the loads are applied incrementally and summed for the entire loading.

For cases where loads are of long duration, temperatures are elevated, and stress levels are high, the creep strain can be significant in comparison to the instantaneous strains. Creep strains tend to consume the ductility of metals and cause metals to approach failure. When a structure may be susceptible to creep, rational design requires that the creep strain be evaluated (or estimated). This is typically accomplished by using a correlation for creep strain, ε^{C}, with the state of stress, σ; time duration of loading, t; and temperature T as independent parameters.

After the instantaneous strains are evaluated at levels 1, 2, and 3 and the creep strain is evaluated at level 4 for particular concurrent thermal and mechanical load cases, the total strain can be evaluated at level 5. At level 6, the design adequacy is evaluated by comparison to allowable

strain values. The strains resulting from various load set combinations should be superimposed to obtain the response to all concurrent loading. Strains should be categorized as membrane or bending stress and individual limits imposed. To evaluate waste package performance, criteria need to be defined for the various strain categories.

3.2.3.2 Generalized Linear Elastic Mechanical and Thermal Constitutive Relationships

In 1678, Robert Hooke published a linear constitutive relationship for elastic materials when loaded in tension. This constitutive relationship is known as Hooke's law and, when generalized to include thermal strains for either tension or compression loads for an isotropic material in three dimensions, becomes

$$\varepsilon_{ij}^{E} = \frac{1}{G}\sigma_{ij} - \delta_{ij}\left[\frac{\sigma_{ij}}{2G} + \frac{\nu}{E}\phi - \alpha T\right] \tag{3.55}$$

$$G = \frac{E}{2(1+\nu)} \tag{3.56}$$

$$\phi = \sigma_x + \sigma_y + \sigma_z = I_1 \tag{3.57}$$

where

E = elastic (or Young's) modulus $[f/\ell^2]$

ν = Poisson's ratio [ ]

G = shear modulus $[f/\ell^2]$

α = coefficient of thermal expansion $[1/\theta]$

T = temperature elevation above reference temperature $[\theta]$

δ_{ij} = Kronecker delta, = 1 for $i = j$ and = 0 for $i \neq j$

δ_{ij} = stress tensor $[f/\ell^2]$

ε_{ij}^E = elastic strain tensor

and where the constitutive equation can be written in terms of the strain components as

$$\varepsilon_x^E = \frac{1}{E}\left[\sigma_x - \nu(\sigma_y + \sigma_z)\right] + \alpha T$$

$$\varepsilon_y^E = \frac{1}{E}\left[\sigma_y - \nu(\sigma_x + \sigma_z)\right] + \alpha T$$

$$\varepsilon_z^E = \frac{1}{E}\left[\sigma_z - \nu(\sigma_x + \sigma_y)\right] + \alpha T$$

$$\varepsilon_{xy}^E = \gamma_{xy}^E = \frac{1}{G}\ \tau_{xy} = \frac{2(1+\nu)}{E}\ \tau_{xy}$$

$$\varepsilon_{yz}^E = \gamma_{yz}^E = \frac{1}{G}\ \tau_{yz} = \frac{2(1+\nu)}{E}\ \tau_{yz}$$

$$\varepsilon_{xz}^E = \gamma_{xz}^E = \frac{1}{G}\ \tau_{xz} = \frac{2(1+\nu)}{E}\ \tau_{xz} \qquad (3.58)$$

Equation 3.58 can be presented in matrix form as:

$$\begin{Bmatrix} \varepsilon_x^E \\ \varepsilon_y^E \\ \varepsilon_z^E \\ \varepsilon_{xy}^E \\ \varepsilon_{yz}^E \\ \varepsilon_{xz}^E \end{Bmatrix} = \begin{bmatrix} \frac{1}{E} & -\frac{\nu}{E} & -\frac{\nu}{E} & 0 & 0 & 0 & 1 \\ -\frac{\nu}{E} & \frac{1}{E} & -\frac{\nu}{E} & 0 & 0 & 0 & 1 \\ -\frac{\nu}{E} & -\frac{\nu}{E} & \frac{1}{E} & 0 & 0 & 0 & 1 \\ 0 & 0 & 0 & \frac{1}{G} & 0 & 0 & 0 \\ 0 & 0 & 0 & 0 & \frac{1}{G} & 0 & 0 \\ 0 & 0 & 0 & 0 & 0 & \frac{1}{G} & 0 \end{bmatrix} \begin{Bmatrix} \sigma_x \\ \sigma_y \\ \sigma_z \\ \tau_{xy} \\ \tau_{yz} \\ \tau_{zx} \\ \alpha T \end{Bmatrix} \tag{3.59}$$

Hooke's law applies to isotropic materials. For orthotropic materials, the properties E, ν, G, and α used in the formulation have values that can be different in each of the three coordinate directions.

The generalized Hooke's law can be written for the stress tensor as

$$\sigma_{ij} = \lambda\delta_{ij}\,(\theta^E - 3\alpha T) + G\left[\varepsilon_{ij}^E + \delta_{ij}\,(\varepsilon_{ij}^E - \alpha T)\right] \tag{3.60}$$

where

$$\theta^E = \varepsilon_x^E + \varepsilon_y^E + \varepsilon_z^E = I_1' \tag{3.61}$$

and where λ is known as Lame's constant and G is the shear modulus. Lame's constant, λ, can be expressed in terms of the elastic modulus, E, and the Poisson ratio, ν:

$$\lambda = \frac{\nu E}{(1 + \nu)(1 - 2\nu)} \tag{3.62}$$

The other functions in Equation 3.60 have been defined previously.

The Cartesian stress tensor written in terms of the various strain components is

$$\begin{aligned}
\sigma_x &= \lambda(\varepsilon_x^E + \varepsilon_y^E + \varepsilon_z^E - 3\alpha T) + 2G(\varepsilon_x^E - \alpha T) \\
\sigma_y &= \lambda(\varepsilon_x^E + \varepsilon_y^E + \varepsilon_z^E - 3\alpha T) + 2G(\varepsilon_y^E - \alpha T) \\
\sigma_z &= \lambda(\varepsilon_x^E + \varepsilon_y^E + \varepsilon_z^E - 3\alpha T) + 2G(\varepsilon_z^E - \alpha T) \\
\sigma_{xy} &= G\varepsilon_{xy}^E = \tau_{xy} = G\gamma_{xy}^E \\
\sigma_{yz} &= G\varepsilon_{yz}^E = \tau_{yz} = G\gamma_{yz}^E \\
\sigma_{xz} &= G\varepsilon_{xz}^E = \tau_{xz} = G\gamma_{xz}^E
\end{aligned} \tag{3.63}$$

In Equations 3.60 and 3.63 for the normal stress components, the first term is the stress associated with dilation or volume change, and the second term is the deviatoric stress associated with distortion of the shape as strain progresses.

Equation 3.63 applies to isentropic material behavior and can be written in matrix form as

$$\begin{Bmatrix} \sigma_x \\ \sigma_y \\ \sigma_z \\ \tau_{xy} \\ \tau_{yz} \\ \tau_{xz} \end{Bmatrix} = \begin{bmatrix} (\lambda+2G) & \lambda & \lambda & 0 & 0 & 0 & -(3\lambda+2G) \\ \lambda & (\lambda+2G) & \lambda & 0 & 0 & 0 & -(3\lambda+2G) \\ \lambda & \lambda & (\lambda+2G) & 0 & 0 & 0 & -(3\lambda+2G) \\ 0 & 0 & 0 & G & 0 & 0 & 0 \\ 0 & 0 & 0 & 0 & G & 0 & 0 \\ 0 & 0 & 0 & 0 & 0 & G & 0 \end{bmatrix} \begin{Bmatrix} \varepsilon_x^{IE} \\ \varepsilon_y^{IE} \\ \varepsilon_z^{IE} \\ \gamma_{xy}^{IE} \\ \gamma_{yz}^{IE} \\ \gamma_{xz}^{IE} \\ \alpha T \end{Bmatrix} \tag{3.64}$$

For orthotropic material behavior, E, G, and λ may have different values in each of the coordinate directions.

The coefficients of thermal expansion for structural metals are typically very small ($10^{-5} < \alpha < 10^{-6}$) when α is expressed in [1/°F] units. For this reason, the thermal strains are usually treated along with the elastic strains. The elastic strains are frequently small in comparison to plastic strains. Thermal strains in structural metals are frequently neglected if plastic strains occur. However, an analyst must be cognizant of the magnitude of the strain components that are being neglected relative to those that are retained.

The values of E, ν, G, λ, and the bulk modulus, K, are all referred to as elastic constants. Only two of these are independent, and thus any two can be used to describe the material behavior. In terms of the modulus of elasticity and Poisson's ratio, the shear modulus, Lame's constant, and the bulk modulus are given by:

$$G = \frac{E}{2(1 + \nu)} \tag{3.56}$$

$$\lambda = \frac{E\nu}{(1 + \nu)(1 - 2\nu)} \tag{3.62}$$

$$K = \frac{E}{3(1 - 2\nu)} \tag{3.65}$$

Table 3.1 gives the complete set of relationships between the elastic constants. These constants are listed in Tables 3.2 through 3.17 for a number of materials of interest in waste package analysis.

3.2.3.3 Yield Strength, Ultimate Tensile Strength, and Ultimate Compressive Strength

Most structural engineering materials have an initial linear elastic region in which deformation can be treated as reversible and time-independent. At the proportional elastic limit, the stress-strain relationship begins to display nonlinear behavior. At the elastic limit (frequently indistinguishable from the proportional elastic limit), some non-recoverable plastic deformation remains after the release of the load. If the stress is increased above the elastic limit, the stress-strain relationship departs more and more from a linear relationship. When a specimen that has been loaded beyond the elastic limit is unloaded, a permanent deformation is observable. This deformation is the basis for determining the yield strength. The stress that causes a 0.20 percent permanent strain upon specimen unloading is defined as the 0.20 percent yield strength.

The ultimate tensile strength is the maximum stress in tension sustained by a material at failure. The ultimate compressive stress is the maximum stress in compression sustained by a material in failure. Most ductile materials (e.g., mild steels) exhibit similar ultimate compression and

Table 3.1

Relationships between Isotropic Elastic Constants

	LAME CONSTANTS		YOUNG'S MOD.	POISSON'S RATIO	BULK MOD.
	λ	G(SHEAR MOD.)	E	ν	K
λ,G	--	--	$\frac{G(3\lambda + 2G)}{\lambda + G}$	$\frac{\lambda}{2(\lambda + G)}$	$\frac{3\lambda + 2G}{3}$
λ,E	--	$\frac{(E-3\lambda) + \sqrt{(E-3\lambda)^2 + 8\lambda E}}{4}$	--	$\frac{-(E+\lambda) + \sqrt{(E+\lambda)^2 + 8\lambda^2}}{4\lambda}$	$\frac{(3\lambda+E) + \sqrt{(3\lambda+E)^2 - 4\lambda E}}{6}$
λ,ν	--	$\frac{\lambda\ (1-2\nu)}{2\nu}$	$\frac{\lambda(1+\nu)\ (1-2\nu)}{\nu}$	--	$\frac{\lambda(1+\nu)}{3\nu}$
λ,K	--	$\frac{3\ (K-\lambda)}{2}$	$\frac{9K(K-\lambda)}{3K-\lambda}$	$\frac{\lambda}{3K-\lambda}$	--
G,E	$\frac{(2G-E)G}{E-3G}$	--	--	$\frac{E-2G}{2-G}$	$\frac{GE}{3(3G-E)}$
G,ν	$\frac{2G\nu}{(1-2\nu)}$	--	$2G(1+\nu)$	--	$\frac{2G(1+\nu)}{3(1-2\nu)}$
G,K	$\frac{3K-2G}{3}$	--	$\frac{9KG}{3K+G}$	$\frac{1}{2}\left[\frac{3K-2G}{3K+G}\right]$	--
E,ν	$\frac{\nu E}{(1+\nu)\ (1-2\nu)}$	$\frac{E}{2(1+\nu)}$	--	--	$\frac{E}{3(1-2\nu)}$
E,K	$\frac{3K(3K-E)}{9K-E}$	$\frac{3EK}{9K-E}$	--	$\frac{1}{2}\left[\frac{3K-E}{3K}\right]$	--
ν,K	$\frac{3K\nu}{1+\nu}$	$\frac{3K(1-2\nu)}{2(1+\nu)}$	$3K(1-2\nu)$	--	--

Table 3.2

Zircaloy 2 Tubing Mechanical Properties as a Function of Temperature in English Units

T (^oF)	E (10^6 psi)	ν (-)	G (10^6 psi)	λ (10^6 psi)	K (10^6 psi)	α ($10^{-6}/^oF$) Longitudinal	Transverse	Radial
75	13.8	.32	5.24	9.06	12.6	4.62	6.58	8.71
100	13.7					4.62	6.58	8.81
200	13.2					4.62	6.58	8.71
300	12.7					4.62	6.58	8.71
332	12.5	.41	4.43	20.41	23.2	4.62	6.58	8.71
400	12.2					4.62	6.58	8.71
500	11.7					4.62	6.58	8.71
600	11.2					4.62	6.58	8.71
700	10.7					4.62	6.58	8.71
800	10.2					4.62	6.58	8.71
900	9.7					4.62	6.58	8.71
1000	9.2					4.62	6.58	8.71
1100	8.7					4.62	6.58	8.71

Legend

E - Elastic Modulus - Longitudinal Direction
ν - Poisson's Ratio
G - Shear Modulus (Lame's Constant μ)
λ - Lame's Constant
K - Bulk Modulus
α - Mean Coefficient of Thermal Expansion from 86^oF to Indicated Temperature
Coordinate definition
z - longitudinal
θ - transverse
r - radial

Source: SC-65

Table 3.3

Zircaloy 2 Mechanical Properties as a Function of Temperature in Metric Units

T (^oC)	E (MPa)	ν (-)	G (MPa)	λ (MPa)	K (MPa)	α $10^{-6}/^oC$ Longitudinal	Transverse	Radial
23.9	9.52×10^4	0.32	3.61×10^4	6.25×10^4	8.69×10^4	8.32	11.84	15.68
37.8	9.45×10^4					8.32	11.84	15.68
93.3	9.10×10^4					8.32	11.84	15.68
148.9	8.76×10^4					8.32	11.84	15.68
166.7	8.62×10^4	0.41	3.06×10^4	14.08×10^4	16.14×10^4	8.32	11.84	15.68
204.4	8.41×10^4					8.32	11.84	15.68
260.4	8.07×10^4					8.32	11.84	15.68
315.6	7.72×10^4					8.32	11.84	15.68
371.1	7.38×10^4					8.32	11.84	15.68
426.7	7.03×10^4					8.32	11.84	15.68
482.2	6.69×10^4					8.32	11.84	15.68
537.8	6.34×10^4					8.32	11.84	15.68
593.3	6.00×10^4					8.32	11.84	15.68

Legend

E - Elastic Modulus-Longitudinal Direction (Transverse Direction)
ν - Poisson's Ratio
G - Shear Modulus (Lame's Constant μ)
λ - Lame's Constant
K - Bulk Modulus
α - Mean Coefficient of Thermal Expansion from 30^oC to the Indicated Temperature
Coordinate definition
z - longitudinal
θ - transverse
r - radial

Source: Derived from data in Table 3.2

Table 3.4

Zircaloy 4 Mechanical Properties as a Function of Temperature in English Units

T (^oF)	E (10^6 psi)	ν (-)	G (10^6 psi)	λ (10^6 psi)	K (10^6 psi)	α ($10^{-6}/^oF$) Longitudinal	α ($10^{-6}/^oF$) Radial
75	15.4	0.296	5.94	8.62	12.58	-	-
100	15.2	0.294	5.87	8.38	12.30	-	-
200	14.3	0.287	5.56	7.49	11.19	2.75	1.60
300	13.5	0.280	5.27	6.71	10.23	3.00	2.22
400	12.6	0.273	4.95	5.95	9.25	3.20	2.31
500	11.8	0.266	4.66	5.30	8.40	3.33	2.82
600	10.9	0.259	4.33	4.65	7.54	3.45	3.24
700	10.0	0.252	3.99	4.06	6.72	3.52	3.52
800	9.2	0.245	3.69	3.55	6.01	3.60	3.72
900	8.3	0.238	3.35	3.05	5.28	3.65	4.00
1000	7.5	0.231	3.05	2.62	4.65	3.70	4.22
1100	6.6	0.224	2.70	2.19	3.99	3.72	4.39

Legend

E - Elastic Modulus
ν - Poisson's Ratio
G - Shear Modulus (Lame's Constant μ)
λ - Lame's Constant
K - Bulk Modulus
α - Mean Coefficient of Thermal Expansion from 86^oF to the Indicated Temperature
Coordinate definition
z - longitudinal
r - radial

Source: SC-65

Table 3.5

Zircaloy 4 Mechanical Properties as a Function of Temperature in Metric Units

T (^oC)	E (MPa)	ν (-)	G (MPa)	λ (MPa)	K (MPa)	α ($10^{-6}/^oC$) Longitudinal	Radial
23.9	10.62×10^4	0.296	4.10×10^4	5.94×10^4	8.68×10^4	-	-
37.8	10.48×10^4	0.294	4.05×10^4	5.78×10^4	8.48×10^4	-	-
93.3	9.86×10^4	0.287	3.83×10^4	5.17×10^4	7.72×10^4	4.95	2.88
148.9	9.31×10^4	0.280	3.63×10^4	4.63×10^4	7.06×10^4	5.40	4.00
204.4	8.69×10^4	0.273	3.41×10^4	4.10×10^4	6.38×10^4	5.76	4.16
260.0	8.14×10^4	0.266	3.21×10^4	3.66×10^4	5.79×10^4	5.94	5.08
315.6	7.52×10^4	0.259	2.99×10^4	3.21×10^4	5.20×10^4	6.21	5.83
371.1	6.90×10^4	0.252	2.75×10^4	2.80×10^4	4.63×10^4	6.34	6.34
426.7	6.34×10^4	0.245	2.54×10^4	2.45×10^4	4.14×10^4	6.48	6.70
482.2	5.72×10^4	0.238	2.31×10^4	2.10×10^4	3.64×10^4	6.57	7.20
537.8	5.17×10^4	0.231	2.10×10^4	1.81×10^4	3.21×10^4	6.66	7.60
593.3	4.55×10^4	0.224	1.86×10^4	1.51×10^4	2.75×10^4	6.70	7.90

Legend

E - Elastic Modulus
ν - Poisson's Ratio
G - Shear Modulus (Lame's Constant μ)
λ - Lame's Constant
K - Bulk Modulus
α - Mean Coefficient of Thermal Expansion from 30^oC to the Indicated Temperature
Coordinate Definition
z - longitudinal
r - radial

Source: Derived from data in Table 3.4

Table 3.6

Carbon Steel Mechanical Properties as a Function of Temperature in English Units

T (^oF)	E (10^6 psi)	ν (-)	G (10^6 psi)	λ (10^6 psi)	K (10^6 psi)	α ($10^{-6}/^oF$)
70	27.9	.29	10.81	14.93	22.14	6.07
100	-					6.13
150	-					6.25
200	27.7					6.38
250	-					6.49
300	27.4					6.60
350	-					6.71
400	27.0					6.82
450	-					6.92
500	26.4					7.02
550	-					7.12
600	25.7					7.23
650	-					7.33
700	24.8					7.44
750	-					7.54
800	-					7.65

Legend

E - Elastic Modulus
ν - Poisson's Ratio
G - Shear Modulus (Lame's Constant μ)
K - Bulk Modulus
α - Mean Coefficient of Thermal Expansion from 70^oF to Indicated Temperature
λ - Lame's Constant

Source: ASME-71

Table 3.7

Carbon Steel Mechanical Properties as a Function of Temperature in Metric Units

T (^oC)	E (MPa)	ν (-)	G (MPa)	λ (MPa)	K (MPa)	α ($10^{-6}/^oC$)
21.1	19.2×10^4	0.29	7.46×10^4	10.30×10^4	15.27×10^4	10.93
37.8	-					11.03
65.6	-					11.25
93.3	19.1×10^4					11.48
121.1	-					11.68
148.9	18.9×10^4					11.88
176.7	-					12.08
204.4	18.6×10^4					12.28
232.2	-					12.46
260.0	18.2×10^4					12.64
287.8	-					12.82
315.6	17.7×10^4					13.01
343.3	-					13.19
371.1	17.1×10^4					13.39
398.9	-					13.57
426.7	-					13.77

Legend

E - Elastic Modulus
ν - Poisson's Ratio
G - Shear Modulus (Lame's Constant μ)
λ - Lame's Constant
K - Bulk Modulus
α - Mean Coefficient of Thermal Expansion from 21.1^oC to the Indicated Temperature

Source: Derived from data in Table 3.6

Table 3.8

304 Stainless Steel Mechanical Properties as a Function of Temperature in English Units

T (^oF)	E (MPa)	ν (-)	G (10^6 psi)	λ (10^6 psi)	K (10^6 psi)	α ($10^{-6}/^oF$)
70	28.3	.29	10.97	15.15	22.46	9.11
100	-					9.16
150	-					9.25
200	27.7					9.34
250	-					9.41
300	27.1					9.47
350	-					9.53
400	26.6					9.59
450	-					9.65
500	26.1					9.70
550	-					9.76
600	25.4					9.82
650	-					9.87
700	24.8					9.93
750	-					9.99
800	24.1					10.05

Legend

E - Elastic Modulus
ν - Poisson's Ratio
G - Shear Modulus (Lame's Constant μ)
λ - Lame's Constant
K - Bulk Modulus
α - Mean Coefficient of Thermal Expansion from 70^oF to the Indicated Temperature

Source: ASME-71

Table 3.9

304 Stainless Steel Mechanical Properties as a Function of Temperature in Metric Units

T (^oC)	E (MPa)	ν (-)	G (MPa)	λ (MPa)	K (MPa)	α ($10^{-6}/^oC$)
21.1	19.5×10^4	0.29	7.57×10^4	10.45×10^4	15.49×10^4	16.40
37.8	-					16.49
65.5	-					16.65
93.3	19.1×10^4					16.81
121.1	-					16.94
148.9	18.7×10^4					17.05
176.7	-					17.15
204.4	18.3×10^4					17.26
232.2	-					17.37
260.0	18.0×10^4					17.46
287.8	-					17.57
315.6	17.5×10^4					17.68
343.3	-					17.77
371.1	17.1×10^4					17.87
398.9	-					17.98
426.7	16.6×10^4					18.09

Legend

E - Elastic Modulus
ν - Poisson's Ratio
G - Shear Modulus (Lame's Constant μ)
λ - Lame's Constant
K - Bulk Modulus
α - Mean Coefficient of Thermal Expansion from 21.1^oC to the Indicated Temperature

Source: Derived from data in Table 3.8

Table 3.10

Defense HLW Glass Mechanical Properties as a Function of Temperature in English Units

T (^oF)	E (10^6 psi)	ν (-)	G (10^6 psi)	λ (10^6 psi)	K (10^6 psi)	α ($10^6/^oF$)
*	10.00	0.20	4.20	2.76	5.51	6.78

Legend

E - Elastic Modulus
ν - Poisson's Ratio
G - Shear Modulus (Lame's Constant μ)
λ - Lame's Constant
K - Bulk Modulus
α - Coefficient of Thermal Expansion

* Temperature not given, assume 68^oF

Source: Derived from data in Table 3.11

Table 3.11

Defense HLW Glass Mechanical Properties as a Function of Temperature in Metric Units

T (^oC)	E (MPa)	ν (-)	G (MPa)	λ (MPa)	K (MPa)	α ($10^{-6}/^oC$)
*	6.9×10^4	0.20	2.9×10^4	1.9×10^4	3.8×10^4	12.2

Legend

E - Elastic Modulus
ν - Poisson's Radio
G - Shear Modulus (Lame's Constant μ)
λ - Lame's Constant
K - Bulk Modulus
α - Coefficient of Thermal Expression

* Temperature not given, assume 20^oC

Source: WE-83

Table 3.12

Commercial HLW Glass Mechanical Properties as a Function of Temperature in English Units

T (^oF)	E (10^6 psi)	ν (-)	G (10^6 psi)	λ (10^6 psi)	K (10^6 psi)	α ($10^{-6}/^oF$)
*	10.0	0.20	4.2	2.76	5.51	5.56

Legend

E - Elastic Modulus
ν - Poisson's Ratio
G - Shear Modulus (Lame's Constant μ)
λ - Lame's Constant
K - Bulk Modulus
α - Coefficient of Thermal Expansion

* Temperature not given, assume 68^oF

Source: Derived from data in Table 3.13

Table 3.13

Commercial HLW Glass Mechanical Properties as a Function of Temperature in Metric Units

T (^oC)	E (MPa)	ν (-)	G (MPa)	λ (MPa)	K (MPa)	α ($10^{-6}/^oC$)
*	6.9×10^4	0.20	2.9×10^4	1.9×10^4	3.8×10^4	10.0

Legend

E - Elastic Modulus
ν - Poisson's Ratio
G - Shear Modulus (Lame's Constant μ)
λ - Lame's Constant
K - Bulk Modulus
α - Coefficient of Thermal Expansion

* Temperature not given, assume 20^oC

Source: WE-83

Table 3.14

Cast Iron Mechanical Properties* as a Function of Temperature in English Units

T (^oF)	E (10^6 psi)	ν (-)	G (10^6 psi)	λ (10^6 psi)	K (10^6 psi)	α ($10^{-6}/^oF$)
32						6.503
70	23.6	0.271	9.3	9.4	17.2	6.626
100						6.724
200						7.048
300						7.372
400						7.697
500						8.021
600						8.346

Legend

E - Elastic Modulus
ν - Poisson's Ratio
G - Shear Modulus (Lame's Constant μ)
λ - Lame's Constant
K - Bulk Modulus
α - Average Linear Coefficient of Thermal Expansion Over the Temperature Range from 32^oF to the Indicated Temperature

* Malleable Iron

Source: BA-78

Table 3.15

Cast Iron* Mechanical Properties as a Function of Temperature in Metric Units

T (^oC)	E (MPa)	ν (-)	G (MPa)	λ (MPa)	K (MPa)	α ($10^{-6}/^oC$)
0.0						11.71
21.1	16.3×10^4	0.271	6.41×10^4	6.48×10^4	11.86×10^4	11.93
37.8						12.10
93.3						12.69
148.9						13.27
204.4						13.85
260.0						14.44
315.6						15.02

Legend

E - Elastic Modulus
ν - Poisson's Ratio
G - Shear Modulus (Lame's Constant μ)
λ - Lame's Constant
K - Bulk Modulus
α - Average Linear Coefficient of Thermal Expansion Over the Temperature Range 0^oC to the Indicated Temperature

* Malleable Iron

Source: Derived from data in Table 3.14

Table 3.16

Ticode 12 Mechanical Properties as a Function of Temperature in English Units

T (^oF)	E (10^6 psi)	ν (-)	G (10^6 psi)	λ (10^6 psi)	K (10^6 psi)	α ($10^{-6}/^oF$)
70	15.0	.21	6.2	4.5	8.6	
600						5.3

Legend

E - Elastic Modulus
ν - Poisson's Ratio
G - Shear Modulus (Lame's Constant μ)
λ - Lame's Constant
K - Bulk Modulus
α - Mean Coefficient of Thermal Expansion from 32^oF to Indicated Temperature

Source: TI

Table 3.17

Ticode 12 Mechanical Properties as a Function of Temperature in Metric Units

T (^oC)	E (MPa)	ν (-)	G (MPa)	λ (MPa)	K (MPa)	α ($10^{-6}/^oC$)
21.1	10.3×10^4	0.21	4.3×10^4	3.1×10^4	5.9×10^4	
315.6						9.54

Legend

E - Elastic Modulus
ν - Poisson's Ratio
G - Shear Modulus (Lame's Constant μ)
λ - Lame's Constant
K - Bulk Modulus
α - Mean Coefficient of Thermal Expansion from 0^oC to Indicated Temperature

Source: Derived from data in Table 3.16

tensile strength. Brittle materials (e.g., glass, geologic materials, cast iron) have higher strengths in compression than tension.

Strength data for candidate waste package materials are presented in Tables 3.18 through 3.31.

3.2.3.4 Plastic Constitutive Relationships

Materials loaded beyond their elastic limit deform plastically. Upon unloading, the plastic portion of the deformation is retained. Thus, the state of strain for plastic deformation is dependent on load history as opposed to being a function of the state of stress. Good design practice requires an analytical knowledge of plastic strains that result from loading on an instantaneous basis. Because of the path dependence of plastic strains on loading, an incremental theory of straining is used.

Saint-Venant proposed in 1870 that the principal axes of the strain components are coincident with the principal stress axes. In 1871, Levy generalized (as did von Mises independently in 1913) the so-called Saint-Venant constitutive relationships to include both normal and shear stress and strain components as follows:

$$d\varepsilon_{ij}^{I} = S_{ij}d\lambda \tag{3.66}$$

which is also called a flow rule where:

ε_{ij}^{I} = total instantaneous strain component directed perpendicular to i and along j (elastic strain is ignored so $\varepsilon_{ij}^{I} = \varepsilon_{ij}^{P}$)

ε_{ij}^{P} = plastic strain component directed perpendicular to i and along j

Table 3.18

Carbon Steel Yield Strength as a Function of Temperature in English Units

T (^oF)	Yield Strength (σ_y) (kpsi)
212	24.0
392	21.9
572	21.3
752	20.6
932	19.4
1112	17.8

Source: ASME-71

Table 3.19

Carbon Steel Yield Strength as a Function of Temperature in Metric Units

T (^oC)	Yield Strength (σ_y) (MPa)
100	165.5
200	151.1
300	146.9
400	142.0
500	133.8
600	122.7

Source: Derived from data in Table 3.18

Table 3.20

304 Stainless Steel Yield Strength as a Function of Temperature in English Units

T (^oF)	Yield Strength (σ_y) (kpsi)
212	30.0
392	25.0
572	22.5
752	20.7
932	19.4
1112	18.2

Source: ASME-71

Table 3.21

304 Stainless Steel Yield Strength as a Function of Temperature in Metric Units

T (^oC)	Yield Strength (σ_y) (MPa)
100	206.8
200	172.4
300	155.1
400	142.7
500	133.8
600	125.5

Source: Derived from data in Table 3.20

Table 3.22

Zircaloy 4 Strength Including Ultimate Tensile Strength (σ_u), 0.2 Percent Offset Yield Strength (σ_y), and Linear Elastic (Proportional) Limit (σ_p) in English Units

T (°F)	σ_u min (kpsi)	σ_u avg (kpsi)	σ_y min (kpsi)	σ_y avg (kpsi)	σ_p min (kpsi)	σ_p avg (kpsi)
75	79	94	52	70	24.0	29.5
100	78	93	52	70	24.5	30.8
200	72	88	50	69	29.0	38.5
300	67	83	48	66	30.0	40.5
400	62	78	45	62	26.7	37.7
500	57	72	40	58	23.0	33.0
600	50	66	36	53	22.6	30.5
700	44	60	31	47	22.4	29.3
800	36	52	27	42	22.3	28.4
900	27	42	23	35	22.2	28.2

Sources: AE-69, BY-69, BY-70, WH-68, BA-67, BE-66, SC-65

Table 3.23

Zircaloy 4 Including Ultimate Tensile Strength (σ_u), 0.2 Percent Offset Yield Strength (σ_y), and Linear Elastic (Proportional) Limit (σ_p) in Metric Units

T (^oC)	σ_u|min (MPa)	σ_u|min (MPa)	σ_y|min (MPa)	σ_y|avg (MPa)	σ_p|min (MPa)	σ_p|avg (MPa)
23.8	544.7	648.1	358.5	486.6	165.5	203.4
37.8	537.8	641.2	358.5	486.6	168.9	212.4
93.3	496.4	606.7	344.7	475.7	200.0	265.4
148.9	462.9	572.3	330.9	455.0	206.8	279.2
204.4	427.5	537.8	310.3	427.5	184.1	255.5
260.0	393.0	496.4	275.8	400.0	158.6	227.5
316.6	344.7	455.0	248.2	365.4	156.5	210.3
371.1	303.4	413.7	213.7	324.0	154.4	202.0
426.6	248.2	358.5	186.2	358.5	153.8	195.8
482.2	181.2	358.5	158.6	241.3	153.1	194.4

Source: Derived from data in Table 3.22

Table 3.24

Zircaloy 2 Ultimate Strength (σ_u) and Yield Strength (σ_y) as a Function of Temperature in English Units

T (^oF)	σ_u (psi) (Transverse)	σ_u (psi) (Longitudinal)	σ_y (kpsi) (Transverse)	σ_y (kpsi) (Longitudinal)
212	69.0	72.0	58.0	45.0
392	59.3	64.0	49.5	42.5
572	51.0	58.0	42.5	38.0
752	42.0	48.8	36.0	31.0
932	36.0	40.0	29.5	26.0

Source: GO-68

Table 3.25

Zircaloy 2 Ultimate Strength (σ_u) and Yield Strength (σ_y) as a Function of Temperature in Metric Units

T (°C)	σ_u (MPa) (Transverse)	σ_u (MPa) (Longitudinal)	σ_y (MPa) (Transverse)	σ_y (MPa) (Longitudinal)
100	475.7	496.4	399.9	310.3
200	408.9	441.3	341.3	293.0
300	351.6	399.9	293.0	262.0
400	289.6	336.5	248.2	213.7
500	248.2	275.8	203.4	179.3

Source: Derived from data in Table 3.24

Table 3.26

Ticode 12 Strength Including Minimum Tensile Strength ($\sigma_{u|min}$), Minimum 0.2 Percent Offset Yield Strength ($\sigma_{y|min}$), and Room Temperature Typical Ultimate Strength (σ_u) and Typical Yield Strength (σ_y) in English Units

T (°F)	$\sigma_{u\|min}$ (kpsi)	$\sigma_{y\|min}$ (kpsi)	σ_u (kpsi)	σ_y (kpsi)
70	70.0	50.0	82.9	64.7
100	68.0			
200	60.5			
300	52.6			
400	45.0			
500	40.0			
600	38.2			

Source: TI-82

Table 3.27

Ticode 12 Strength Including Minimum Tensile Strength ($\sigma_{u|min}$), Minimum 0.2 Percent Offset Strength ($\sigma_{y|min}$), and Room Temperature Typical Ultimate Strength (σ_u) and Typical Yield Strength (σ_y) in Metric Units

T (°C)	$\sigma_{u\|min}$ (MPa)	$\sigma_{y\|min}$ (MPa)	σ_u (MPa)	σ_y (MPa)
23.8	482.6	344.7	571.6	446.1
37.8	468.8			
93.3	417.1			
148.9	362.7			
204.4	310.3			
260.0	275.8			
315.6	263.4			

Source: Derived from data in Table 3.26

Table 3.28

Cast Iron Yield Data* in English Units

% Carbon	σ_t (kpsi)	σ_c (kpsi)	τ (kpsi)
3.3	47.7	159.0	60.8
3.7	40.9	119.1	47.3
4.0	35.1	120.8	47.6
4.1	32.5	120.8	44.6
4.3	29.3	90.9	37.0
4.5	25.0	95.0	35.5
4.6	22.4	91.0	33.0
4.8	20.4	72.8	29.6

* Ultimate tensile strength (σ_t), ultimate compressive strength (σ_c) and ultimate shear (τ) as a function of carbon content (the strength of grey cast iron does not vary significantly with temperature in the temperature range below 700°F)

Source: BA-78

Table 3.29

Cast Iron Yield Data* in Metric Units

% Carbon	σ_t (MPa)	σ_c (MPa)	τ (MPa)
3.3	328.9	1096.2	419.2
3.7	282.0	821.1	326.1
4.0	242.0	832.9	328.2
4.1	224.1	832.9	307.5
4.3	202.0	626.7	225.1
4.5	172.4	655.0	244.8
4.6	154.4	627.4	227.5
4.8	140.7	501.9	204.1

* Ultimate tensile strength (σ_t), ultimate compressive strength (σ_c), and ultimate shear (τ) as a function of carbon content (the strength of grey cast iron does not vary significantly with temperature in the temperature range below 700°F)

Source: Derived from data in Table 3.28

Table 3.30

Defense Waste Glass (131 TDS*) Ultimate Tensile Strength (σ_t) and Ultimate Compressive Strength (σ_c) in English Units

T (^oF)	σ_t (kpsi)	σ_c (kpsi)
68	9.0	100.0

* This glass melts at about 2050^oF.

Source: WI-84

Table 3.31

Defense Waste Glass (131 TDS*) Ultimate Tensile Strength (σ_t) and Ultimate Compressive Strength (σ_c) in Metric Units

T (^oC)	σ_t (MPa)	σ_c (MPa)
20	62.1	689.5

*This glass melts at about 1150^oC.

Source: Derived from data in Table 3.30

S_{ij} = stress deviator tensor

$d\lambda$ = non-negative constant

Equation 3.66 can be written on a component basis as

$$\frac{d\varepsilon_x^{\ I}}{S_x} = \frac{d\varepsilon_y^{\ I}}{S_y} = \frac{d\varepsilon_z^{\ I}}{S_z} = \frac{d\varepsilon_{yz}^{\ I}}{\tau_{yz}} = \frac{d\varepsilon_{zx}^{\ I}}{\tau_{zx}} = \frac{d\varepsilon_{xy}^{\ I}}{\tau_{xy}} = d\lambda \tag{3.67}$$

These equations, known as the Levy-Mises equations, are a constitutive relationship between strain and stress on a component basis. They state that the ratio of the increment of the total instantaneous strain component (with elastic strain being neglected) to the corresponding stress deviator component is a single constant for all components. The assumption that the elastic strains are negligible in comparison to the instantaneous plastic strains limits the theory to large strain conditions such as would be encountered in metal-forming applications rather than structural responses where strains must be closely controlled. The Levy-Mises equations (3.66 and 3.67) were restated by Prandtl in 1925 and Reuss in 1930 as

$$d\varepsilon_{ij}^{IP} = S_{ij}\,d\lambda \tag{3.68}$$

where ε_{ij}^{IP} is the instantaneous plastic strain component directed perpendicular to i and along j and the other quantities are as previously defined.

On a component basis, the Prandtl-Reuss constitutive relationship for instantaneous plastic strain is

$$\frac{d\varepsilon_x^{IP}}{S_x} = \frac{d\varepsilon_y^{IP}}{S_y} = \frac{d\varepsilon_z^{IP}}{S_z} = \frac{d\varepsilon_{xy}^{IP}}{\tau_{xy}} = \frac{d\varepsilon_{yz}^{IP}}{\tau_{yz}} = \frac{d\varepsilon_{zx}^{IP}}{\tau_{zx}} = d\lambda \tag{3.69}$$

Equation 3.69 can be rewritten in terms of the principal strains and stresses as

$$\frac{d\varepsilon_1^{IP} - d\varepsilon_2^{IP}}{S_1 - S_2} = \frac{d\varepsilon_2^{IP} - d\varepsilon_3^{IP}}{S_2 - S_3} = \frac{d\varepsilon_3^{IP} - d\varepsilon_1^{IP}}{S_3 - S_1} = d\lambda \tag{3.70}$$

where the terms are the ratios of the diameters of the Mohr's circles for instantaneous plastic strain to the diameters of the Mohr's circles for the stress written in terms of the principal stresses.

The constant $d\lambda$ can be shown to be equal to

$$d\lambda = \frac{3}{2}\frac{d\varepsilon^{IP}}{\sigma_e} \tag{3.71}$$

The Prandtl-Reuss equations can be written for the instantaneous plastic strain components in terms of the stress components as:

$$d\varepsilon_x^{IP} = \frac{d\varepsilon^{IP}}{\sigma_e}\left[\sigma_x - \frac{1}{2}(\sigma_y + \sigma_z)\right]$$

$$d\varepsilon_y^{IP} = \frac{d\varepsilon^{IP}}{\sigma_e}\left[\sigma_y - \frac{1}{2}(\sigma_x - \sigma_z)\right]$$

$$d\varepsilon_z^{IP} = \frac{d\varepsilon^{IP}}{\sigma_e}\left[\sigma_z - \frac{1}{2}(\sigma_x + \sigma_y)\right]$$

$$d\gamma_{xy}^{IP} = \frac{3}{2}\frac{d\varepsilon^{IP}}{\sigma_e}\tau_{xy}$$

$$d\gamma_{yz}^{IP} = \frac{3}{2}\frac{d\varepsilon^{IP}}{\sigma_e}\tau_{yz}$$

$$d\gamma_{zx}^{IP} = \frac{3}{2}\frac{d\varepsilon^{IP}}{\sigma_e}\tau_{zx} \tag{3.72}$$

where

$$\sigma_e = \sqrt{3J_2} \tag{3.73a}$$

$$\sigma_e = \frac{1}{\sqrt{2}}\left[(\sigma_1-\sigma_2)^2 + (\sigma_2-\sigma_3)^2 + (\sigma_3-\sigma_1)^2\right]^{1/2} \tag{3.73b}$$

$$\sigma_e = \frac{1}{\sqrt{2}}\left[(\sigma_x-\sigma_y)^2 + (\sigma_y-\sigma_z)^2 + (\sigma_z-\sigma_x)^2 + 6(\tau_{xy}^2 + \tau_{yz}^2 + \tau_{zx}^2)\right]^{1/2} \tag{3.73c}$$

Equations 3.73a through 3.73c express the von Mises yield criterion. This criterion states that when the state of stress is equal to the uniaxial yield stress in a tensile specimen, then yielding will occur.

In 1924, Henckey developed a deformation theory for plastic stress-strain behavior in which the strains are related to the current state of

stress. This theory is limited in its applicability because plastic strains are typically dependent on the load path and better represented by an incremental (local) relationship.

The Prandtl-Reuss constitutive relationship and von Mises yield criterion as given in Equations 3.72 and 3.73 are frequently used to describe the instantaneous plastic stress-strain relationship.

3.2.3.5 Creep Constitutive Relationships

When tensile tests are performed, the stress-strain relationship depends in part on the duration of the test. At elevated temperatures, there is more dependence on test duration. As the duration of the test is increased, the load at fracture decreases. Also, if two specimens are tested so that they are stressed in the range that includes some plastic instantaneous strain but not rupture, the specimen that is subsequently subjected to the longer duration loading will retain more deformation on unloading. This time effect of loading on deformation or strain is called creep. The creep strain retained on unloading is conceptually similar to the instantaneous plastic strain discussed in the previous section.

The structural analyst must be concerned with creep because the associated strain consumes part of the ductility of the material. Figure 3.5 shows the creep strain versus time superimposed on the instantaneous elastic and plastic strains. The instantaneous elastic strain will always precede the creep strain. The instantaneous plastic strain may or may not occur, depending on the proximity of the state of stress to yielding as discussed in the previous section and in Appendix C (von Mises yield criterion). The primary creep is a short duration process, on the order of a day, in which the structure "shakes down" or flows to a more stable condition to resist the imposed loading condition. Secondary creep occurs within the time during which the rate of creep strain can be approximated as a constant.

The creep rate, which is the slope of the strain versus time curve of Figure 3.5, is at a minimum in the secondary creep range. This is an approximately constant strain rate region. The actual curve may be concave downward over the initial time interval and concave upward over the later time interval. In the tertiary creep range, the strain rate is accelerating until rupture occurs. This is an unstable range, and the stress levels should be kept low enough for the service temperature so that the stable secondary creep range exceeds the service life of the structure.

A typical family of creep curves for a given temperature and stress level is shown in Figure 3.6. Creep tests are performed for a limited number of hours, and the service life of a structure may be greater than the test duration. Assumptions are typically made and data extrapolated to longer loading durations. In general, structural system development does not wait until creep test data are available for the entire loading duration.

The family of creep curves shown in Figure 3.7 can be used in conjunction with the instantaneous stress versus strain curve to give the stress versus strain behavior for a given duration of the stress application. These curves, known as isochronous stress-strain curves, give a clear indication of creep effects in terms of the additional strain incurred. Waste package performance objectives will require keeping the stress low enough so that the required service life can be endured without exceeding specified strain limits. There may be several strain limits, as higher limits can be applied to bending than to membrane stress categories, etc. For example, the ASME boiler and pressure vessel code specifies a maximum membrane plus bending strain of 2 percent and a maximum membrane strain of 1 percent away from welds.

In a review of the creep rate data for various steels, Timoshenko observed that, initially, when the creep rate is decreasing (TI-56),

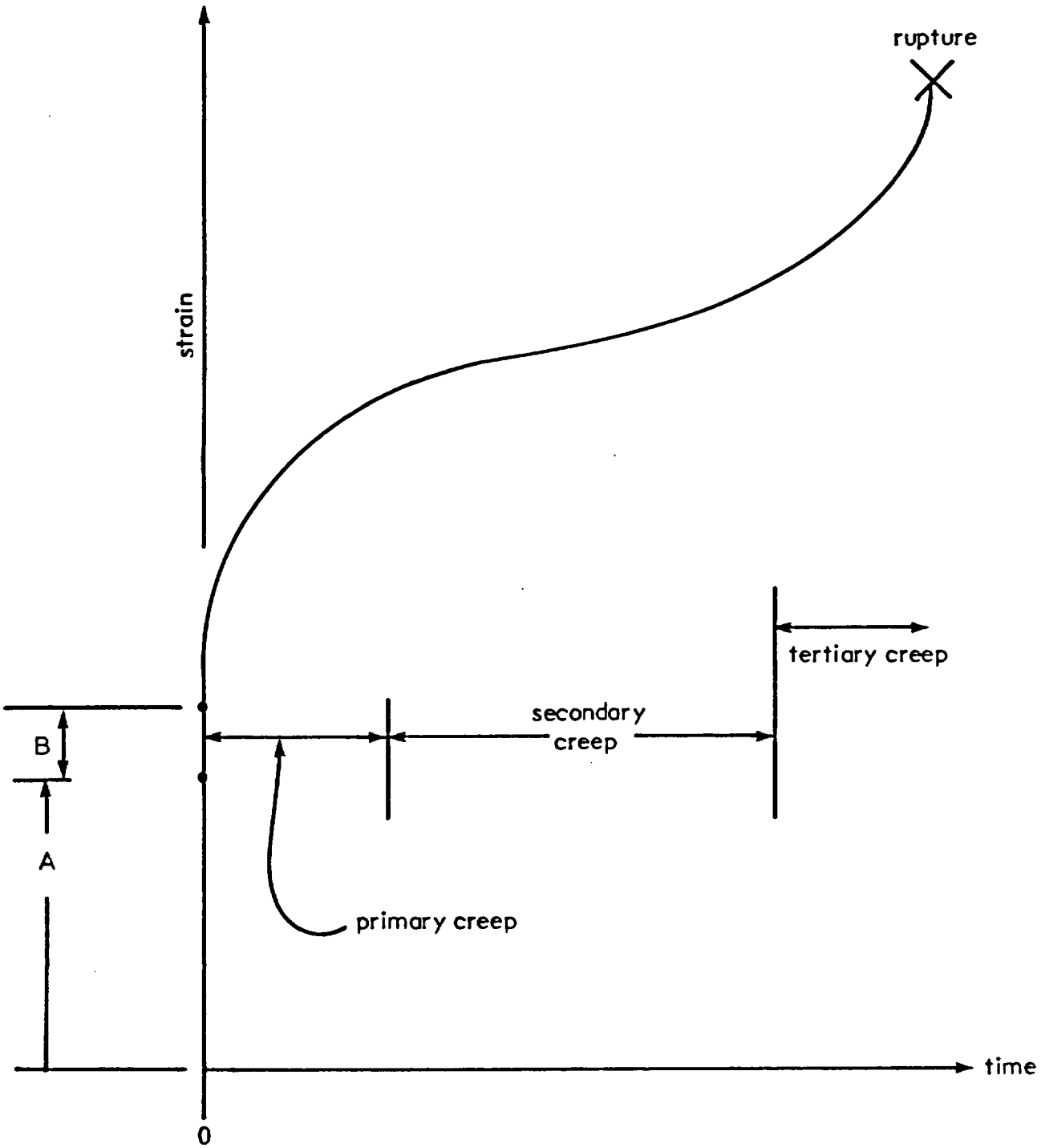

Figure 3.5

Plot Showing Instantaneous Elastic Strain A, Instantaneous Plastic Strain B Plus Primary, Secondary and Tertiary Creep Ranges for Constant Stress and Constant Temperature Controlled Uniaxial Tensile Loading

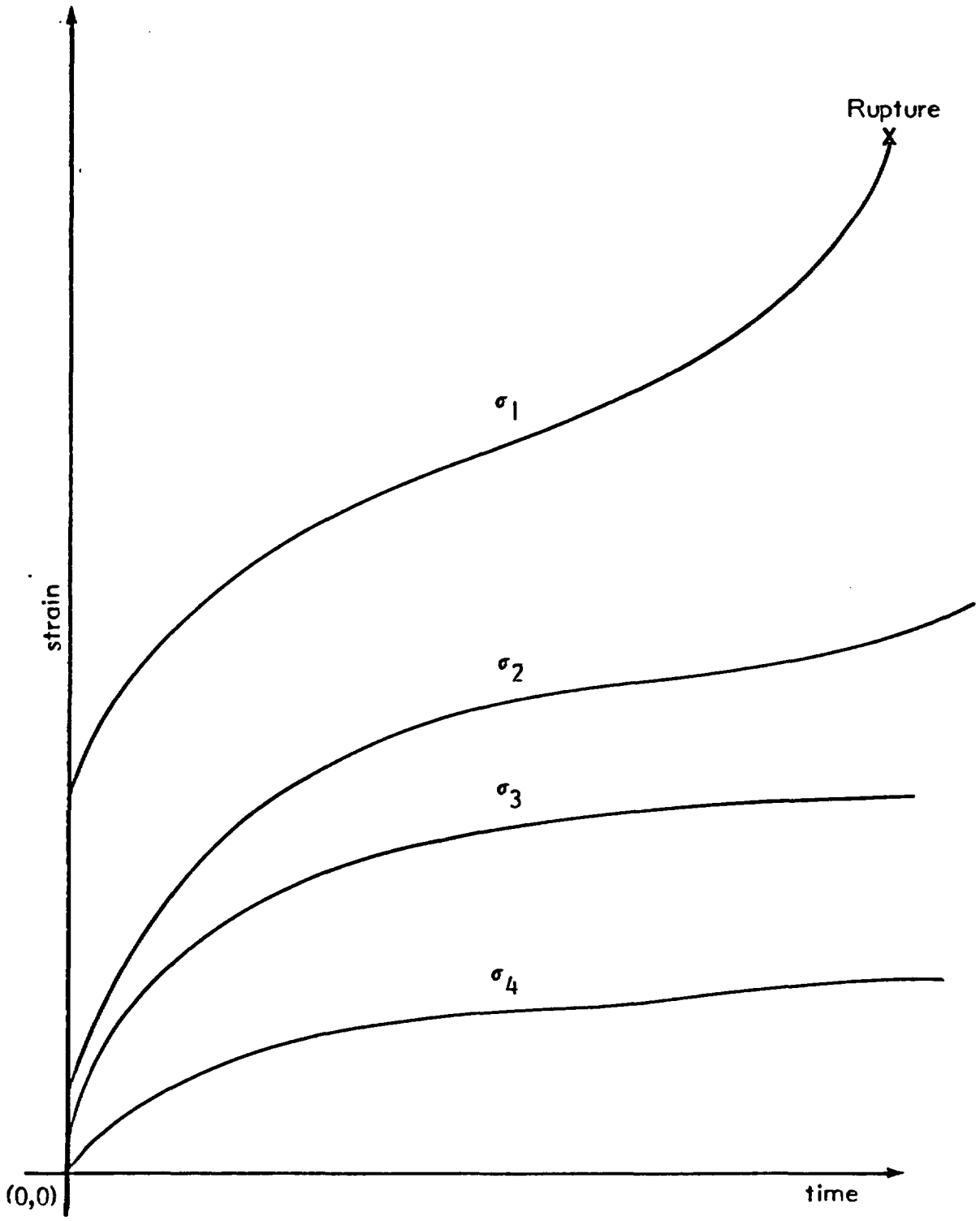

Figure 3.6

Creep Strain Versus Time Curves for the Same Temperature but Different Stress Levels $\sigma_1 > \sigma_2 > \sigma_3 > \sigma_4$. The Instantaneous Strain Is the Value at Time = 0.

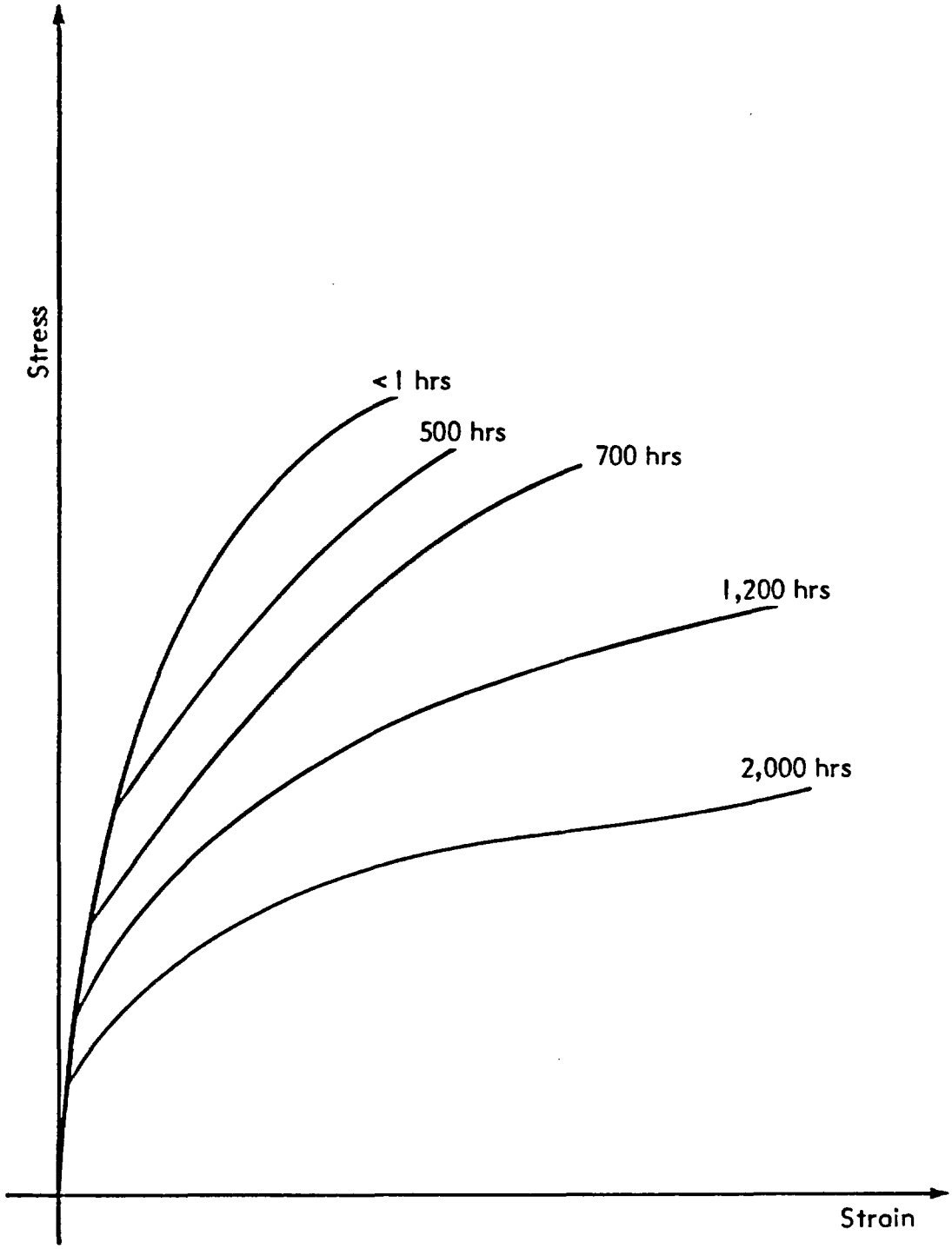

Figure 3.7

Isochronal Stress Versus Strain Behavior
for a Given Temperature

the excess of creep rate above the minimum (which applies over the secondary creep range or at the point of inflection if concavity changes from down to up somewhere in the defined secondary creep range) decreases geometrically as time increases arithmetically.

The creep rate can be written as a function of time as

$$\dot{\varepsilon}^c = \frac{d\varepsilon^c}{dt} = \dot{\varepsilon}^c_{min} + ae^{-bt} \tag{3.74}$$

in which a, b, and $\dot{\varepsilon}^c_{min}$ are constants that can be determined from creep curves such as those shown in Figure 3.8.

Equation 3.74 can be integrated in time to give:

$$\varepsilon^c = \varepsilon_o{}^c + \dot{\varepsilon}^c_{min}t - \frac{a}{b}e^{-bt} \tag{3.75}$$

where $\varepsilon_o{}^c$ and $\dot{\varepsilon}^c_{min}$ are as shown in Figure 3.8. $\dot{\varepsilon}^c_{min}$ is the slope of the creep curve at the point of inflection. The dotted line is tangent to the creep curve at the point of inflection.

Another plot is constructed from Figure 3.6 by taking the slopes of the curves at given time intervals and plotting them on a logarithmic scale against time as shown in Figure 3.9. This set of curves for different values of stress can be used to determine values of the constants a and b in the last term of Equation 3.75. The exponential is a correction term which is added to the linear value given by the first two linear terms on the right side of Equation 3.75. The exponential term is used to approximate the distance parallel to the strain axis between the straight dashed line and the curve of Figure 3.8 on the left side of the inflection point of the curve. For large values of time, the term can be neglected because it decays exponentially.

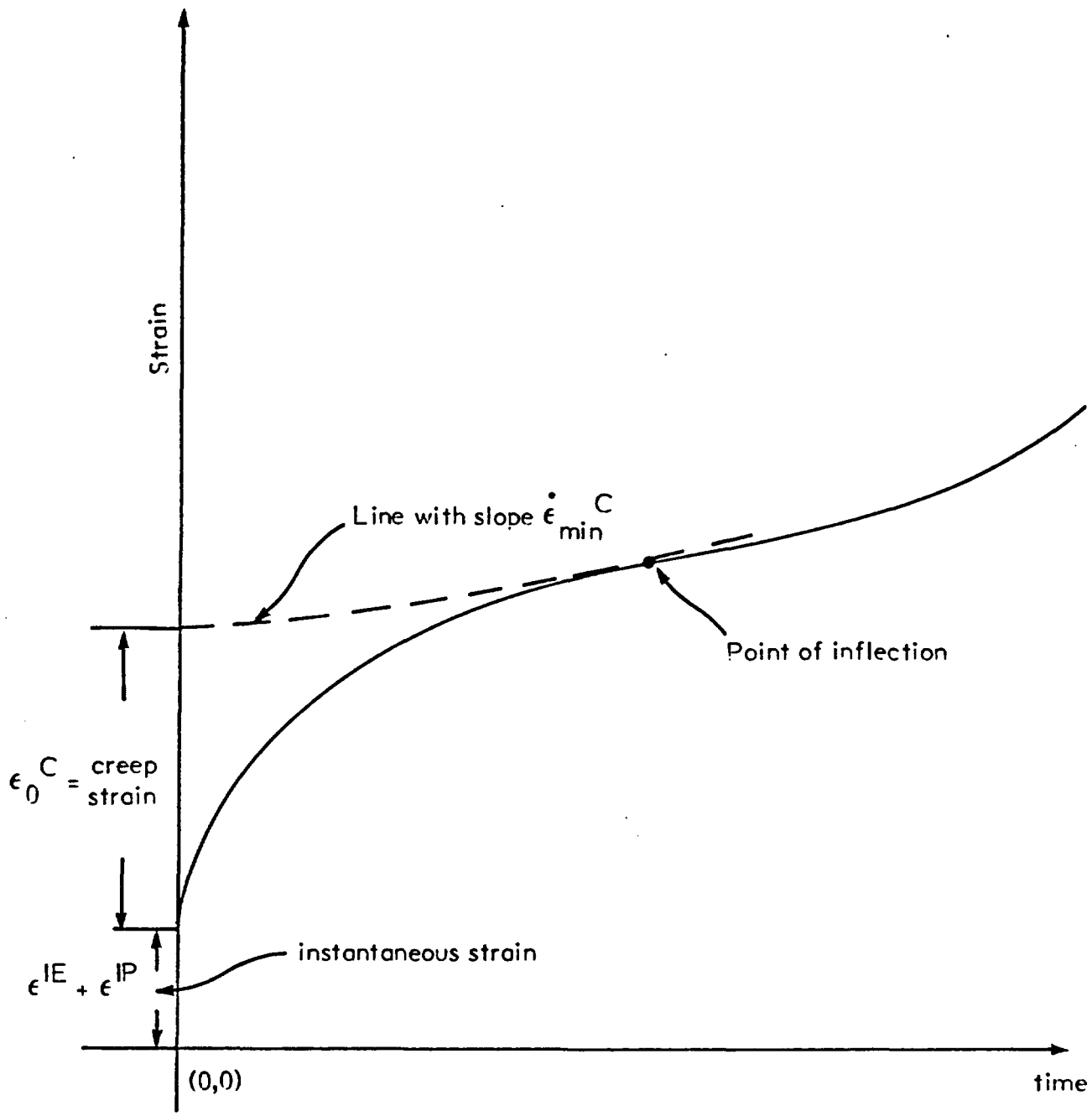

Figure 3.8

Strain Versus Time Curve Which Includes Instantaneous and Creep Strains

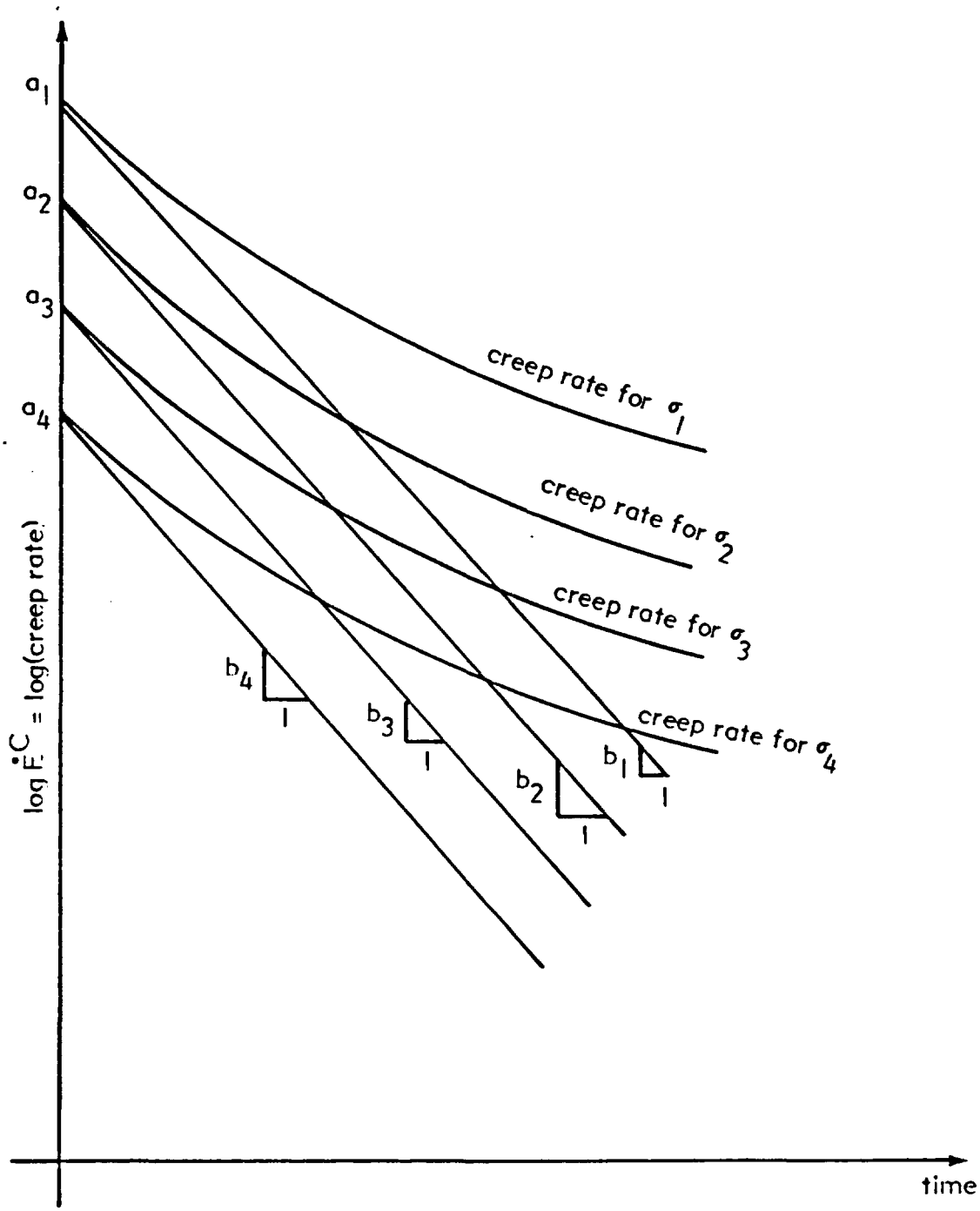

Figure 3.9

Creep Rate Versus Time Plotted from Figure 3.6 Data

A study of experimental data by many investigators indicates that the minimum creep rate can be represented empirically as a power function of the stress value

$$\dot{\varepsilon}^{c}_{min} = k\sigma^{n} \tag{3.76}$$

where, for a family of curves as shown in Figure 3.6, k and n are constants for a given material and temperature.

Creep data measurements require a long-term commitment of laboratory facilities and monitoring by technicians. The three principal parameters governing the creep rate are stress state, duration of loading, and temperature:

$$\varepsilon^{c} = f(\sigma, t, T) \tag{3.77}$$

where

ε^{c} = creep rate $[t^{-1}]$

σ = state of stress $[f/\ell^{2}]$

t = duration of loading condition causing the stress state $[t]$

T = temperature of material $[\theta]$

The developer of the correlation has some freedom in choosing the functional form of the correlation. It is convenient if the independent parameters are separated into three functions obeying the commutative law

$$\varepsilon^{c} = f_{\sigma}(\sigma) f_{t}(t) f_{T}(T) \tag{3.78}$$

This form is arbitrary and does not represent the true functional relationship. Therefore, its derivatives are not meaningful. However, functions of the form of Equation 3.78 provide representative values of creep strain when properly developed. An appropriate set of constants can often make a mediocre functional form yield acceptable values within a limited range of the independent variables.

Data for a particular alloy and range of stress, temperature, and time (of loading) are often difficult to obtain. Furthermore, most experimental data are obtained from uniaxial tensile loading.

The most commonly used stress function is one given by Norton in 1929 as

$$f_\sigma(\sigma) = k\sigma^m \tag{3.79}$$

where k and m are experimentally correlated constants. Other correlation forms have been proposed by McVetty in 1934, Soderberg in 1936, Johnson in 1963, and Garafalo in 1965 (Reference PE-71).

Time functions are like stress functions in that they represent approximately the dependence of the creep strain within a limited range of time. The physics of creep can not be inferred from these functions. A time function was developed by Andrade in 1910

$$f_t(t) = (1+bt^{1/3}) \exp(kt)-1 \tag{3.80}$$

where b and k are empirically determined constants. Other time functions were developed by McVetty in 1934 and Graham and Walles in 1955 (Reference PE-71).

For material absolute temperatures below about 40% of the melting temperature, creep occurs primarily by a slip mechanism at grain boundaries. This slip creep straining is very similar to instantaneous plastic straining. The creep straining occurs over an interval of time but can occur at much lower stress levels than the instantaneous plastic strain. Dorn in 1955 (Reference PE-71) suggested that the temperature function should be of the form

$$f_T(T) = \exp\left(-\frac{Q}{RT}\right) \tag{3.81}$$

where

Q = material's activation energy [e/molecule]

R = Boltzmann's constant
(= 1.38066×10^{-23} Joules/molecule ^{o}K) [e/molecule θ]

T = material's absolute temperature [θ]

It is also common for experimentalists to develop creep correlations using a mixed stress and time function. Equation 3.77 is represented as

$$\varepsilon^c = f_{\sigma t}(\sigma,t)\ f(T) \tag{3.82}$$

rather than by Equation 3.78. Marin gives various stress-time functions. One given by Finnie in 1959 (Reference MA-62) is

$$f_{\sigma t}(\sigma,t) = k_1 \sigma^{k_2} t^{k_3} \tag{3.83}$$

where

k_1, k_2, and k_3 = empirical constants

σ = tensile stress $[f/\ell^2]$

t = duration of stress condition $[t]$

Equations 3.77 through 3.83 are based on the creep correlation technique. Because so many stress, time, stress-time, and temperature functions have been developed, their detailed review is beyond the scope of this report.

It should be remembered that the correlations are primarily for uniaxial tensile loading and that they are data representations rather than mathematical expressions of the physics of creep. Usually, creep correlations apply over the secondary range of creep where the creep rate is nearly constant over a significant period of time. Also, deviations from the constant creep rate can be corrected for limited loading durations by the last term in Equation 3.75.

In 1950, Drucker unified the flow rule relationships for elastic and inelastic deformation by defining the plastic potential function

$$p = p(\sigma_{ij}) \tag{3.84}$$

as a scalar function of the stress components σ_{ij}. He then expressed the incremental creep shown in terms of the plastic potential function as:

$$d\varepsilon_{ij}^{c} = \frac{\partial p}{\partial \sigma_{ij}} d\lambda \tag{3.85}$$

and where

$$d\lambda = \frac{d\varepsilon_e^c}{\sqrt{\frac{2}{3} \frac{\partial p}{\partial \sigma_{mn}} \frac{\partial p}{\partial \sigma_{mn}}}} \tag{3.86}$$

where $d\varepsilon_e^c$ = equivalent creep strain increment.

Equation 3.85 can be written as

$$d\varepsilon_{ij}^{c} = \frac{\partial p}{\partial \sigma_{ij}} \frac{d\varepsilon_e^c}{\sqrt{\frac{2}{3}\frac{\partial p}{\partial \sigma_{mn}}\frac{\partial p}{\partial \sigma_{mn}}}} \tag{3.87}$$

The plastic potential function is written in terms of an equivalent stress. The stress components are summed so that the equivalent stress is comparable to the uniaxial stress in a tensile test. The von Mises equivalent stress is most often used although multicomponent creep data verifying its applicability are very limited. The form of the von Mises yield is given by Equation 3.73c for isotropic materials. Its derivative is given as

$$\frac{\partial \sigma_e}{\partial \sigma_x} = \frac{1}{\sigma_e}\left[\sigma_x - \frac{1}{2}(\sigma_y + \sigma_z)\right] \tag{3.88}$$

If the potential function is assumed to have a form of

$$p(\sigma_{ij}) = k_1 \sigma_e^{k_2} \tag{3.89}$$

and it is further assumed that

$$p(\sigma_{ij}) = J_2 = \frac{1}{6}\left[(\sigma_1-\sigma_2)^2 + (\sigma_2-\sigma_3)^2 + (\sigma_3-\sigma_1)^2\right] \tag{3.90}$$

then the constants k_1 and k_2 can be determined from Equations 3.89 and 3.90:

$$k_1 = \frac{1}{3}$$

$$k_2 = 2$$

(3.91)

The effective creep strain ε_e^c can be defined as

$$d\varepsilon_e^c = \sqrt{\frac{2}{3}\, d\varepsilon_{ij}^c\, d\varepsilon_{ij}^c}$$

(3.92)

The constitutive relationship in incremental form becomes

$$d\varepsilon_{ij}^c = \frac{3}{2}\frac{d\varepsilon_e^c}{\sigma_e}\, S_{ij}$$

(3.93)

where S_{ij} is the stress deviator tensor.

Differentiating Equation 3.78 with respect to time gives

$$\frac{d\varepsilon^c}{dt} = f_\sigma(\sigma)\,\frac{df_t(t)}{dt}\, f_T(T)$$

(3.94)

This is known as the time hardening law for uniaxial creep.

The flow law can be written on a multi-axis basis as

$$d\varepsilon_{ij}^c = f_\sigma(\sigma_e)\,\frac{\partial\sigma_e}{\partial\sigma_{ij}}\,\frac{df_t(t)}{dt}\, f_T(T)dt$$

(3.95)

The flow rule or constitutive relationship applies to constant volume creep straining processes where straining is a result of deviatoric stresses, S_{ij}, only and where the axes of principal stresses and strains coincide.

By substituting the value of $\partial\sigma_e/\partial\sigma_x$ from Equation 3.88, Equation 3.95 can be written for the various incremental strain components as:

$$d\varepsilon_x{}^c = \frac{f_\sigma(\sigma_e)}{\sigma_e}\left[\sigma_x - \frac{1}{2}(\sigma_y + \sigma_z)\right]\frac{df_t(t)}{dt}\ f_T(T)dt$$

$$d\varepsilon_y{}^c = \frac{f_\sigma(\sigma_e)}{\sigma_e}\left[\sigma_y - \frac{1}{2}(\sigma_x + \sigma_z)\right]\frac{df_t(t)}{dt}\ f_T(T)dt$$

$$d\varepsilon_z{}^c = \frac{f_\sigma(\sigma_e)}{\sigma_e}\left[\sigma_z - \frac{1}{2}(\sigma_x + \sigma_y)\right]\frac{df_t(t)}{dt}\ f_T(T)dt$$

$$d\gamma_{xy}{}^c = \frac{3f_r(\sigma_e)}{\sigma_e}\ \tau_{xy}\ \frac{df_t(t)}{dt}\ f_T(T)dt$$

$$d\gamma_{yz}{}^c = \frac{3f_r(\sigma_e)}{\sigma_e}\ \tau_{yz}\ \frac{df_t(t)}{dt}\ f_T(T)dt$$

$$d\gamma_{zx}{}^c = \frac{3f_r(\sigma_e)}{\sigma_e}\ \tau_{zx}\ \frac{df_t(t)}{dt}\ f_T(T)dt \qquad (3.96)$$

This constitutive relationship is the most important analytical element of the mechanics of creep. The discussion of creep can be extended to encompass the creep strain's dependence on time and temperature so the relative influence of these two parameters is appreciated. Response curves are shown in Figure 3.10. These curves are generated by the locus of constant strain points or failure points on a stress versus

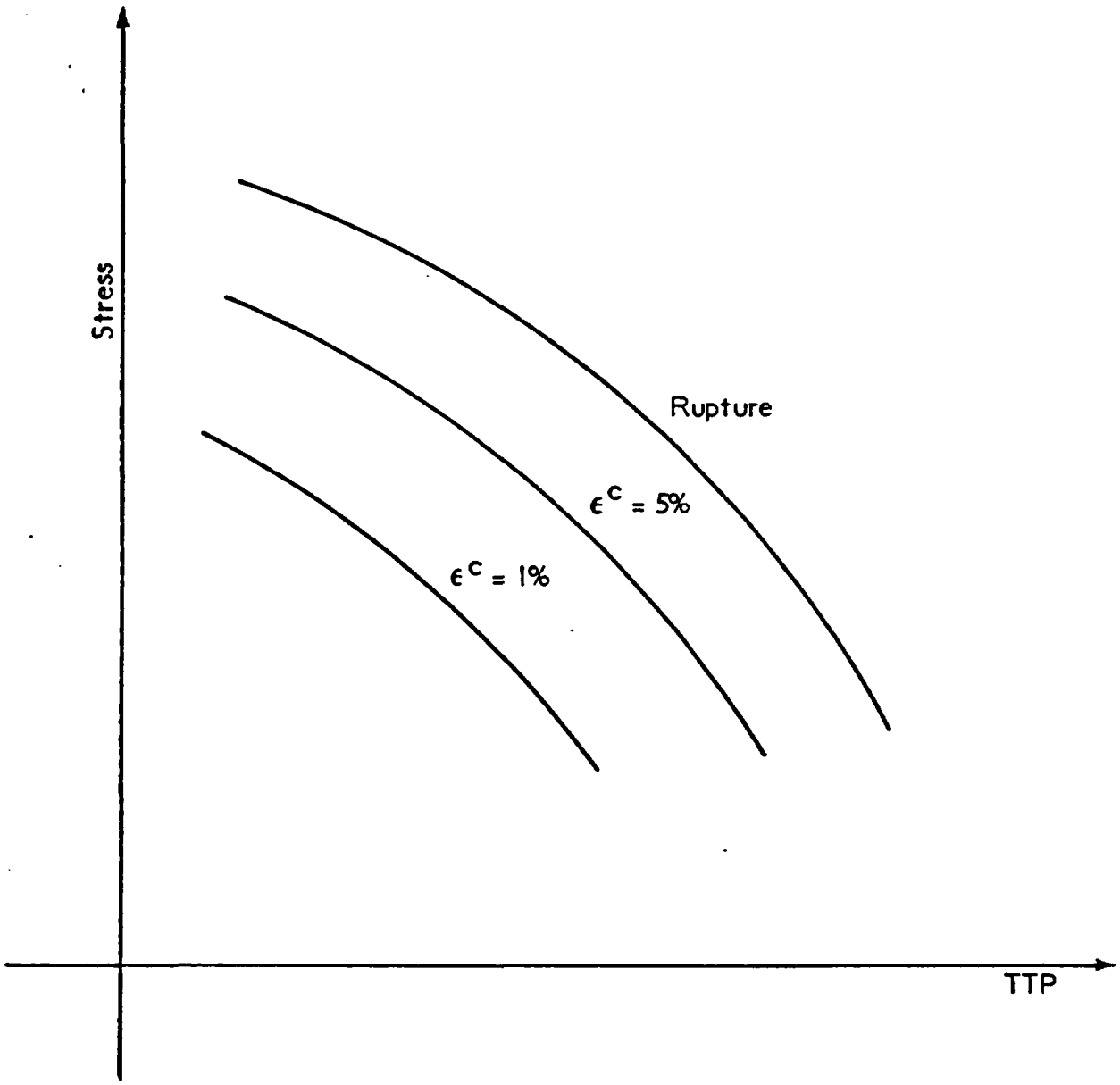

Figure 3.10

Curves of Constant Creep Strain and Rupture
on Stress Versus Time-Temperature Parameter (TTP)

time-temperature parameter (TTP) plane. The curves are useful for selecting a design stress based on an allowable creep strain for a given load duration and material temperature.

It should be noted that the data in Figure 3.10 are based on uniaxial tensile loading and uniaxial stress. For performance evaluation of an actual structure, the state of stress may be bi-axial or tri-axial and hence more complex. The upper curve shown in Figure 3.10 is known as a stress rupture curve. It indicates what stresses cause failure for a given load duration and temperature. The various curves can indicate what limits on stress levels are needed to keep the creep strain and deformations within acceptable limits. The creep strain is related to the total strain as

$$\varepsilon^C = \varepsilon - \varepsilon^I \tag{3.97}$$

where

ε = total strain at a point [ ]

ε^I = instantaneous strain at a point due to instantaneous elastic, thermal, and instantaneous plastic deformations [ ]

ε^C = creep strain at a point [ ]

The most commonly used TTP is the Larson-Miller parameter (LMP) published by Larson and Miller in 1952:

$$TTP = LMP = T(k_1 + \log_{10} t) \tag{3.98}$$

where

T = absolute temperature (^oR)

k_1 = constant (usually 20.0)

t = time (hr)

Other TTPs have been developed by Dorn, Manson and Haeford, Fisher and Dorn, and other investigators (Reference PE-71).

The fifth line in Table 3.32 presents the LMP value for a temperature of 200°C and a loading duration of 1,000 hours. As shown in the fourth line, dropping the temperature by 10°C allows the loading duration to increase by a factor of 3.1 to 3,140 hours for the same value of the LMP. In line seven, an increase of 50°C to 250°C causes the loading duration to drop to 6.32 hours. When the LMP is evaluated for different temperature values, a very strong variation in the allowable loading duration is apparent. For a given allowable stress or a given allowable total strain, small increases in temperature drastically reduce the allowable duration of the stress associated with the load condition. Alternately, reducing the temperature greatly lengthens the allowable load duration.

Tables 3.33 through 3.36 provide primary creep rates for potential waste package structural materials.

3.3 Mechanical Properties of Packing Materials

The Department of Energy has proposed a number of packing materials to impede the flow of water and migration of radionuclides from a waste package. Many of the proposed backfill materials are clays or clay-rock mixtures. The mechanical properties of these backfill materials will vary widely depending on:

- Clay mineralogy
- Clay mineral content
- Water content and composition
- Exchange cation composition (if any)

Table 3.32

Different Temperature and Load Durations
Consistent with a Constant LMP

T (^oC)	T (^oR)	t (hrs)	LMP
50	581.4	4.80×10^{13} (5.5×10^9 years)	19585.2
100	671.4	1.47×10^9 (1.7×10^5 years)	19585.2
150	761.4	5.23×10^5 (6 years)	19585.2
190	833.4	3.14×10^3	19585.2
200	851.4	1.00×10^3	19585.2
210	869.4	3.34×10^2	19585.2
250	941.4	6.32×10^0	19585.2
300	1031.4	9.68×10^{-2} (5.8 minutes)	19585.2
400	1211.4	1.46×10^{-4} (0.53 seconds)	19585.2
500	1391.4	1.19×10^{-6} (4.3×10^{-3} seconds)	19585.2

Table 3.33

Carbon Steel Creep Rate

The creep rate of 0.3% carbon steel at 300°C is given by

$$\dot{\varepsilon}^{c} = 2 \times 10^{-38} \sigma^{6.9}$$

where

$\dot{\varepsilon}_c$ = creep strain rate (1/hr)
σ = stress (psi)

Source: TI-56

Table 3.34

Zircaloy 2 Creep Rate

The creep rate of cold worked Zircaloy tubing is given by

$$\dot{\varepsilon}^c = 3.96 \times 10^{-9} \text{ Sin h } \left(\frac{\sigma}{8700}\right)$$

where

$\dot{\varepsilon}^c$ = creep strain rate (1/hr)

σ = stress (psi)

This correlation is applicable to stresses $\sigma < 29{,}000$ psi and for a material temperature of 300°C.

Source: PH-69

Table 3.35

304 Stainless Steel Creep Rates

Temperature (°F)	Temperature (°C)	Stress (psi)	Creep Rate (%/hr)
300	148.9	5,000	1.25 E-23
300	148.9	10,000	2.01 E-23
300	148.9	15,000	9.57 E-20
300	148.9	20,000	3.33 E-18
300	148.9	25,000	1.05 E-16
300	148.9	30,000	3.24 E-15
400	204.4	5,000	2.03 E-19
400	204.4	10,000	3.65 E-17
400	204.4	15,000	2.04 E-15
400	204.4	20,000	8.53 E-14
400	204.4	25,000	3.30 E-12
400	204.4	30,000	1.24 E-10
500	260	5,000	4.67 E-16
500	260	10,000	9.42 E-14
500	260	15,000	6.18 E-12
500	260	20,000	3.13 E-10
500	260	25,000	1.48 E-8
500	260	30,000	6.86 E-7
600	315.6	5,000	2.63 E-13
600	315.6	10,000	5.99 E-11
600	315.6	15,000	4.65 E-9
600	315.6	20,000	2.86 E-7
600	315.6	25,000	1.65 E-5
600	315.6	30,000	9.43 E-4
700	371.1	5,000	5.23 E-11
700	371.1	10,000	1.35 E-8
700	371.1	15,000	1.24 E-6
700	371.1	20,000	9.28 E-5
700	371.1	25,000	6.59 E-3
700	371.1	30,000	4.63 E-1
800	426.7	5,000	4.68 E-9
800	426.7	10,000	1.37 E-6
800	426.7	15,000	1.51 E-4
800	426.7	20,000	1.37 E-2
800	426.7	25,000	1.20 E+0
800	426.7	30,000	1.03 E+2

Source: PH-69

Table 3.36

Ticode 12 Creep Rate

T Temperature (°F)	(°C)	σ Stress (Ksi)	$\dot{\varepsilon}^c$ (% ε per 1000 hrs)
77	25	20.0	0
77	25	30.0	9.2×10^{-5}
77	25	42.0	3.6×10^{-2}
77	25	48.0	3.94×10^{-2}
300	148.9	15.6	0
300	148.9	26.0	7.2×10^{-3}
300	148.9	32.0	4.8×10^{-3}
600	315.6	7.0	3.3×10^{-3}
600	315.6	12.0	8.2×10^{-3}
600	315.6	15.0	1.4×10^{-2}
600	315.6	18.0	1.5×10^{-2}
600	315.6	20.0	1.86×10^{-2}

Source: TI-84

- Degree of compaction
- Degree of cementation
- Fabric or structure

Environmental factors that affect the stress-strain behavior of clay include temperature, stress history, strain rate, and confining pressure. Since the mechanical properties of clay and clay-rock mixtures vary depending on many factors, this section consists of a qualitative discussion of material properties taken from Reference ME-83. Prior to use in a repository, the packing material should be tested to determine the quantitative material properties. General patterns of plasticity and strength for several clay mineral types are discussed below.

3.3.1 Plasticity

Water content is one of the most important parameters affecting the stress-strain behavior of clays. The plastic behavior of soils is conveniently described by index properties known as Atterberg Limits, which are reported in weight percent water. Table 3.37 gives Atterberg Limits for relatively pure clays. The plastic limit is the approximate minimum water content at which the material exhibits plasticity. The liquid limit is the approximate minimum water content at which the material behaves as a liquid. Plastic behavior occurs only within a limited range of water contents, defined by the plasticity index (PI = liquid limit - plastic limit). Atterberg Limits are a function of clay mineral content, clay mineralogy, particle sizes, and the degree of aggregation.

Plasticity of clays involves a combination of attractive forces between particles and the lubricating action of the adsorbed water on these particles. Plastic behavior occurs when sufficient water is adsorbed to overcome these attractive interparticle forces and reduce the shear strength of the clay significantly. The variation in values for plastic limits of clay reflects the amount of interlayer water associated with each clay (Reference GR-62). Clay structure and exchangeable cations are most

Table 3.37

Plastic (PW) and Liquid (LW) Limits for Common Clay Minerals

Clay		Ca^{+2}		Mg^{+2}		K^{+}		Na^{+}	
		PW %	LW %	PW %	LW %	PW %	LW %	PW %	LW %
Smectite	(1)	65	166	59	158	57	161	93	344
	(2)	65	155	51	199	57	125	89	433
	(3)	63	177	53	162	60	297	97	700
	(4)	79	123	73	138	76	108	86	280
Illite	(5)	40	90	39	83	43	81	34	61
	(6)	36	69	35	71	40	72	34	59
	(7)	42	100	43	98	41	72	41	75
Kaolinite	(8)	36	73	30	60	38	69	26	52
	(9)	26	34	28	39	28	35	28	29

(1) Pontotoc, MS
(2) Cheto, AZ
(3) Belle Fourche, SD
(4) Omsted, IL (25% illite layers)
(5) Fithian, IL
(6) Jackson County, OH
(7) Grundy County, IL (5% smectite layers)
(8) Anna, IL
(9) Dry Branch, FL

Source: GR-62

important in determining plastic limits for smectites, while other clays with few or no exchangeable cations show less variability. Na-smectites have the largest plastic limits, and because of the large water content, these values are not as well-defined as those for Ca- and Mg-smectites.

Smectites with Na^+ and Li^+ as exchangeable cations can adsorb the most water before losing strength and exhibiting plastic behavior. The high plastic limits associated with smectites result from their ability to disperse into fine particles and maximize the amount of water that can be adsorbed. The Na^+ or Li^+ exchange cations maximize the dispersion of clay particles. Other clay minerals are not as effectively dispersed by the presence of interlayer Na^+ or Li^+. These cations have a limited effect in determining plastic limits of illites, for example.

The clay mineral content in a soil or clay also strongly affects its plastic behavior. Figure 3.11 shows the relation between the plasticity index and clay content for three clay mineral groups. It is apparent that even small amounts of montmorillonite added to a non-clay material such as sand will impart significant plasticity.

3.3.2 Strength

The strength of a material reflects the stress required to cause a loss of load-bearing capacity or cracking. Unconfined compression tests of clays and other materials are very common but are less relevant to clay behavior in confined conditions in repository seals than are triaxial shear strengths.

Values for shear strengths of clays depend on clay mineral composition, particle size distribution, shape and arrangement of particles, and the composition of the non-clay fraction (References GR-62 and GR-71). The most important determinant of a clay's strength appears to be its moisture content and, more specifically, how the water is oriented on the clay surfaces. The clay mineralogy, the quantity of exchange sites, and the

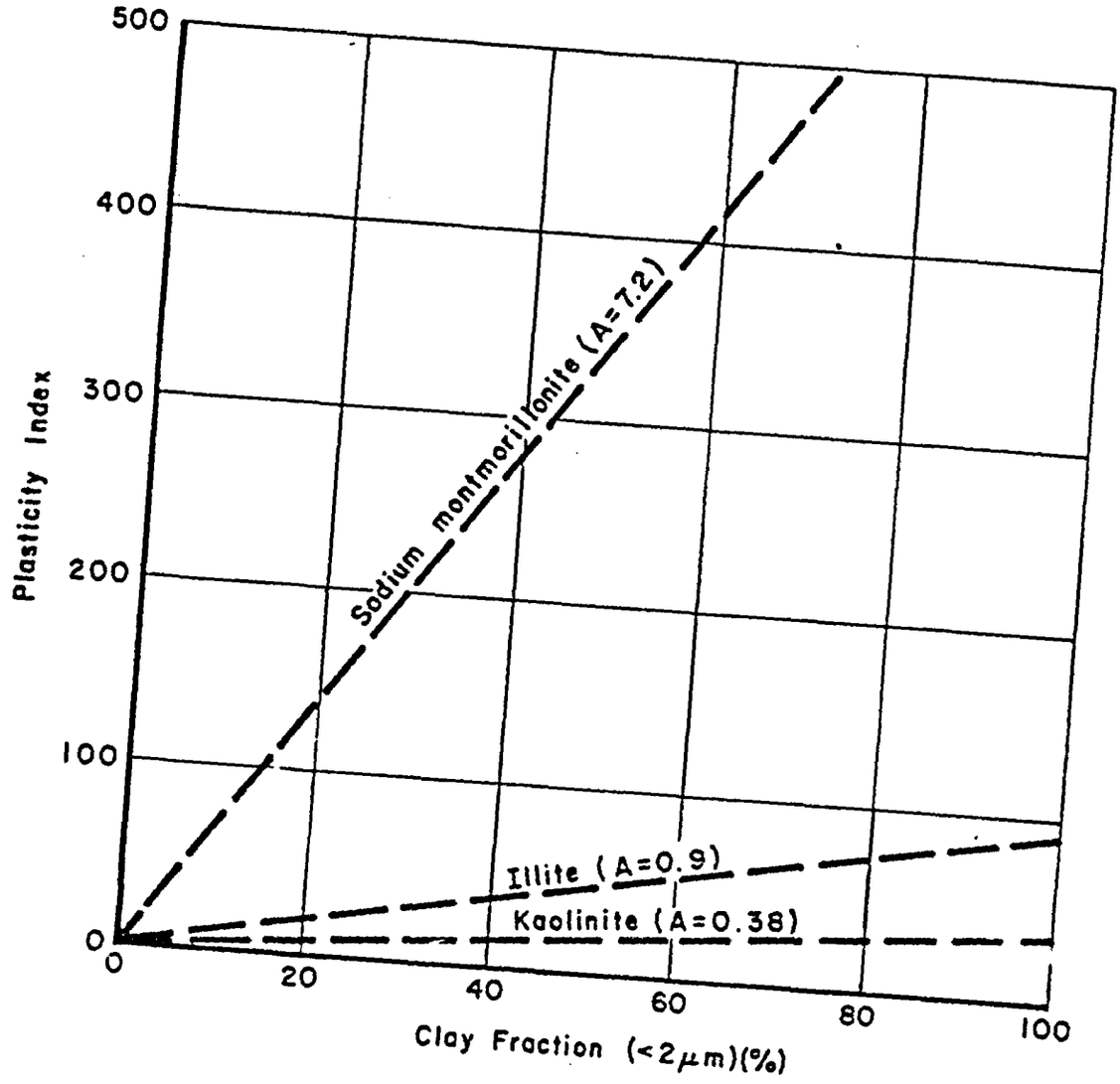

$$A = \text{activity of clay} = \frac{\text{plasticity index}}{\text{\% by weight finer than } 2\mu m}$$

Non-clay fraction composed of quartz sand

Source: LA-69

Figure 3.11

Effect of Clay Content and Clay Mineralogy on the Plastic Behavior of Soils

cations located in these sites are the major factors that determine the thickness of adsorbed water layers. Smectites that have relatively thick adsorbed water layers tend to have lower shear strengths than illites or kaolinite that have thinner water layers.

The influence of clay mineral type and content is best illustrated by observing effects on the residual friction angle, a measure of minimum strength achieved at large shear displacements (Figure 3.12). Smectites have lower shear strengths than kaolinite and illite; also, the clay mineral content required to have a marked influence on shear strength in clays is less for smectite (montmorillonite) than for other varieties. The moisture content of the clay also greatly influences the shear strength of a compacted clay. In clays that contain little water, the shear strength is a log function of the moisture content, decreasing with increasing moisture content (Reference GR-62). This exponential behavior does not hold, however, at higher moisture contents because of the increasing importance of adsorbed water layers and a shift from frictional to cohesive forces. Clays used in repository seals may be emplaced at relatively low moisture contents, so their strength under compressive load will be directly related to water saturation. Subsequent to closure, however, clay seals and backfills may reach much higher moisture contents. Clay strength must be known for a range of moisture contents.

The strength of clays is affected by parameters other than clay mineral type and content, including stress history (e.g., precompaction), fabric (especially as affected by compaction), confining pressure, the rate of loading, the rate of deformation, and temperature. Pre-compacted materials may display greater strength at the same effective normal stress than materials that have not been pre-compacted. Strength frequently increases in a clay with increased loading and deformation rates. The effect of temperature on the strength of clays is highly variable and depends on both the temperature during consolidation and the temperature during shear. Increased confining pressure also results in increased strength of the material.

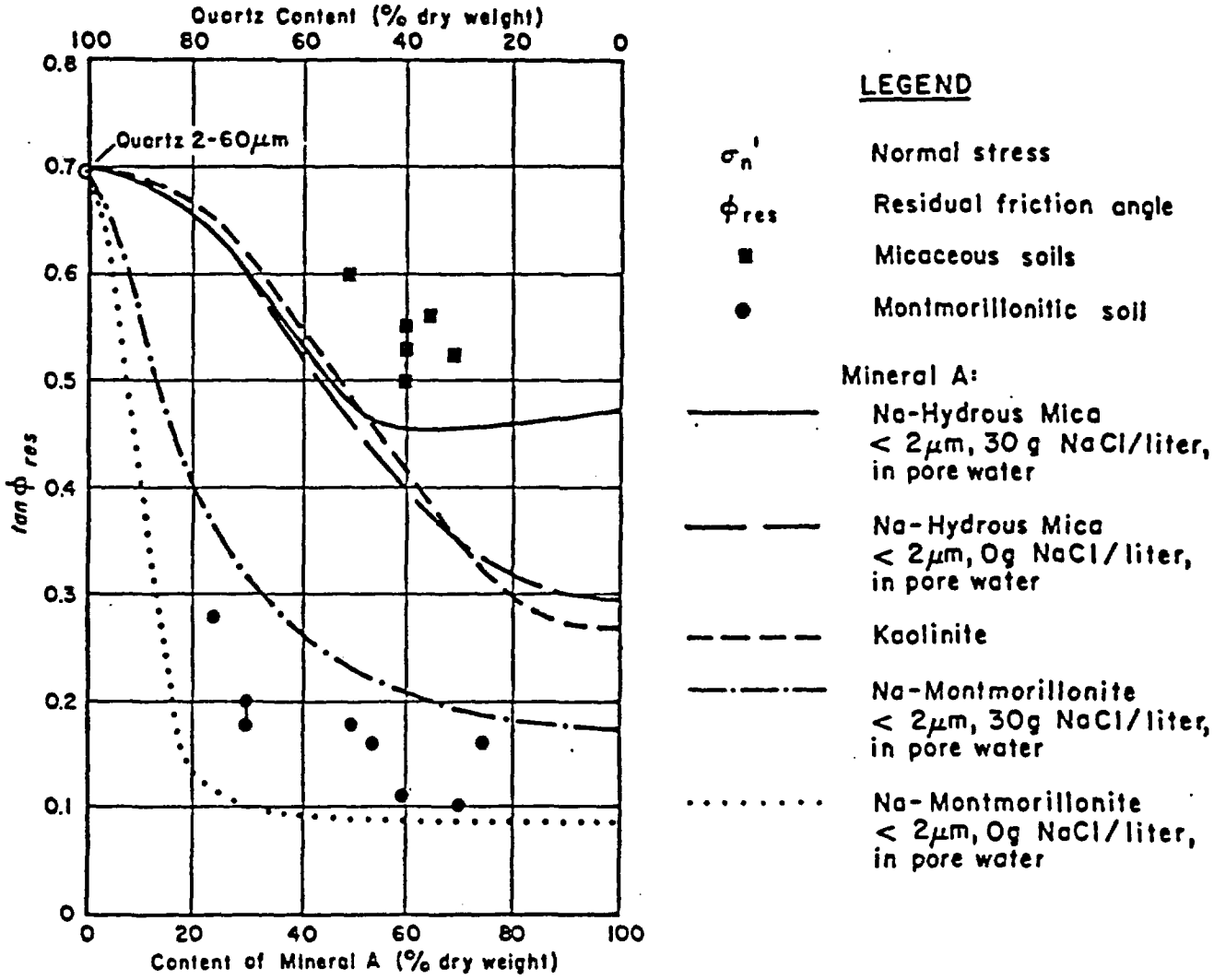

NOTE
$\sigma_n' = 1.0\ kg/cm^2$ for all tests.

Source: MI-76

Figure 3.12

Effect of Clay Content and Clay Mineralogy, Including Hydrous Micas, on the Residual Friction Angle of Soil Under Shear Stress

Under some conditions, clay materials will undergo plastic deformation, while other conditions can promote brittle behavior. Plastic behavior is promoted by isotropic, dispersed clay fabric; freedom from cementation; freedom from leaching and thixotropy; and a high moisture content.

3.4 Loads and Constraints

The finite element method uses nodes whose initial position and velocity are specified. These nodes can be translated along three orthogonal axes and rotated about each of the three axes. These six components allow for the description of any general motion condition.

For a structure to perform its primary function of transmitting loads without failing (generally without breaking or incurring excessive deformation), it must be constrained. The constraints have many forms depending on the physical nature of the structural anchors and foundation. To use the finite element method, the structural analyst must interpret the physics of the structure and must specify a representative assemblage of elements that are connected at nodes. Then, any or all of the six degrees of freedom of any node can be constrained throughout the response simulation. By specifying the various degrees of freedom that are constrained (eliminated) for any of the nodes in the model, the analyst effectively constrains the structure. The constraints allow the loads imposed on the structure to be reacted, causing loads (forces and moments) and associated stresses internal to the structure.

Analytical problems that are solved using continuous functional relationships typically involve the use of constraints in the form of algebraic equations. They specify a particular point on the structure that is prevented from translating or rotating in a particular direction. For differential equations expressing displacement, the constraints are the differential equation's boundary conditions.

For the finite element method of analysis, the external loads may be specified as:

- Forces and moments applied at specific nodes (this is usually in terms of three force components and three moment components for the coordinate systems)
- Pressures acting on a particular element face
- Gravitational body force acting on the mass associated with each of the elements

Some programs allow for the centrifugal body force associated with the mass of any element that is rotating at a specified velocity. This is used in conjunction with particular element types for modeling rotating cylinders or annuli.

External forces may also be applied indirectly by specifying the displacement or rotation from a previous equilibrium position of various nodes. This is done in terms of the three displacement components and three rotational components that specify the position of a node.

The finite element method of analysis allows the treatment of various types of loading and superimposes the responses. Very general loading conditions are represented with ease. It is not practical to obtain analytical solutions for complex loading conditions.

3.5 Equations of Motion

Equations of motion describe the motion at discrete points or nodes. These equations relate element conditions and behavior to node motion. The mass of each element is allocated to the various nodes of the element. The equation of motion then relates the element properties to the node motion.

For a simple two degree of freedom (u_1, u_2) system as shown in Figure 3.13, the equations of motion are:

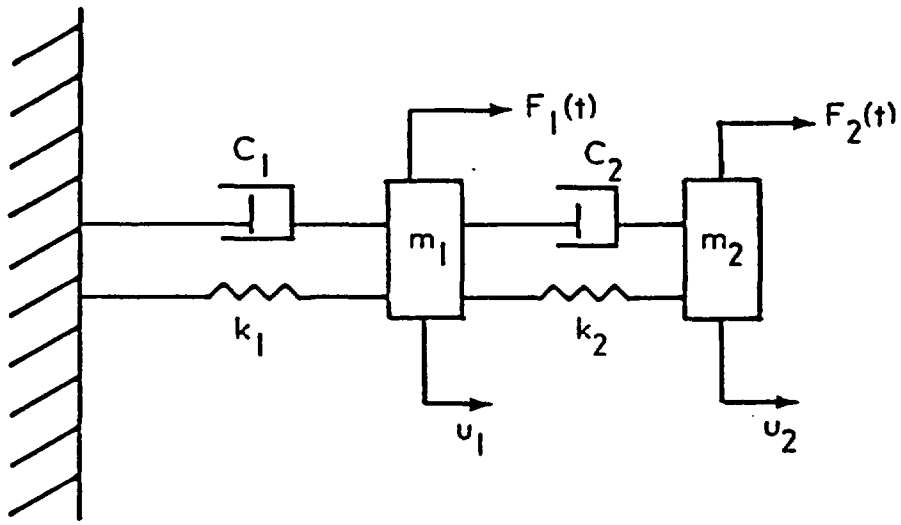

Figure 3.13

Simple Two Degree of Freedom System (Two Translations u_1 and u_2) with Mass, Damping and Stiffness, and Transient Forcing Functions

$$\begin{bmatrix} m_1 & 0 \\ 0 & m_2 \end{bmatrix} \begin{Bmatrix} \ddot{u}_1 \\ \ddot{u}_2 \end{Bmatrix} + \begin{bmatrix} (C_1+C_2) & -C_2 \\ -C_2 & C_2 \end{bmatrix} \begin{Bmatrix} \dot{u}_1 \\ \dot{u}_2 \end{Bmatrix} + \begin{bmatrix} (k_1+k_2) & -k_2 \\ -k_2 & k_2 \end{bmatrix} \begin{Bmatrix} u_1 \\ u_2 \end{Bmatrix} =$$

$$\begin{Bmatrix} F_1(t) \\ F_2(t) \end{Bmatrix} \tag{3.99}$$

where:

m_i = mass at node i [m]

C_i = damping of element i [ft/ℓ]

k_i = stiffness of element i [f/ℓ]

u_i = displacement of node i [ℓ]

$\dot{u}_i$ = velocity of node i [ℓ/t]

$\ddot{u}_i$ = acceleration of node i [ℓ/t^2]

$F_i(t)$ = transient forcing function applied to node i [f]

There is one equation of motion for each active degree of freedom for each node. In general, each node has three translational and three rotational degrees of freedom. The general form of Equation 3.99 in matrix notation is:

$$[m]\{\ddot{u}\} + [c]\{\dot{u}\} + [k]\{u\} = \{F(t)\} \tag{3.100}$$

where:

$[m]$ = mass (and rotational inertia) matrix

$[c]$ = damping matrix

$[k]$ = stiffness (including rotational) matrix

$\{u\}$ = vector of node displacement (and rotations)

$F(t)$ = node transient forcing function (including moments)

Equation 3.100, sometimes referred to as the dynamic equilibrium equation, is a statement of how externally applied loads are distributed between node displacement, velocity, and acceleration terms. The distribution is governed by the physical aspects (stiffness, damping, and mass) of the elements associated with the nodes. Various techniques are used to solve Equation 3.100 depending on which affects are present and dominant. In general, the solution $u(t)$ is determined, from which $\dot{u}(t)$ and $\ddot{u}(t)$ are determined.

For structures subject to static loading where their final displacements are of interest, Equations 3.99 and 3.100 become:

$$\begin{bmatrix} k_1 + k_2 & -k_2 \\ -k_2 & k_2 \end{bmatrix} \begin{Bmatrix} u_1 \\ u_2 \end{Bmatrix} = \begin{Bmatrix} F_1 \\ F_2 \end{Bmatrix} \tag{3.101}$$

$$k\{u\} = \{F\} \tag{3.102}$$

where the quantities are as previously defined except that the force vector components do not vary with time. This is the relationship between externally applied loading, element stiffness, and node displacement.

3.6 Equilibrium Relationships

Structural performance is always in accord with the principle of force and moment equilibrium. Structures that are subjected to static loading and that have no sustained motion obey the equilibrium principle at all locations throughout the structure. The static equilibrium condition is expressed in terms of each of the six degrees of freedom of motion:

$$\Sigma F_r = 0, \ \Sigma F_\theta = 0, \ \Sigma F_z = 0$$

$$\Sigma M_r = 0, \ \Sigma M_\theta = 0, \ \Sigma M_z = 0 \tag{3.103}$$

where:

F_i = force exerted on a node in the i direction (externally applied force component and internal element stiffness type forces) [f]

M_i = moment exerted on a node about a line parallel to the i axis (externally applied moment component and internal element rotational stiffness type moments) [fℓ]

Some structures experience accelerations associated with transient or periodic motion during their responses to loading conditions. These structures conform to a special form of the equilibrium principle which, for a particle, includes pseudo force (and moment) components directed opposite to the acceleration and having a magnitude equal to the product of the translational (rotational) acceleration and the mass (mass moment of inertia) of the particle. The finite element method includes procedures for associating distributed mass from various elements with the acceleration at discrete points (nodes). The node is usually the point of connection

of the elements contributing mass to the node. The pseudo force and moment components are named in honor of D'Alembert who stated the principle of dynamic equilibrium in 1743. The dynamic equilibrium relationships are:

$$\Sigma F_r - ma_r = 0,\ \Sigma F_\theta - ma_\theta = 0,\ \Sigma F_z - ma_z = 0$$

$$\Sigma M_r - I_r\alpha_r = 0,\ \Sigma M_\theta - I_\theta\alpha_\theta = 0,\ \Sigma M_z - I_z\alpha_z = 0 \tag{3.104}$$

where:

F_i = force exerted on a node in the i direction (externally applied force component and internal element stiffness and damping type forces) [f]

M_i = moment exerted on a node about a line parallel to the i axis (externally applied moment component and internal element rotational stiffness and damping type forces) [ℓf]

m = mass associated with particle or node at which dynamic equilibrium condition is being applied [m]

I_i = mass moment of inertia of the mass of a node about axis i [$m\ell^2$]

a_i = translational acceleration of the mass in the i direction [ℓ/t^2]

α_i = angular acceleration of the mass about the i axis [$1/t^2$]

This dynamic equilibrium principle states that a particle can be considered to be in force equilibrium if the inertial force of the mass corresponding to its current acceleration magnitude is included with the external forces in the summation of forces on the particle.

This form of the equilibrium principle given by D'Alembert is consistent with Newton's second and third laws (about 1664) and of profound consequence to the development of analytical mechanics and in particular to Hamilton's principle.

The equilibrium condition is important because it is used to verify the finite element solution. The finite element solution involves equations of motion, load condition, and constraints, which are used to solve for the structure displacement, which generally includes six degrees of freedom at each node, and the internal forces and moments at each node of each element. The load path and displacements are established in accord with the stiffness, damping, and mass distributions of the structure and the nature and location of the constraints. The equilibrium relationship requires the force and moment interactions among the elements to be in force and moment equilibrium at each node with respect to each axis.

The equilibrium condition described in this section can be used as a check on the solution accuracy. It must be satisfied to within an acceptable tolerance. The force balance is similar to that given in the equation of motion but differs in that it deals with internal forces, which have been determined based on deflection, velocity, and acceleration calculated by solving the equations of motion, which contain only external force terms. The equations of motion are coupled and more difficult to solve than the uncoupled equilibrium relationships.

Equilibrium checks are also useful when done for the entire structure. They should indicate that the sum of the reactions in any of the six degrees of freedom is of equal magnitude to the externally applied load (including body forces such as gravity). The sum of all reactions (at the constraints) should be opposite in direction to the externally applied loads.

3.7 Analytical Responses

The purpose of structural analysis is to simulate mathematically a constrained structure's response to a particular loading condition. The response quantities of a finite element analysis generally include:

- Node positions (after loading)
- Element deformation (between nodes based on position before and after loading)

- Element strain (at each node of the element based on deformation and previous dimensions)
- Internal force and moment interaction for each element at each node

Linear-elastic force versus displacement material behavior is most common where a constant value of element stiffness is used. Optional response quantities usually include the stress tensor components at each node of each element.

When the structure and its model are especially complex, static loads may be imposed in steps so that the finite element model will go through the entire calculational procedure a number of times. This affords the program the opportunity to perform node equilibrium checks and provides the analyst with incremental response versus incremental loading information. For structures that respond dynamically, solutions are obtained at discrete time increments. The values of the externally applied loads can be changed at the end of each time step. This solution technique allows for the responses to be determined incrementally over time. In this process, equilibrium checks are optional after each time step. Equilibrium is attained to within a particular tolerance value when it is imposed. To speed up the calculation, the analyst can specify a multiple of calculational time increments per equilibrium check. When equilibrium checks are made, they are made for all unconstrained degrees of freedom of all nodes.

Strains associated with changes of temperature of the structure are calculated as though the structure was free to expand without constraints (free thermal expansion). The displacements are then considered in conjunction with the constraints on the structure, the structural stiffness distribution, and node force and moment equilibrium. The constraints and element stiffness give rise to internal forces and moments for which stresses can be calculated on a linear elastic basis.

The analyst must also be concerned with instantaneous plastic or creep strains. This involves specification of the parameters appearing in the

pertinent constitutive relationship. These are used in place of the generalized Hooke's law applicable to linear elastic behavior. The solution procedure is very similar except that it is necessary to calculate the stress tensor so that the instantaneous plastic flow rule can be evaluated in terms of the current state of stress. The creep flow rule is evaluated in terms of the current state of stress and the current duration of loading.

Responses of greatest interest to the waste package performance analyst are those indicating pending undesirable performance. This undesirable performance is likely to take the form of excessive strain either in regions of the structure that experience instantaneous plastic strain or in regions where creep strains accumulate over long durations of loading. In the absence of these two phenomena, elastic strain limits would be imposed by the familiar technique of limiting the stress tensor. This is accomplished by limiting the stress in accordance with one of the yielding criteria. Several yielding criteria are described in Appendix C.

4.0 REFERENCES

AE-69 Atomic Energy Commission, Eighth Annual Report - AEC Fuels and Materials Development Program," GEMP-1012, Part II, March 31, 1969.

ASME-71 American Society of Mechanical Engineers, 1971 ASME Boiler and Pressure Vessel Code, Section III, Nuclear Power Plant Components, 1971.

BA-67 Babcock and Wilcox, "Corrosion and Hydriding of Zircaloy," Quarterly Technical Progress Report #3, April - June 1967, 3765-3, August 1967.

BA-78 Theodore Baumeister, et al., Marks Standard Handbook for Mechanical Engineers, McGraw-Hill Book Co., 1978.

BE-66 R.M. Berman, et al., Properties of Zircaloy-4 Tubing, WAPD-TM-585, December 1966.

BY-69 S.T. Byrne, "Analysis of Additional Wolverine Mechanical Properties Data on Zircaloy-4 Tubing," Memo, November 6, 1969.

BY-70 S.T. Byrne, "Mechanical and Silicon Evaluation of Omaha Core Materials," Memo, NLM-70-255, July 7, 1970.

CO-66 W.A. Coffman, et al., "A Large Range Thermodynamic and Transport Water Properties FORTRAN IV Computer Program," WAPD-TM-568, December 1966.

CU-83 R.H. Curtis, R.J. Wart, and E.L. Skiba, Parameters and Variables Appearing in Repository Design Models, NUREG/CR-3586, December 1983.

DA-82 M.S. Davis, et al., Nuclear Waste Management Technical Support in the Development of Nuclear Waste Form Criteria for the NRC, NUREG/CR-2333, Vol. 1-4, February 1982.

DA-82a M.S. Davis and D.G. Schweitzer, Review of DOE Waste Package Program, NUREG/CR-2482, February 1982.

FI-50 M. Fishenden and O.A. Saunders, An Introduction to Heat Transfer, p. 97, Oxford University Press, London, 1950.

GE-61 Warren H. Geidt, Principles of Engineering Heat Transfer, Van Nostrand, 1961.

GO-68 J.G. Goodwin and W.L. Davis, Predictions of Tensile Properties at Temperatures Other Than the Testing Temperature, WAPP-TM-77, May 1968.

GR-62 R.E. Grim, Applied Clay Mineralogy, McGraw-Hill Book Co., 1968.

GR-68 R.E. Grim, Clay Mineralogy, McGraw-Hill Book Co., 1968.

GR-71 R.W. Grimshaw, The Chemistry and Physics of Clays, 4th ed., John Wiley and Sons, 1971.

HO-67 H.C. Hottel and A.F. Sarofin, Radiation Heat Transfer, McGraw-Hill Book Co., 1967.

HO-81 Jack P. Holman, Heat Transfer, McGraw-Hill Book Co., 1981.

KR-61 Frank Krieth, Principles of Heat Transfer, International Textbook Co., 1961.

LA-69 T.W. Lambe and R.V. Whitman, Soil Mechanics, John Wiley and Sons, 1969.

MA-62 Joseph Marin, Mechanical Behavior of Engineering Materials, Prentice-Hall, 1962.

ME-83 D. Meyers and J.J. Howard, eds., Evaluation of Clays and Clay Minerals for Application to Repository Sealing, ONWI-486, July 1983.

MI-76 J.K. Mitchell, Fundamentals of Soil Behavior, John Wiley and Sons, 1976.

MI-83 M. Mills, D. Vogt, and B. Mann, Parameters and Variables Appearing in Radiological Assessment Codes, NUREG/CR-3160, June 1983.

OR-77 Oak Ridge National Laboratory, "Documentation for the CCC-217/ ORIGEN Computer Code Package," June 1977.

PE-71 R.K. Penny and D.L. Marriott, Design for Creep, McGraw-Hill Book Co., 1971.

PE-73 R.H. Perry and C.H. Chilton, Chemical Engineers Handbook, McGraw-Hill Book Co., 1973.

PH-69 P.L. Phennigworth, "Solid Mechanics with Applications to Pressurized Water Reactors, WAPD-TM-762, September 1969.

SC-65 D.B. Scott, Physical and Mechanical Properties of Zircaloy 2 and 4, Westinghouse Electric Corporation, WCAP-3269-41, May 1965.

SI-68 Siegel and Howell, Thermal Radiation Heat Transfer, NASA SP-164, 1968.

SI-83 Dale R. Simpson, Some Characteristics of Potential Backfill Materials, ONWI-449, May 1983.

TI Titanium Metals Corporation of America, "TIMET-TiCode-12," Pittsburgh, Pennsylvania.

TI-56 S. Timoshenko, Strength of Materials, Part II, Advanced Theory and Problems, Third Edition, Van Nostrand, 1956.

TI-82 Titanium Metals Corporation of America, "TIMET, TiCode-12 Mechanical and Physical Properties Brochure," May 1982.

TI-84 M. Timko, TIMET, Private Communication, Pittsburgh, Pennsylvania, February 1984.

WE-73 Westinghouse Electric Corporation, Reference Safety Analysis Report, RESAR-3, Vol. II, 1973.

WE-83 Westinghouse Electric Corporation, Engineered Waste Package System Design Specification, ONWI-423, May 1983.

WH-68 J.F. White, Interim Summary of Work Applicable to ECC on Physico-Chemical Studies of Clad UO_2 under Reactor Accident Conditions, GEMP-619, June 1968.

WI-84 G. Wicks, Savannah River Laboratory, Personal communication, 1984.

APPENDIX A

RELATIONSHIP BETWEEN TEMPERATURE DEPENDENCE OF MASS DENSITY AND TEMPERATURE DEPENDENCE OF THERMAL EXPANSION

The mass density varies slightly with temperature for most structural metals. Therefore, experimenters tend not to focus attention on the temperature dependence of mass density. Frequently, only the room temperature value is given in property tables. However, the thermal expansion coefficient of temperature is frequently given as a function of temperature. This appendix indicates how the thermal expansion coefficient data can be used to quantify the dependence of mass density on temperature.

Assume that an isotropic cube with a side dimension L at the initial uniform temperature T_1 is raised in temperature to T_2. Geometrically, each side will increase in length by an amount $\overline{\Delta L}$ when the cube reaches temperature equilibrium at T_2. The increase in length

$$\overline{\Delta L} = \overline{\alpha} L \Delta T \tag{A-1}$$

where

$\overline{\Delta L}$ = increase in length of one side of cube [ℓ]

$\overline{\alpha}$ = mean value of thermal expansion coefficient of temperature in the temperature range from T_1 to T_2 [$\ell/\ell\theta$]

L = initial length of cube side [ℓ]

$\Delta T = T_2 - T_1$ = increase in temperature of the cube [θ]

During transition from the lower temperature T_1 to the higher temperature T_2, the mass of the cube remains constant

$$m_1 = m_2$$

$$\rho_1 V_1 = \rho_2 V_2 \tag{A-2}$$

where

m is mass of cube [m]

ρ is mass density of the material $[m/\ell^3]$

V is volume of cube $[\ell^3]$

and the subscripts refer to the two isothermal states at temperature T_1 and T_2.

Equation A-2 can be written

$$\rho V = (\rho + \Delta\rho)(V + \Delta V)$$

where

$$\rho_1 = \rho$$
$$V_1 = V$$
$$\rho_2 = \rho + \Delta\rho$$
$$V_2 = V + \Delta V$$

The terms $\Delta\rho$ and ΔV are incremental quantities that are negative if $\rho_2 < \rho_1$ or $V_2 < V_1$.

Dividing both sides by ρV gives

$$1 = (1 + \frac{\Delta\rho}{\rho})\ (1 + \frac{\Delta V}{V})$$
$$1 = 1 + \frac{\Delta\rho}{\rho} + \frac{\Delta V}{V} + (\frac{\Delta\rho}{\rho})(\frac{\Delta V}{V})$$

and

$$\frac{\Delta V}{V} = \frac{-\Delta\rho/\rho}{(1+\Delta\rho/\rho)}$$

or

$$\frac{\Delta V}{V} = -\frac{\Delta\rho}{\rho} \tag{A-3}$$

when higher order terms are assumed to be negligible (i.e., $\Delta\rho/\rho<<1$).

The change in volume can also be related to the change in the side dimension

$$\Delta V = (L + \overline{\Delta L})^3 - L^3$$

which can be written as

$$\Delta V = 3L^2\overline{\Delta L} + 3L\overline{\Delta L}^2 + \overline{\Delta L}^3$$

and

$$\frac{\Delta V}{V} = \frac{3\overline{\Delta L}}{L} + \frac{3\overline{\Delta L}^2}{L^2} + \frac{\overline{\Delta L}^3}{L^3}$$

Substituting Equation A-3 in the previous relationship yields

$$-\frac{\Delta\rho}{\rho} = \frac{3\overline{\Delta L}}{L} + \frac{3\overline{\Delta L}^2}{L^2} + \frac{\overline{\Delta L}^3}{L^3} \tag{A-4}$$

as the density variation term. Substituting Equation A-1 for ΔL gives

$$-\frac{\Delta\rho}{\rho} = 3\bar{\alpha}\Delta T + 3(\bar{\alpha}\Delta T)^2 + (\bar{\alpha}\Delta T)^3 \tag{A-5}$$

For carbon steel in the temperature range ($0°F \leq 1000°F$)

$$\bar{\alpha} \approx 8.0 \times 10^{-6} \text{ (in/in°F)}$$

$$\Delta T = 1000(°F)$$

$$\bar{\alpha}\Delta T = 8.0 \times 10^{-3} \quad \text{(in).}$$

Using Equation A-5

$$\frac{-\Delta\rho}{\rho} = 3\bar{\alpha}\Delta T + 3(\bar{\alpha}\Delta T)^2 + (\bar{\alpha}\Delta T)^3$$

$$\frac{-\Delta\rho}{\rho} = 24 \times 10^{-3} + 192 \times 10^{-6} + 512 \times 10^{-9}$$

The magnitude of the second and third terms on the right side of the equation is negligible in comparison to the first term. For carbon steel, the density variation ($-\Delta\rho$), which decreases as the material increases in temperature by 1000°F, is only 2.4%. The assumption used in stating Equation A-3 can also be reviewed:

$$\left|\frac{\Delta\rho}{\rho}\right| << 1.0$$

$$0.024 << 1.0$$

This is acceptable for engineering calculations where amounts up to several percent are negligible in comparison to unity.

Equation A-5 can be simplified and written as

$$\frac{-\Delta\rho}{\rho} = 3\bar{\alpha}\Delta T \tag{A-6}$$

where

ρ = mass density $[m/\ell^3]$

$\bar{\alpha}$ = mean value of thermal expansion coefficient of temperature over the temperature range from T_1 to T_2 $[\ell/\ell\theta]$

$\Delta T = T_2 - T_1$ = temperature increase between isothermal states 1 and 2 $[\theta]$

$\Delta\rho = \rho_2 - \rho_1$ = mass density increase of a given mass for a specific temperature increase (ΔT from T_1 to T_2) $[m/\ell^3]$

$-\Delta\rho = \rho_1 - \rho_2$ = mass density decrease of a given mass for specific temperature increase (ΔT from T_1 to T_2) $[m/\ell^3]$

Equation A-6 can be used to give an approximate but acceptable definition of the mass density's temperature dependence in terms of available thermal expansion coefficient data over a common temperature range.

In this report, we choose not to ignore the temperature dependence of the mass density and approximate it by using Equation A-6 when the temperature coefficient of thermal expansion data is available. Analysts who use these data will be free to decide whether to treat mass density as a temperature-dependent property or as a constant property for the temperature variations anticipated in their particular application. This report presents consistent data to facilitate general analysis.

When finite element structural analysis methods are used, the analyst must consider the effects of using temperature-dependent mass density. Most finite element methods assume that no significant volume change occurs with temperature changes. Therefore, constant (non-temperature-dependent) values of density generally should be used. In this instance, the mass of the structure is calculated as the product of the mass density and the volume. To conserve mass, a constant mass density should be used.

APPENDIX B
MOHR'S DIAGRAMS

Mohr's diagrams are graphic techniques that are used primarily for illustrating principal stresses and the maximum shear stress for a state of stress and the principal strains and maximum shear strain for a state of strain. In the case of stress, the maximum shear stress τ_{max} is a key failure parameter for ductile materials as stated by the Tresca criterion (see Appendix C, Equation C-1). Mohr's diagrams for stress are more common than those for strain because structural analysis tends to be done in terms of stress quantities.

In general, principal stresses are determined by extracting the three real roots of Equation 3.34 with invariant coefficients as defined in terms of stress components by Equations 3.35 through 3.37 and illustrated in Figure B-1. If the principal stress values are known, the Mohr's diagram for stress can be constructed directly as depicted in Figure B-2. The circles have diameters on the σ axis equal to the difference in principal stress values.

The three Mohr's circles are drawn on the σ,τ plane. One circle circumscribes the other two, and each circle has a point in common with each of the other two. The points in common are the principal stresses which lie on the σ axis.

The Mohr's diagram for stress is applicable to the case of plane stress, e.g., in the x,y plane shown in Figure B-3. The sign convention defining positive stress components for the purpose of constructing the Mohr's diagram directly from the stress components is defined in Figure B-4.

For the plane stress case where stress components not in the x,y plane are all zero, Equations 3.35-3.37 yield

$$
\begin{aligned}
I_1 &= \sigma_x + \sigma_y \\
I_2 &= \sigma_x\sigma_y - \tau_{xy}^2 \\
I_3 &= 0
\end{aligned}
\qquad \text{(B-1)}
$$

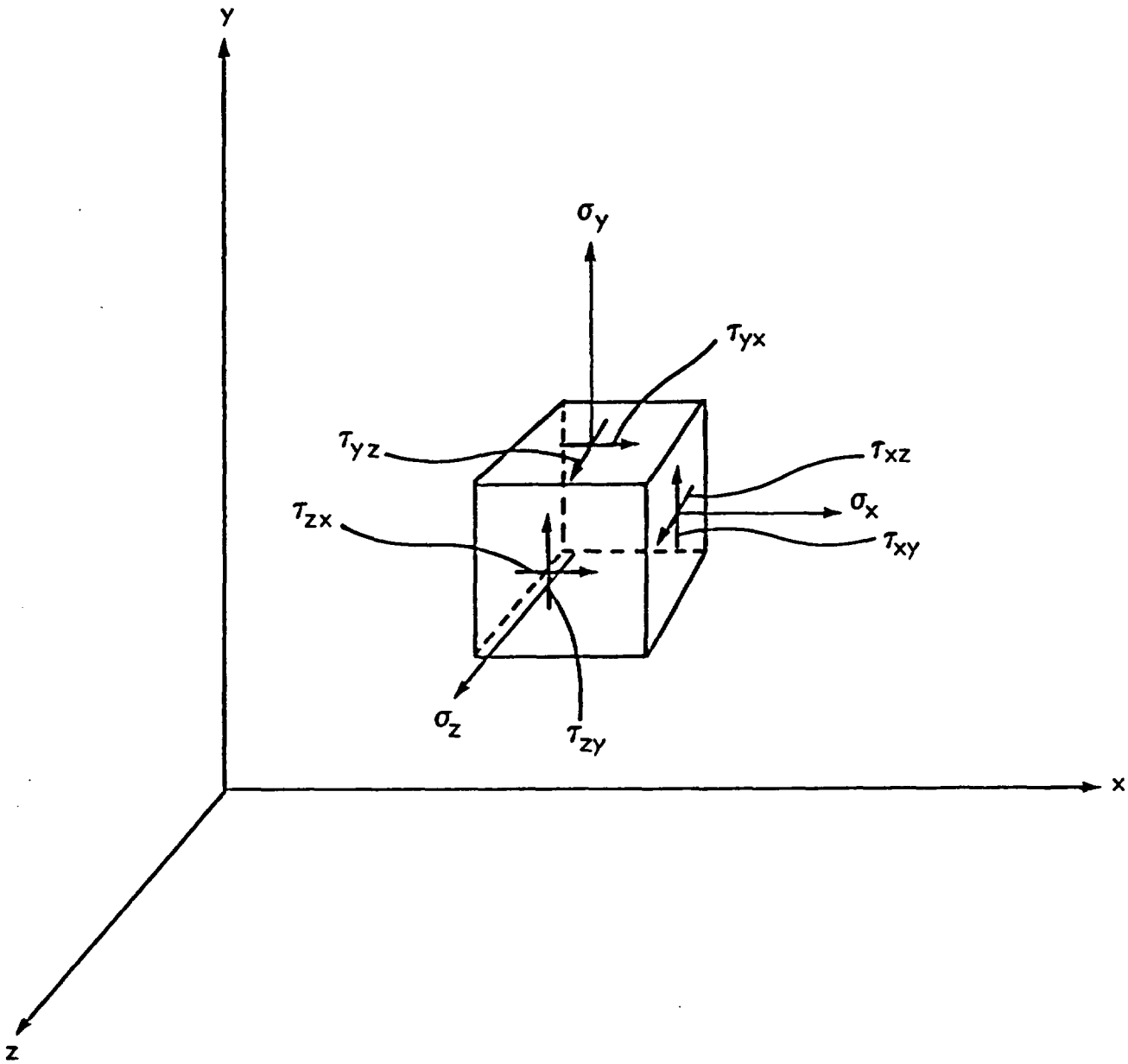

Figure B-1

Infinitesimal Cube Used to Define the State of Stress at a Point in a Structure. Stress Components Are Shown Only on the Positive Axis Faces. Components of Equal Magnitude but Opposite Direction Act on the Faces Which Project along the Negative Axes.

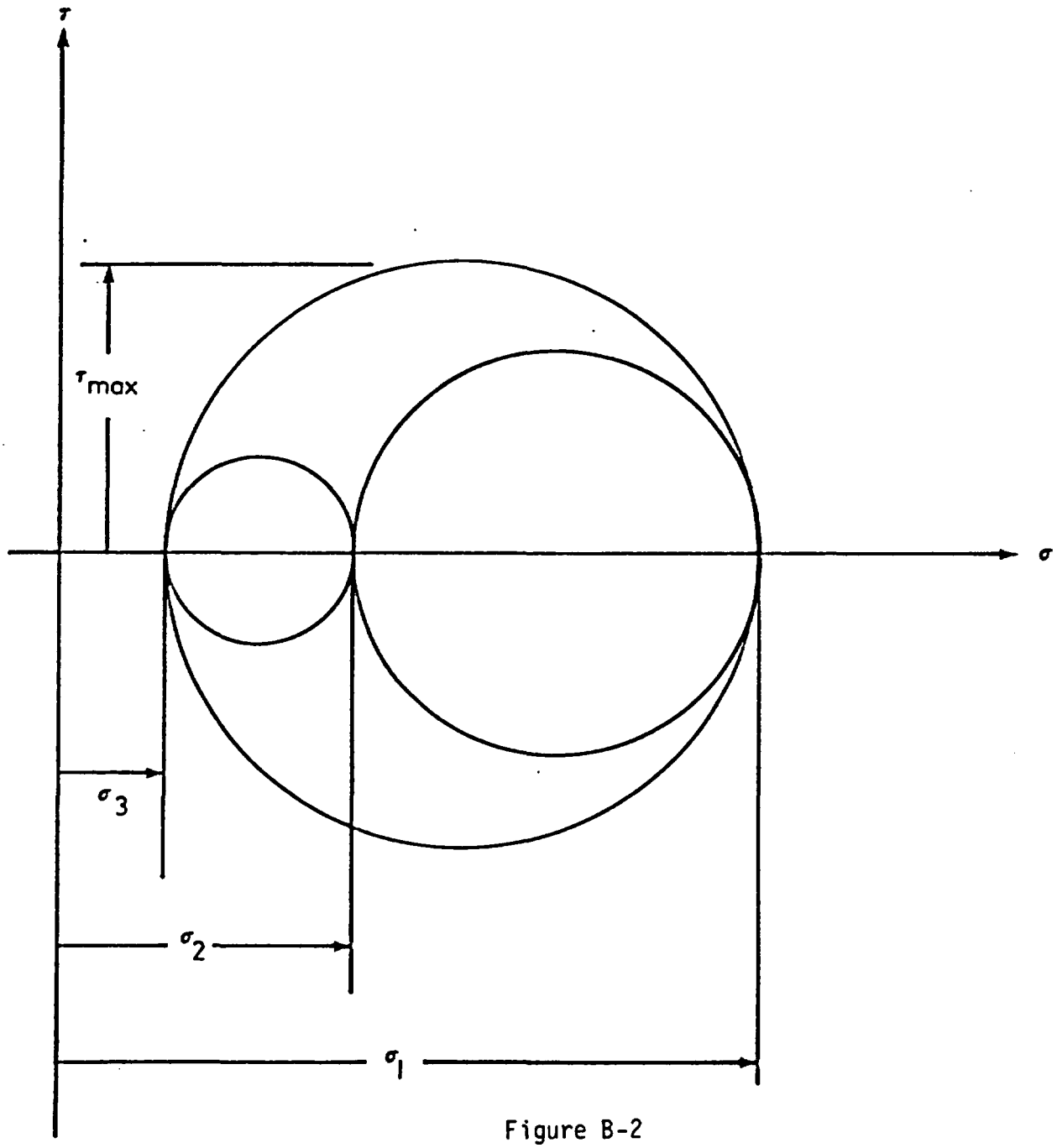

Figure B-2

Mohr's Circles for Stress with Principal Stresses σ_1, σ_2, σ_3 and Maximum Shear Stress $\tau_{max} = {}^1/_2 \max\{|\sigma_1-\sigma_2|, |\sigma_2-\sigma_3|, |\sigma_1-\sigma_3|\}$

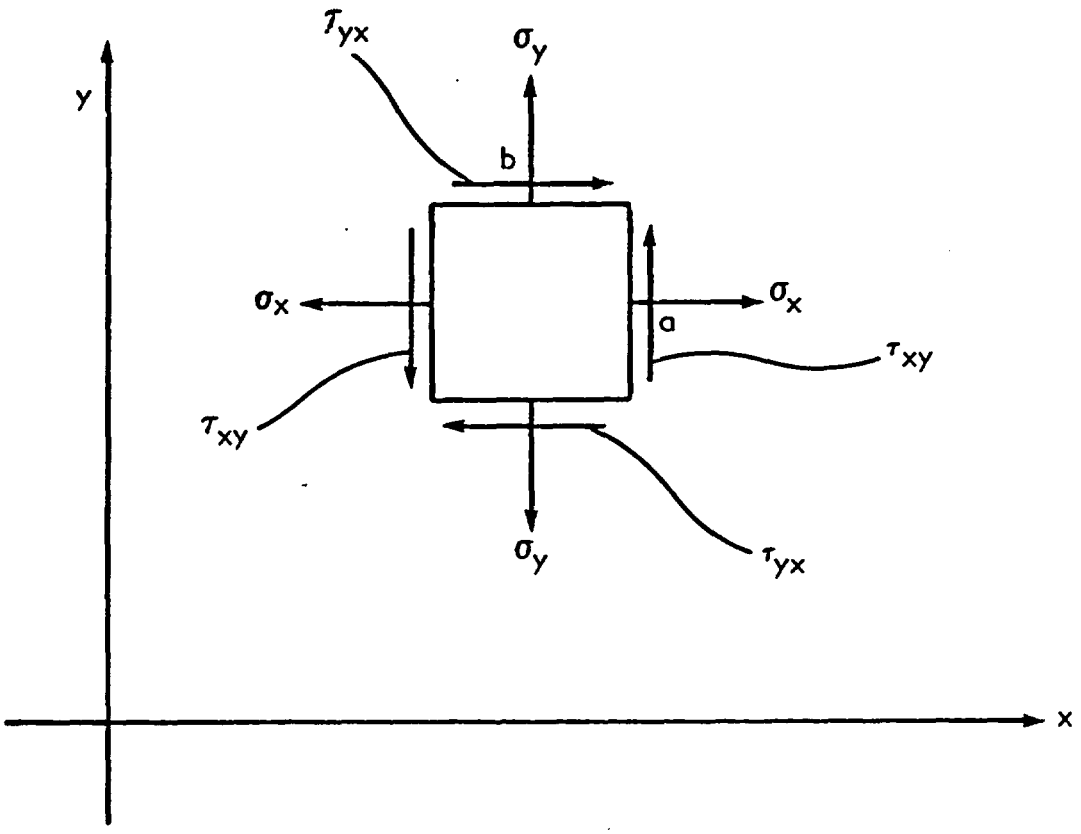

Figure B-3

Two Dimensional x-y Plane View of Infinitesimal Cube Used to Define State of Stress at Point p.

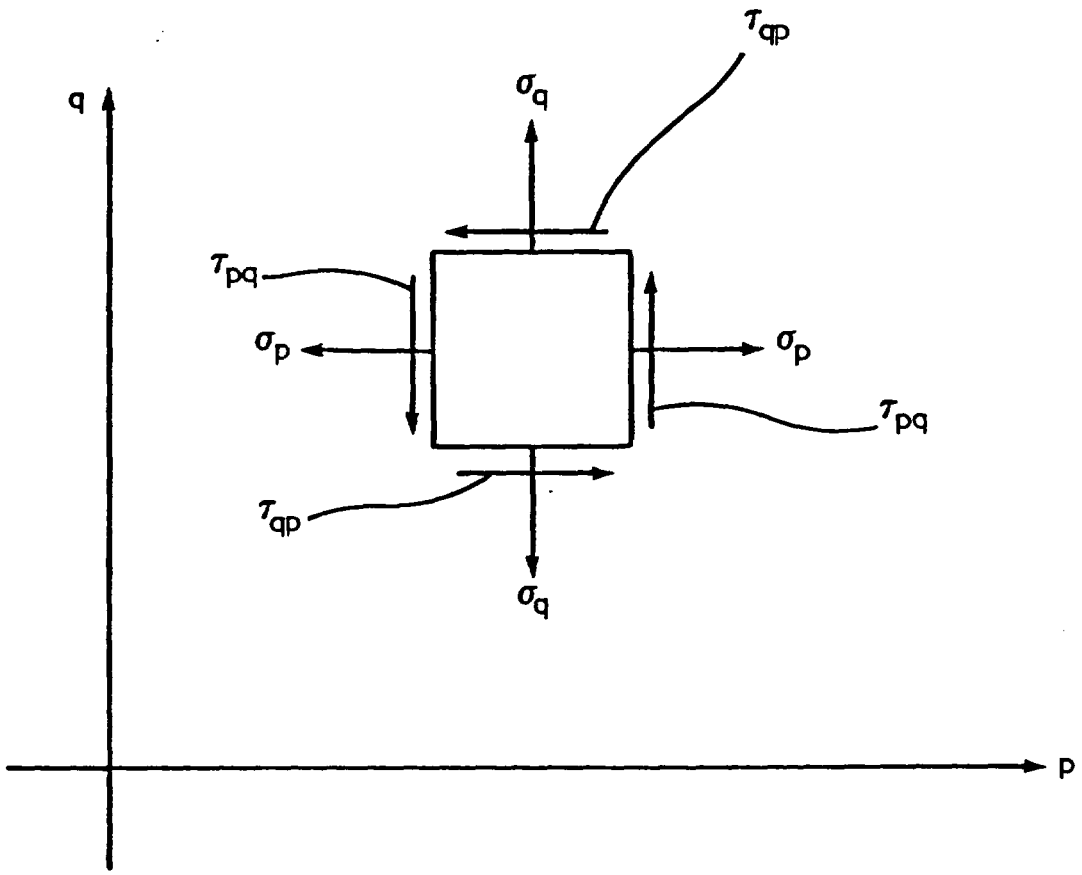

Figure B-4

Sign Convention for Stress Components Used in Constructing Mohr's Circle in the Generalized p-q Plane. Components Are Shown in the Positive Direction. (Note: This sign convention is only for constructing Mohr's Circle.)

For this condition, Equation 3.34 can be factored to give

$$S(S^2 - I_1 S + I_2) = 0 \tag{B-2}$$

The quadratic factor has a solution

$$\begin{matrix}\alpha_1 \\ \alpha_2\end{matrix} = \frac{1}{2}(\alpha_x + \alpha_y) \pm \sqrt{\left(\frac{\alpha_x - \alpha_y}{2}\right)^2 \pm \tau_{xy}^2} \tag{B-3}$$

and the maximum shear stress is given by

$$\tau_{max} = \sqrt{\left[\frac{1}{2}(\sigma_x - \sigma_y)\right]^2 + \tau_{xy}^2} \tag{B-4}$$

If the magnitudes of the components are

$$\begin{aligned} \sigma_x &= 20{,}000 \text{ (psi)} \\ \sigma_y &= 5{,}000 \text{ (psi)} \\ \tau_{xy} &= \tau_{xy} = 5{,}000 \text{ (psi)} \end{aligned} \tag{B-5}$$

and are directed as shown in Figure B-3, the Mohr's circle can be constructed directly using the sign convention of Figure B-4 as shown in Figure B-5.

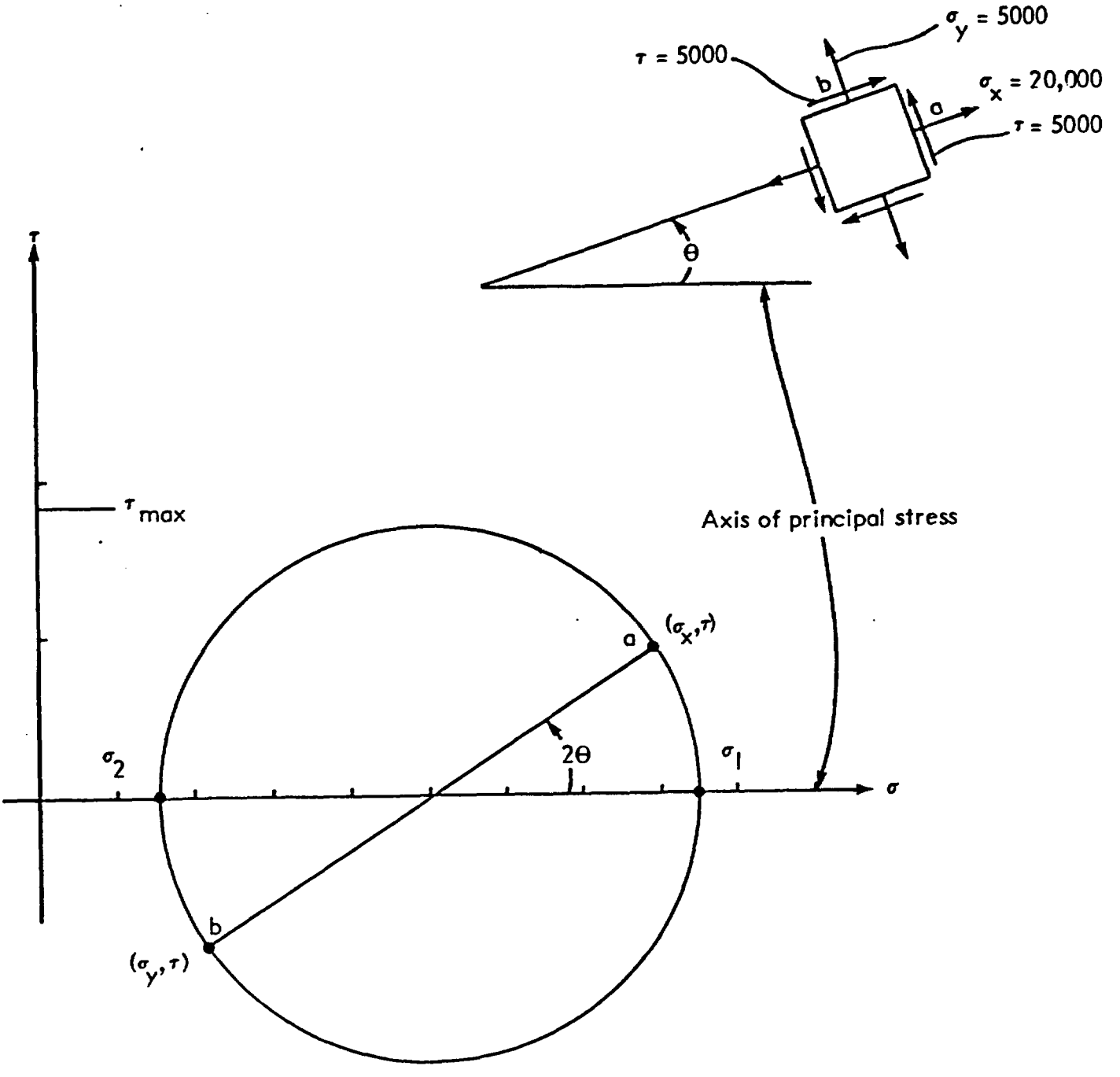

Figure B-5

Mohr's Circle for Stress Components Directed as Defined in Figure B-3. An Angle of θ in the xy Plane of the Structure Corresponds to 2 θ on the Mohr's Circle Plot

The angle θ is related to the stress components according to

$$\theta = \frac{1}{2} \tan^{-1} \left[\frac{2\tau_{xy}}{\sigma_x - \sigma_y} \right] \tag{B-6}$$

For any angle θ, the normal and shear stress components can be determined from

$$\sigma_\theta = \frac{1}{2} (\sigma_1 + \sigma_2) + \frac{1}{2} (\sigma_1 - \sigma_2) \cos 2\theta \tag{B-7}$$

$$\tau_\theta = \frac{1}{2} (\sigma_1 - \sigma_2) \sin 2\theta \tag{B-8}$$

Equation B-6 applies only to the x,y plane stress case of Equation B-5 and Figure B-3. Equations B-7 and B-8 are written in terms of the two principal stresses, σ_1 and σ_2, and are more general. These equations apply to the intermediate size circle of Figure B-2, as well as to the circle of Figure B-5. As shown in Figure B-5, an angle of θ in the x,y plane corresponds to an angle of 2θ on the Mohr's circle.

A Mohr's diagram for stress provides an opportunity to look at contrasting cases of biaxial stress. Supposing that the normal stress component in the y direction shown in Figure B-3 is compressive, tending to compact the material, instead of tensile, and that the other components remain unchanged, then

$$\begin{aligned} \sigma_x &= 20{,}000 \text{ psi} \\ \sigma_y &= -5{,}000 \text{ psi} \\ \tau_{xy} &= \tau_{yx} = 5{,}000 \text{ psi} \end{aligned} \tag{B-9}$$

The Mohr's circle shown in Figure B-6 is much larger in diameter than the circle in Figure B-3. The yielding criteria as given by Tresca would indicate that the stress state with σ_y of opposite sign to σ_x is much worse than when they have the same sign (for the same magnitude). This is consistent with the deviatorial stress causing the distortion. The normal stress in the z direction is zero in the cases of Figures B-5 and B-6. The mean stresses for Figure B-4 are:

$$\sigma_m = (20{,}000 + 5{,}000)/3$$
$$\sigma_m = 8{,}333 \text{ psi}$$

(B-10)

For Figure B-6

$$\sigma_m = (20{,}000 - 5{,}000)/3$$
$$\sigma_m = 5{,}000 \text{ psi}$$

(B-11)

The deviator stress components for Figure B-4 are:

$$D_{ij} = \sigma_{ij} - \delta_{ij}\sigma_m$$

$$D_{ij} = \begin{bmatrix} 11{,}667 & 5{,}000 & 0 \\ 5{,}000 & -3{,}333 & 0 \\ 0 & 0 & -8{,}333 \end{bmatrix}$$

(B-12)

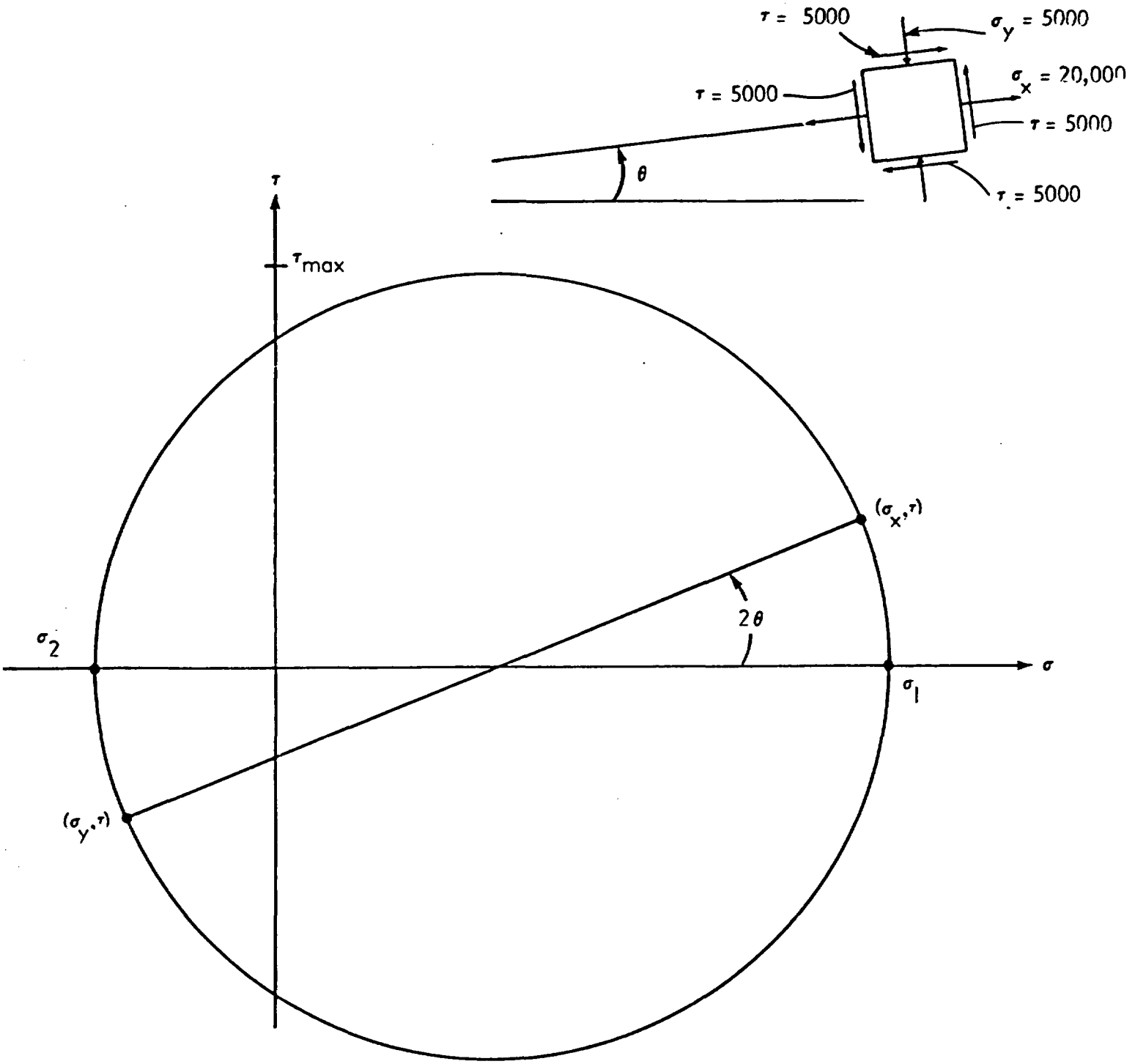

Figure B-6

Mohr's Circle Stress in x-y Plane When y Directed Normal Stress Is Compressive Rather Than Tensile. An Angle of θ in the xy Plane of the Structure Corresponds to 2 θ on the Mohr's Circle Plot.

The biaxial x,y states of stress for Figure B-6 are:

$$D_{ij} = \begin{bmatrix} 15,000 & 5,000 & 0 \\ 5,000 & -10,000 & 0 \\ 0 & 0 & -5,000 \end{bmatrix} \tag{B-13}$$

The state of stress represented in Figure B-6 is more severe than that represented in Figure B-5 because the deviatorial stress components are larger. An other way of considering the difference is that the first case (Figure B-5) has a higher mean stress which does not contribute to failure for ductile structural metals such as most steels.

A simple, uniaxially stressed tensile specimen and its Mohr's circle for stress are shown in Figure B-7.

It is helpful when applying the Tresca criterion (Equation C-1) to construct the particular Mohr's diagram for stress as shown for the three examples in Figures B-2, B-5, and B-6. This procedure involves determining and displaying τ_{max} for the particular state of stress that the Tresca criterion compares to the value of τ_{max} in the uniaxial tensile specimen at yielding.

A comparison of Equations 3.5 - 3.8 with Equations 3.34 - 3.37 indicates that the Mohr's diagram for strain is analogous to the Mohr's diagram for stress. In general, the three real roots of Equation 3.5 are the principal strains for a particular state of strain as defined by the components on the right side of the strain invariant relationships (Equations 3.6 - 3.8). When the principal strains are determined, the Mohr's diagram for strain can be constructed by the same procedure used to construct Figure B-2 for stress.

For biaxial (x,y) only straining, Equations 3.6 through 3.8 become

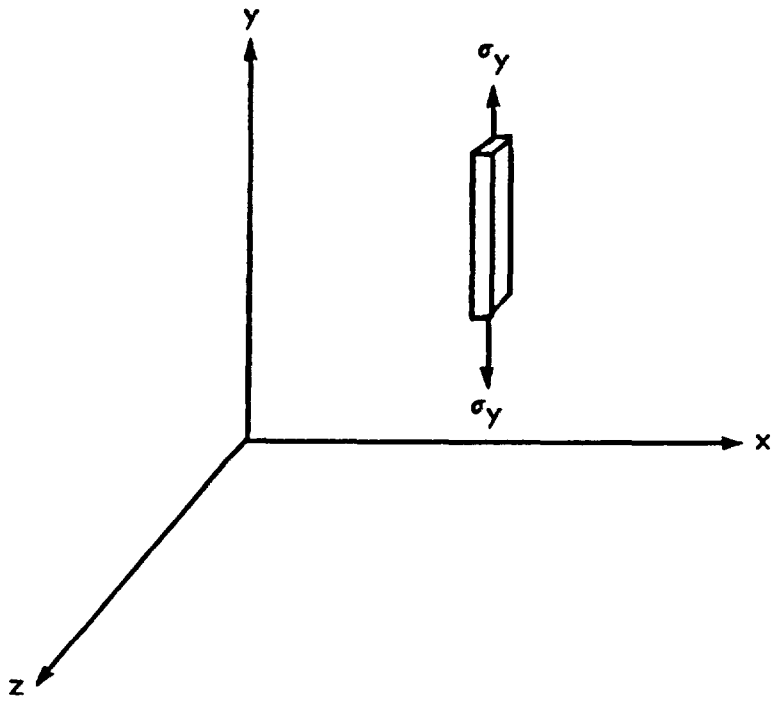

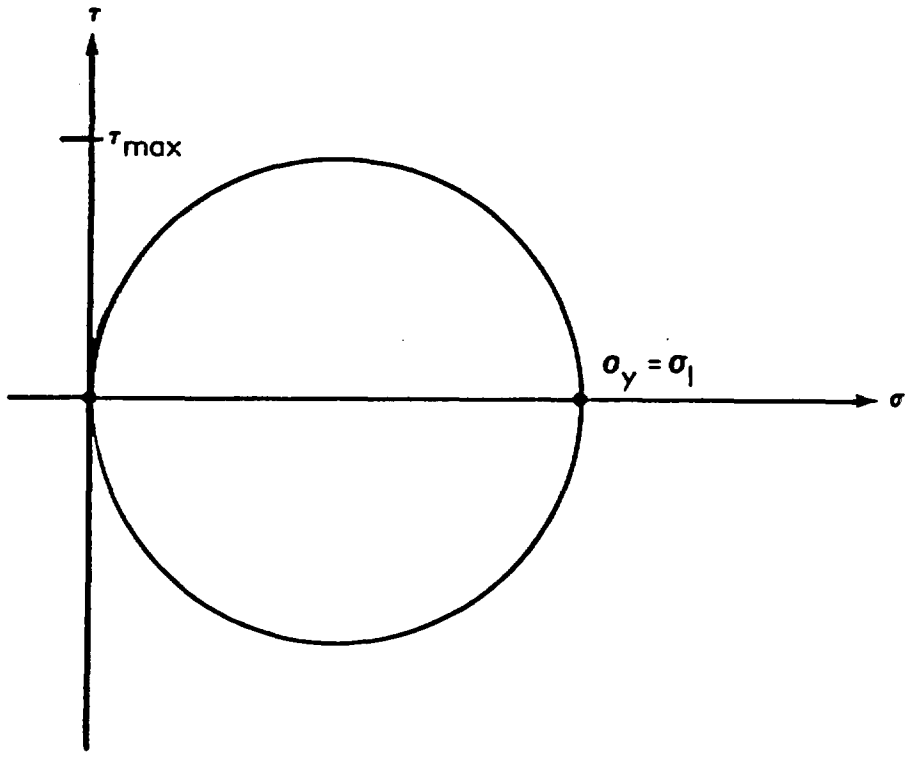

Figure B-7

Mohr's Circle for a Simple Uniaxial Tension Specimen without Shear on the Cube. Two of the Mohr's Circles Can Be Considered as Points (0,0).

$$I_{\varepsilon 1} = \varepsilon_x + \varepsilon_y$$

$$I_{\varepsilon 2} = \varepsilon_x \varepsilon_y - \frac{\gamma_{xy}^2}{4}$$

(B-14)

and Equation 3.5 can be factored to give

$$\varepsilon\left(\varepsilon^2 - \frac{I}{\varepsilon_1}\varepsilon + \frac{I}{\varepsilon_2}\right) = 0$$

(B-15)

The quadratic factor in Equation B-15 can be solved to give

$$\begin{matrix}\varepsilon_1 \\ \varepsilon_2\end{matrix} = \frac{1}{2}(\varepsilon_x + \varepsilon_y) \pm \sqrt{\left(\frac{\varepsilon_x - \varepsilon_y}{2}\right)^2 + \left(\frac{\gamma_{xy}}{2}\right)^2}$$

(B-16)

where the first term on the right side is the abscissa (along the ε axis) of the center of the Mohr's circle for strain and the last term is the radius of the circle. The circle is shown in Figure B-8 for a case of plane (x,y) strain. The angle θ shown in Figure B-8 is related to the strain components by

$$\theta = \frac{1}{2}\,\mathrm{Tan}^{-1}\left[\frac{\gamma_{xy}}{\varepsilon_x - \varepsilon_y}\right]$$

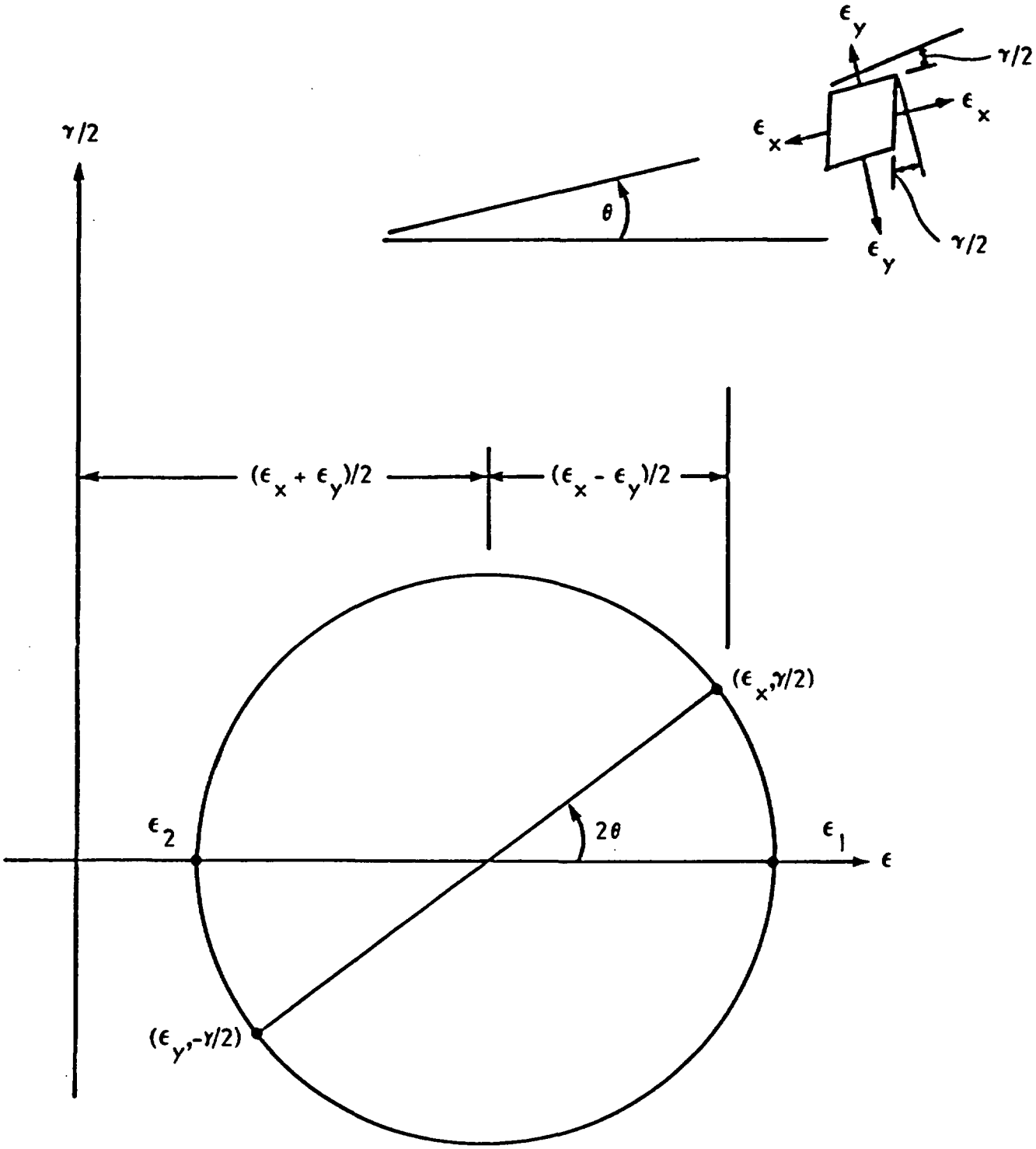

Figure B-8

Mohr's Circle for Strain

APPENDIX C
MATERIAL YIELD CRITERIA

The state of stress at which yielding occurs is related to the yield stress for a specimen in a simple tensile test by yield criteria. These equations prescribe the means of determining how close, at a point, the material's state of stress is to yielding. The state of stress that is compared to the yield stress can be used as a generalized stress condition for design. It would be legitimate to use it to indicate when the state of stress reached a magnitude equivalent to a design criterion such as 75% of the yield stress in a uniaxial tensile specimen.

For ductile metals that are commonly used as structural materials, there are two reliable and commonly used yield criteria. They are the Tresca and von Mises criteria. The Mohr-Coulomb criteria is often used to predict yielding of soils and geologic media.

Tresca Yield Condition

The Tresca criterion, published in 1868, postulates that yielding will occur at a point when the maximum shear stress at that point is equal to the maximum shear stress in a tensile specimen at yielding. For simple tension, two of the principal stresses are zero, and the maximum shear stress is

$$\tau_{max} = 0.5\ \sigma_o \tag{C-1}$$

where

τ_{max} = maximum shear stress $[f/\ell^2]$

σ_o = tensile stress in simple tensile specimen at yielding $[f/\ell^2]$

The shear stress at a point for any stress state is determined from the principal stresses as

$$\tau_{max} = 0.5 \max (|\sigma_1 - \sigma_2|; |\sigma_2 - \sigma_3|; |\sigma_3 - \sigma_1|) \tag{C-2}$$

Equations C-1 and C-2 are a statement of the Tresca criterion. They can be combined to eliminate τ_{max} and give a relationship between the absolute value of the maximum difference in principal stresses and the yield stress for a uniaxially loaded tensile specimen:

$$\sigma_o = \max (|\sigma_1 - \sigma_2|; |\sigma_2 - \sigma_3|; |\sigma_3 - \sigma_1|) \tag{C-3}$$

Since the Tresca criterion is stated in terms of the principal stresses, the principal stresses must be determined in terms of the stress components. Either the equations given in Appendix B for biaxial stress, the Mohr's diagram methods (biaxial stress), or Equation 3.34 (triaxial stress) may be used to determine the principal stresses.

<u>von Mises Yield Condition</u>

The von Mises yield condition, developed in 1913, states that yielding will occur at a point when the state of stress at that point reaches a value as prescribed by the von Mises formula that is equal to the tensile stress in a simple tensile test at yielding:

$$\sigma_o = \frac{1}{\sqrt{2}} \left[(\sigma_1 - \sigma_2)^2 + (\sigma_2 - \sigma_3)^2 + (\sigma_3 - \sigma_1)^2 \right]^{\frac{1}{2}} \tag{C-4}$$

where

$\sigma_1, \sigma_2, \sigma_3$ = principal stresses in the stress field $[f/\ell^2]$

σ_0 = tensile stress in simple tensile specimen at yielding $[f/\ell^2]$

The Tresca and von Mises yield surfaces for ductile metals are shown in Figure C-1 in the Haigh-Westergaad stress space looking in along the hydrostat, which is a line passing through all points where $\sigma_1 = \sigma_2 = \sigma_3$. The Tresca yield surface projects as a hexagon on planes normal to the hydrostat. The von Mises yield surface projects as a circle on this plane and has a diameter equal to the major diameter of the hexagon. These yield surfaces indicate that yielding occurs at the same stress magnitude in compression as in tension. These yield surfaces are independent of position along the hydrostat and are thus independent of the hydrostatic state of stress.

Mohr-Coulomb Criterion

For compressible soil type media (e.g., bentonite backfill), yielding is reasonably well described in terms of the Mohr-Coulomb failure criterion. This yield criterion relates shear stress on a plane to the normal stress on the same plane. The criterion can be stated as

$$\tau_y = c + \sigma_n \tan \theta \tag{C-5}$$

where:

τ_y = shear stress at yield on shear plane $[f/\ell^2]$

c = cohesion force per unit area $[f/\ell^2]$

σ_n = normal compressive stress on shear plane when yielding in shear occurs $[f/\ell^2]$

θ = material internal angle of friction [ ]

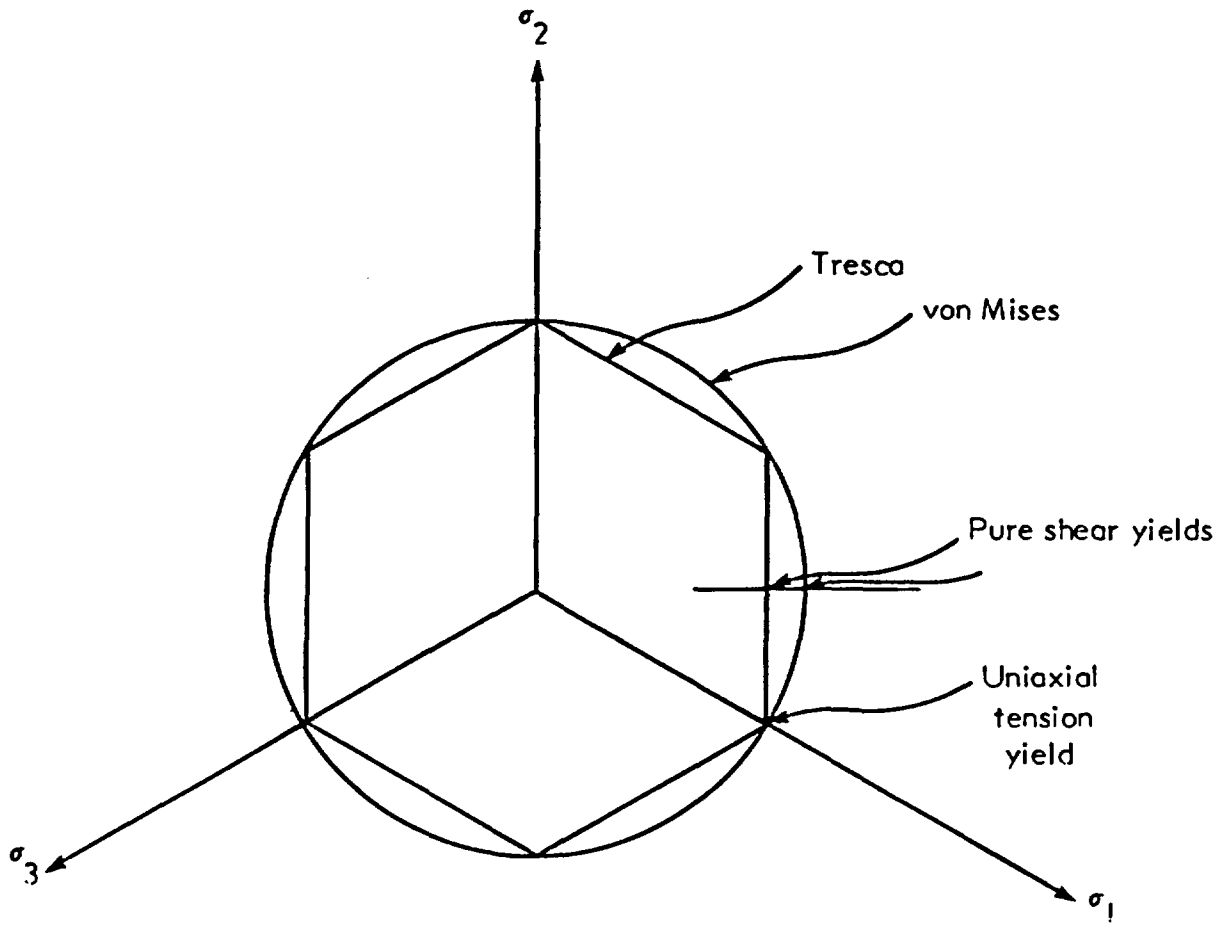

Figure C-1

Von Mises Yield Surfaces Projected on a Plan Normal to the Line Intersection Points Where $\sigma_1 = \sigma_2 = \sigma_3$.

APPENDIX D

HEATING Thermal Property Data

Table D-1

HEATING Thermal Property Data*

Material	Temperature-Dependent Specific Heat (watt-hr/kg°C) Temperature (°C)	Value	Data Uncertainty**	Temperature-Dependent Conductivity (watts/m°C) Temperature (°C)	Value	Data Uncertainty**
Aluminum	0	0.250	0	0	226.	2
	500	0.314	0	400	222.	2
				660	209.	2
Copper	0	0.107	0	0	402.	0
	1083(M.P.)	0.140	0	1083(M.P.)	335.	0
Graphite	-73	0.116	0	10	167.	2
	100	0.262	0	100	151.	2
	200	0.326	0	200	130.	2
	300	0.372	0	300	113.	2
	400	0.411	0	400	100.	2
	600	0.468	0	500	92.	2
Iron	0	0.122	0			
	763	0.223				
Iron, Nodular Cast (Ferritic)	0	0.123	3	0	39.4	0
	100	0.130	3	500	29.7	0
	400	0.178	3			
	700	0.221	3			
Iron, Nodular Cast (Pearlitic)	0	0.123	3	0	38.9	0
	100	0.130	3	900	18.8	0
	400	0.178	3			
	700	0.221	3			
Iron, Gray Cast (Ferritic) 2.3-3.0%C	0	0.113	0	125	51.1	0
	100	0.130	0	300	42.7	0
	400	0.178	0	425	39.8	0
	700	0.221	0			

Table D-1 (continued)

Material	Temperature-Dependent Specific Heat (watt-hr/kg°C) Temperature (°C)	Value	Data Uncertainty**	Temperature-Dependent Conductivity (watts/m°C) Temperature (°C)	Value	Data Uncertainty**
Iron, Gray Cast (Ferritic) 3.2-3.8%C	0	0.113	3	125	53.6	0
	100	0.130	3	300	53.6	0
	400	0.178	3	425	44.4	0
	700	0.221	3			
Iron, Gray Cast (Pearlitic) 2.3-3.0%C	0	0.113	3	0	44.0	0
	100	0.130	3	300	38.5	0
	400	0.178	3	500	32.7	0
	700	0.221	3			
Iron, Gray Cast (Pearlitic) 3.0-3.2%C	0	0.113	3	0	50.2	0
	100	0.130	3	300	43.1	0
	400	0.178	3	500	36.8	0
	700	0.221	3			
Iron, Gray Cast (Pearlitic) 3.4%C	0	0.113	3	0	58.6	0
	100	0.130	3	300	46.5	0
	400	0.178	3	400	44.4	0
	700	0.221	3	700	36.8	0
Iron, Gray Cast (Pearlitic) 3.7-3.8%C	0	0.113	3	0	67.0	0
	100	0.130	3	300	53.6	0
	400	0.178	3	500	41.0	0
	700	0.221	3			
Iron, Gray Cast (Pearlitic) 4.12%C	0	0.113	3	0	80.4	0
	100	0.130	3	300	57.8	0
	400	0.178	3	500	45.2	0
	700	0.221	3			
Titanium	25	0.145	0	0	20.9	2
	300	0.165	0	400	18.8	2
	880	0.186	0	700	18.0	2

Table D-1 (continued)

Material	Temperature-Dependent Specific Heat (watt-hr/kg°C) Temperature (°C)	Value	Data Uncertainty**	Temperature-Dependent Conductivity (watts/m°C) Temperature (°C)	Value	Data Uncertainty**
Zirconium	25	0.079	0	0	32.7	2
	500	0.088	0	200	23.4	2
4130 Carbon Steel	-18	0.145	0	-18	43.1	2
	204	0.145	0	204	42.3	2
	427	0.172	0	427	38.6	2
	648	0.209	0	648	32.2	2
1020 Carbon Steel	0	0.122	0	25	71.2	0
	75	0.144	0			
	200	0.157	0			
	400	0.169	0			
	600	0.198	0			
304 SS	0	0.140	0	0	13.4	0
	400	0.157	0	100	16.3	0
				500	21.8	0
Lead	0	0.0355	0	20	34.6	0
	100	0.0366	0	98.3	33.9	0
	327.5(M.P.)	0.0393	0	204.5	31.7	0
	327.6	0.0395	0	259.4	29.3	0
	1000	0.0381	0	305.0	25.1	0
				332.2	20.9	0
				408.6	16.7	0
				426.6	15.6	0
				526.7	15.1	0
Inconel-X	0	0.120	0	0	13.4	1
	200	0.136	0	400	22.6	1
	700	0.165	0	900	36.8	1

Table D-1 (continued)

Material	Temperature-Dependent Specific Heat (watt-hr/kg°C) Temperature (°C)	Value	Data Uncertainty**	Temperature-Dependent Conductivity (watts/m°C) Temperature (°C)	Value	Data Uncertainty**
Inconel-600	0	0.122	3	0	14.7	0
	200	0.151	3	400	16.4	0
				500	22.9	0
Alumina (ρ = .5g/cm^3)	0	0.202	0	350	0.0419	2
	100	0.258	0	800	0.176	2
	200	0.285	0			
	300	0.308	0			
	500	0.326	0			
Alumina (ρ = 1.9 g/cm^3)	0	0.202	0	150	5.23	0
	100	0.258	0	300	3.77	0
	200	0.285	0	500	2.93	0
	300	0.308	0			
	500	0.326	0			
Glass - Borosillicate	0	0.174	0	0	1.05	2
	100	0.209	0	100	1.13	2
	300	0.256	0			
	600	0.285	0			
Glass - Pyrex	0	0.190	0	0	1.09	0
	100	0.237	0	600	1.76	0
	200	0.276	0			
	300	0.303	0			
	400	0.319	0			
Glass - Soda Lime	0	0.17	3	100	1.47	2
	100	0.21	3	300	1.82	2
	500	0.27	3	500	2.35	2
	900	0.30	3	650	2.81	2

Table D-1 (continued)

Material	Temperature-Dependent Specific Heat (watt-hr/kg°C) Temperature (°C)	Value	Data Uncertainty**	Temperature-Dependent Conductivity (watts/m°C) Temperature (°C)	Value	Data Uncertainty**
Uranium Dioxide (UO_2)	0	0.065	0	0	8.79	0
	100	0.073	0	200	7.53	0
	200	0.079	0	300	6.28	0
	400	0.084	0	500	5.53	0
	1200	0.092	0	700	5.15	0
	2000	0.095	0	800	5.19	0
Sand - Dry	25	0.0009	5			
Sand - 4-10% Water	25	0.005	5			
Sand - Quartz, wet (4-23% water)	25	0.002	5			
Argon	25	0.144	0	0	0.0166	0
				100	0.0214	0
				300	0.0295	0
				500	0.0351	0
Helium	25	1.44	0	0	0.142	0
				100	0.170	0
				200	0.21	0
				500	0.291	0
Krypton	25	0.0337	0	25	0.0921	0
Neon	25	0.287	0	0	0.0456	0
				100	0.0565	0
				200	0.0661	0
				300	0.0750	0
				500	0.0908	0

Table D-1 (continued)

Material	Temperature-Dependent Specific Heat (watt-hr/kg°C) Temperature (°C)	Value	Data Uncertainty**	Temperature-Dependent Conductivity (watts/m°C) Temperature (°C)	Value	Data Uncertainty**
Xenon	25	0.0441	0	0	0.00586	0
				100	0.00708	0
				200	0.00842	0
				300	0.00967	0
				500	0.01206	0
Air	100	0.276	0	0	0.0242	0
				100	0.0318	0
				200	0.0387	0
				300	0.0449	0
				400	0.0566	0
Nitrogen	0	0.284	0	0	0.0240	0
	100	0.290	0	100	0.0313	0
	400	0.302	0	200	0.0380	0
	700	0.322	0	300	0.0442	0
				400	0.0483	0

* Source: A.L. Edwards, A Compilation of Thermal Property Data for Computer Heat-Conduction Calculation, UCRL-50589, February 1969.

** Data uncertainty type descriptions

Data Uncertainty Type 0:
Data was good or no statement was made in data source restricting its accuracy. No conflicting data were found in any other data sources. Most data in this category is probably accurate to within 5-10 percent for specific heat and 10-20 percent for thermal conductivity.

Data Uncertainty Type 1:
Good data, but specific heat or thermal conductivty was reported only for a limited temperature range. The temperature range has been extended by extrapolation and the resulting values are probably as accurate as reported values.

Data Uncertainty Type 2:
Either the accuracy of the data was poor or values reported by different sources disagreed. The best values were used whenever a judgment could be made, or average values were used with consideration given to data for similar materials.

Data Uncertainty Type 3:
No data could be found in the literature; however, values are an estimate based on theoretical or empirical grounds, or on data for similar materials. These estimates were included whenever they reported data for similar materials.

Data Uncertainty Type 4:
No data could be found in the literature, and no accurate estimate could be made. The data, therefore, are considered to be a rough estimate based, in most cases, on data for similar materials.

Data Uncertainty Type 5:
No data could be found in the literature and no estimate was made. A minimum requirement for inclusion of a material in the alphabetical index and material data list is the availability of at least estimated constant values of density, specific heat, and thermal conductivity.